POLITECNICO
MILANO 1863

SCUOLA DI INGEGNERIA INDUSTRIALE
E DELL'INFORMAZIONE

Validation of IMU-based simulation for water exercises kinematics

Tesi di Laurea Magistrale in
Biomedical Engineering - Ingegneria Biomedica

Authors: **Cristina Chieffo and Filippo Motta**

Student ID: 970854 , 969102
Advisor: Prof. Manuela Galli
Co-advisors: Prof. Jeffrey A. Tuhtan, Cecilia Monoli
Academic Year: 2021-22

Contents

List of Figures

List of Tables

List of Symbols

Abbreviation	Description
IMU	Inertial Measurement Unit
MOCAP	Optoelectronic motion capture systems
TT	TinyTag
ROM	Range of Motion
RMSE	Root Mean Squared Error
ICC	Intraclass Correlation Coefficient
S	Squat
FLS	Frontal Leg Swing
KTC	Knee To Chest
HTH	Heel To Hamstring
SD	Standard Deviation

Abstract

Nowadays Inertial Measurement Unit (IMU) based systems are an alternative to the passive marker-based MOtion CAPture (MOCAP) procedure for clinical movement analysis. Although IMU-based motion capture is minimally invasive, faster, cheaper, and more versatile than MOCAP, a straightforward and immediate visualization of the data recorded via customized IMUs remains challenging.
The first phase of the thesis aims to develop an algorithm for rapid and precise analysis and visualisation of body kinematics, using OpenSim software driven by IMUs prototypes, developed by Tallinn University of Technology, called "TinyTag". This will help to bridge the gap of visualisation lack for experimental IMUs.
The algorithm is validated by comparing kinematic estimates, of four simple exercises (squat, frontal leg swing, knee to chest and heel to hamstring) performed by two healthy young adults (Age: 24 ($\pm$0) years; Height: 176 ($\pm$4) cm; Weight: 72.5 ($\pm$7)Kg), obtained from OpenSense driven by TinyTag against the MOCAP system. An additional comparison is made with the results obtained by OpenSense (OpenSim toolkit) driven by commercial Xsens IMUs. The study demonstrated the reliability of the kinematic variables processed by OpenSense using TinyTag data by comparing them with those obtained from the MOCAP system with an RMSE below the eligibility threshold of 5° for the Squat and Knee to Chest exercises. The bias of the difference between the two techniques is less than 10° for all exercises taken into analysis. In addition, Spearman's and Intraclass correlation coefficients demonstrated a perfect monotone correlation between the obtained results. Future studies could enlarge the population acquired and focus on reducing even more the difference with the gold standard.
Furthermore, in the second phase of this work, the application of the developed algorithm in a water environment, exploiting the water-resistant feature of TinyTag sensors, is discussed. It is well known that there are benefits of physical activity in an aquatic setting, including buoyancy, hydrostatic pressure, and temperature. The use of water is indeed applied in sports and clinical fields for recovery from fatigue and treatment of chronic conditions, but no quantitative data are present for the exercises performed underwater, therefore is not possible to know whether the subject is correctly performing the exercise.

In the second phase of the study, the aim is to define the physiological range of motion (ROM) for a distinct young healthy adult population performing four simple exercises commonly used in aquatic physical therapy.
Twenty-five healthy young adult participants (Age: 22.4 ±1.7 years; Height: 176 ±7.8 cm; Weight: 70.16 ±10.4 Kg) are acquired while performing four exercises in two environments, on land and underwater. The joint angles of the subjects are computed starting from the data of experimental IMUs, processed by OpenSense. The results demonstrated that the ROM underwater is larger than the one on land in every exercise, except for the Squat. The latter show, negligible differences as the participants, due to the non-adjustable height of the water, did not perform the required exercise to their highest potential. The obtained results could be used as a baseline for comparison with pathological subjects or to follow the progress in a rehabilitation process. Future studies could incorporate the possibility of recruiting more people and using a pool whose height is adjustable.

Keywords: IMUs prototype, OpenSense, ROM assessment, human motion underwater, OpenSim using IMU

Abstract in lingua italiana

Oggi i sistemi basati su unità di misura inerziale (IMU) sono un'alternativa alla procedura di MOtion CAPture (MOCAP) basata su marcatori passivi per l'analisi clinica del movimento. Sebbene la cattura del movimento basata su IMU sia minimamente invasiva, più veloce, più economica e più versatile della MOCAP, la visualizzazione immediata e diretta dei dati registrati tramite IMU personalizzate rimane una sfida. La prima fase della tesi mira a sviluppare un algoritmo per l'analisi e la visualizzazione rapida e precisa della cinematica corporea, utilizzando il software OpenSim guidato da prototipi di IMU, sviluppati dalla Tallinn University of Technology, chiamati "TinyTag". Questo aiuterà a colmare la mancanza di visualizzazione per le IMU sperimentali.
L'algoritmo è stato validato confrontando le stime cinematiche di quattro semplici esercizi (squat, frontal leg swing, knee to chest and heel to hamstring) eseguiti da due giovani adulti sani (età: 24 (±0) anni; altezza: 176 (±4) cm; peso: 72,5 (±7)Kg), ottenute da OpenSense guidato dai dati dei TinyTag, con il sistema MOCAP. Un ulteriore confronto viene fatto con i risultati ottenuti da OpenSense (OpenSim toolkit) pilotato da IMU commerciali Xsens. Lo studio ha dimostrato l'affidabilità delle variabili cinematiche elaborate da OpenSense utilizzando i dati TinyTag, confrontandole con quelle ottenute dal sistema MOCAP con un RMSE inferiore alla soglia di ammissibilità di 5° per gli esercizi Squat e Knee to Chest. Il bias della differenza tra le due tecniche è inferiore a 10° per tutti gli esercizi presi in analisi. Inoltre, i coefficienti di correlazione di Spearman e Intraclasse hanno dimostrato una perfetta correlazione monotona tra i risultati ottenuti. Studi futuri potrebbero ampliare la popolazione acquisita e concentrarsi sulla riduzione della differenza con il gold standard.
Nella seconda fase, viene discussa l'applicazione dell'algoritmo sviluppato in un ambiente acquatico, sfruttando la caratteristica di resistenza all'acqua dei sensori TinyTag. È noto che l'attività fisica in un ambiente acquatico presenta dei vantaggi, tra cui: il galleggiamento, la pressione idrostatica e la temperatura. L'uso dell'acqua è infatti comune in ambito sportivo e clinico per il recupero dalla fatica e il trattamento di patologie croniche, ma non sono presenti dati quantitativi per gli esercizi eseguiti sott'acqua, quindi non è possibile sapere se il soggetto sta eseguendo correttamente l'esercizio. Nella seconda fase

dello studio, l'obiettivo è quello di definire il range fisiologico di movimento (ROM) per una popolazione distinta di giovani adulti sani che eseguono quattro semplici esercizi comunemente utilizzati nella terapia fisica acquatica.
Venticinque partecipanti giovani adulti sani (età: 22.4 ±1.7 anni; altezza: 176 ±7.8 cm; peso: 70.16 ±10.4 Kg) sono stati ripresi mentre eseguivano quattro esercizi in due ambienti, a terra e sott'acqua. Gli angoli articolari dei soggetti sono calcolati a partire dai dati delle IMU sperimentali ed elaborati da OpenSense. I risultati hanno dimostrato che il ROM sott'acqua è maggiore di quello a terra in ogni esercizio, tranne che per lo Squat. Quest'ultimo presenta differenze trascurabili in quanto i partecipanti, a causa dell'altezza non regolabile dell'acqua, non hanno eseguito l'esercizio richiesto al massimo delle loro potenzialità. I risultati ottenuti potrebbero essere utilizzati come baseline per il confronto con soggetti patologici o per seguire i progressi di un processo di riabilitazione. Studi futuri potrebbero prevedere la possibilità di reclutare un maggior numero di persone e di utilizzare una piscina ad altezza regolabile.

Parole chiave: IMUs prototipi, OpenSense, valutazione ROM, movimento umano in acqua

1 | Introduction

1.1. General framework

The general scope of this master's thesis is the analysis of human motion in the water environment aided by wearable devices and virtual modeling. The first pillar of this thesis is the kinematic motion analysis, whose purpose is to describe the characteristics of the movement, such as position, speed, and acceleration, without taking into account the masses and forces that cause it [5], subjects of interest of dynamic motion analysis. In recent years, studies on this topic have been widely increasing, given the important information that can be gained for both the clinical and sports field, but also for everyday life [6].

For this purpose, the technologies related to the measurements of motor parameters are becoming widely used and, among these, the accuracy of Inertial Measurement Units (IMUs) stands out. Integrating the information from the gyroscope, magnetometer and accelerometer was seen to produce accurate results in terms of kinematic outcomes, such as the joint angles. The second pillar of this work is the creation of an algorithm that allows, through the use of computer software and virtual modeling of the human body, rapid and precise analysis of body kinematics from data collected by waterproof inertial sensors. The results of this analysis will also be valuable for personnel not specialized in the field of computer science, such as coaches and athletic trainers, or even clinicians.

The third pillar is the water environment, this algorithm is used to define a benchmark physiological range of motion (ROM) for lower limbs' joints during simple exercises. A population of 15 healthy subjects is evaluated in the aquatic setting, which offers a beneficial place for physical activities. Water activities may have a clinical purpose, as rehabilitation, or sporting nature, as functional training for performance enhancement [7].

The following subsections set out and define the three pillars presented above.

1.1.1. Kinematic analysis

The study of human movement has a very long history and a wide range of possible fields of application. The first field is undoubtedly the clinical one, where the measurement of the movement's parameters is useful in the choice and design of the surgical intervention, or in evaluating pathological data with respect to the physiological ones [6]. Additionally, kinematics analysis can play a very important role in the rehabilitation pathway; both in its design and customization phases, but also in the monitoring of results after a treatment period. [8]
The second domain is sport and sports medicine, where the possibility of quantitatively measuring the movement has opened the way to new horizons in the study of athletic performances and tailored training protocols aimed at their improvement. Concerning sports medicine, motion analysis can be used to understand the origins of an injury and, consequently, design specific exercises to prevent it.
There are various techniques and tools to perform movement analysis, some of which will be better described in Section 2.1.1. When considering these technologies it is important to remember that each one has its advantages and disadvantages and that no tool is better than any other in an absolute sense, but the context and investigation purpose have a crucial role in choosing what to use [9]. The most commonly used, considered the *gold standard* reference technology for motion analysis is the Optoelectronic MOtion CAPture system (MOCAP) (detailed in a specific paragraph of Section 2.1.1), able to ensure accurate three-dimensional measurements of kinematics parameters through infrared cameras and light-reflecting markers. Nonetheless, with the establishment of new technologies, its limitations are becoming more evident. For instance, the fact that it cannot be used outside of a controlled environment limits its applicability in sports science and sports biomechanics. The best option to overcome this restriction is the IMUs system, which exploits wearable sensors, easily applicable in the motion analysis laboratory set, but also outside, like in a sports court, on a race track, or inside a pool.
In most cases, however, when one problematic aspect is addressed compared to old technology, another is created, which is why the IMUs are still far from being considered the gold standard. It should be taken into account that IMUs acquire motor information very easily and fast, but the same cannot be said for the visualization and processing of the data.

1.1.2. OpenSim modelling

Regarding the way to visualize the inverse kinematic analysis results, the MOCAP requires powerful software able to reconstruct the body kinematics and evaluate the joint displacements, this is typically licensed and expensive to purchase. In the same way, with the advancement of the use of IMUs devices, it arose the need for direct visualization of the results, in a manner that it would be feasible to withdraw conclusions also for people who are not specialized in data processing and interpretation of raw inertial data or graphs, such as general practitioners, coaches of professional athletes but also by the analyzed subjects themselves. For this reason, the University of Stanford in the early 2000s worked on the development of an open-source modeling software called OpenSim (graphic interface shown in Figure 1.1), able to create fast and accurate simulations of movements [1]. The tool is normally driven by data from marker-based MOCAP already in the *.trc* format storing the 3D position of every marker. This information is used on a body model to move it accordingly to the motion captured and to analyze the kinematics of the subject. So, the two greatest potentialities of this software are, to have an easy visualization of the motor gesture performed and at the same time the possibility of depicting inverse kinematics parameters such as joint angles in all three dimensions or even their sum in time. Another feature of this software is enabling the comparison of different rehabilitation processes by evaluating, for example, how the length of the muscle fibers of interest changes [10]. Even though the OpenSim tool can analyze how the muscular fibers change their length during the exercises, studying the muscular activity and synchrony through OpenSim, electromyographic (EMG) data are still necessary.
Furthermore, OpenSim is an open-source platform in which users are encouraged to modify models and codes to suit their applications and share their contributions to the community.
The major restriction of using this method is the need to have an accessible human motion capture system, based on the concept of retro-reflexive markers with all the above-mentioned limitations related to it: being time-consuming, the possibility of making only circumscribed movements within the calibration volume where the infrared cameras are pointing, and above all the impossibility of making acquisitions outside a highly-controlled environment. For these reasons, the advancements in the field of biomechanical modeling have led to the design of an OpenSim toolkit called *"OpenSense"* that allows the possibility of obtaining a virtual twin of the subject from the data provided by wearable sensors and thus exploiting all their advantages explained before.

The tutorial on OpenSim's official website [11] describes step-by-step how to use the software with the data recorded by IMUs already on the market from a well-known company,

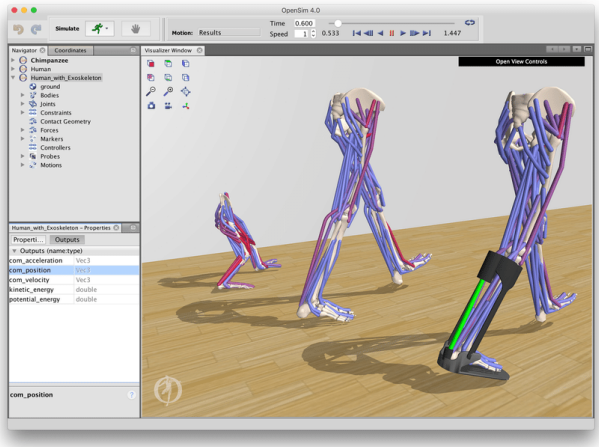

Figure 1.1: Graphic interface of OpenSim software. Simulate different muscle lengths and the use of an ankle-foot orthosis [1]

.

Xsens, but leaves as a future application the possibility of using the software with other customized sensors.

1.1.3. Aquatic environment

The circumstance that this study aims to investigate is the aquatic setting since it represents a welcoming environment for physical activity, thanks to the physical properties of water, well known to the scientific community.
The first of them is buoyancy. Archimedes's principle states that a body immersed in a fluid is subjected to two forces: gravitation, related to the body weight and buoyancy, linked to the volume of fluid moved. This property causes flotation, that on the human body results in the reduction of the loads on the joints. It is estimated that a person immersed in the navel reduces by 50% their weight implying a lessening of the strength applied on joints, better cartilaginous irrigation and better postural control. To have a schematic representation of this concept in Figure 1.2 the forces acting on a subject on the earth are illustrated, the red arrow is the body weight acting toward the center of the earth and in an equal and opposite manner the muscle force, in green, acts to support the subject. On the right, the same concept is detailed but in water circumstances: muscle force is joined by buoyancy, the resultant of which, in yellow, allows the body to remain on the surface of the water.

Another beneficial property of water is the hydrostatic pressure which, according to Pascal's law, is uniformly and orthogonally distributed to the surface of the body. The hydrostatic pressure and water's higher density with respect to the air cause stronger

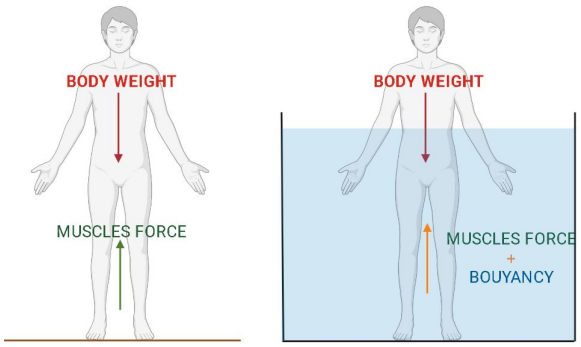

Figure 1.2: Schematic representation of how the buoyancy force helps the subject to support his body weight in water (on the right) with respect to the land (on the left)

resistance to the movement, generating higher training intensity and stimulating proprioceptivity. This last effect is ensured by the fact that each performed action moves a certain amount of water, therefore the subject is more self-conscious of their motion. The higher resistance also improves equilibrium, performances of respiratory and cardiovascular systems, muscle tone and flexibility. The third welcoming property of water is the temperature (usually around 30°C in rehabilitation pools), which can reduce muscle spasticity, increase blood pressure, decrease heart rate and improve tissue perfusion by vessel dilatation [7].
Water's properties find application in several fields. Considering athletes, for example, active water exercises allow strengthening and improvement of the overall physical performances but also enable fast recovery from fatigue [12]. Differently, in the clinical field, the water environment is exploited both during the rehabilitation protocol to recover from injuries and in the treatment of various chronic conditions such as neurological diseases, asthma, spinal cord injury, hemophilia, or stroke survivors [13]. These benefits are related also to psychological reasons: performing exercises in a fun, relaxing and safe environment allows the patient to do them correctly in a more comfortable situation.
Unfortunately the quantitative assessment of underwater motion is limited due to a small number of techniques able to work effectively underwater. For example, the gold standard method, MOCAP, can't work properly due to the effect of water on the infrared electromagnetic waves used by the cameras.

1.2. Brief description of the work

As previously mentioned, the main shortcoming of customized IMUs for motion analysis is the absence of a straightforward user interface to enable processing visualization, analysis and interpretation of the motor data collected [14].

This thesis attempts at solving this drawback by exploiting OpenSense software to process and visualize motor data from customized IMUs collected on land and in water. The IMU sensors used in this project are prototypes, called *Tinytag* entirely developed by the Environmental Sensing and Intelligence laboratory of Tallinn University of Technology (TalTech, Estonia) [1], created specifically to be water resistant. The project is organized into two distinct phases.

Phase 1: Validation of experimental IMU in OpenSense
The open-source OpenSim toolkit OpenSense has already proven to be useful in the representation of kinematic data graphs and for human motor simulations using the measurements obtained from the commercially-available IMU sensors of the company Xsens. Until now, OpenSense's estimates have never been tested with customized sensors. Hence, the first milestone is the establishment of a procedure allowing OpenSense to be driven by the customized IMUs developed at TalTech. Afterward, the kinematic estimates obtained through OpenSense driven by TinyTag are validated by comparison against established tools. A three-way performance comparison is therefore required between the kinematic analysis of simple motor tasks and the evaluation of joints angles, juxtaposing: (1) OpenSense's estimates driven by TinyTag, (2) OpenSense's calculations driven by Xsens wearables and (3) the MOCAP as the gold standard of motion capture. This first phase is summarized in a block diagram shown in Figure 1.3.

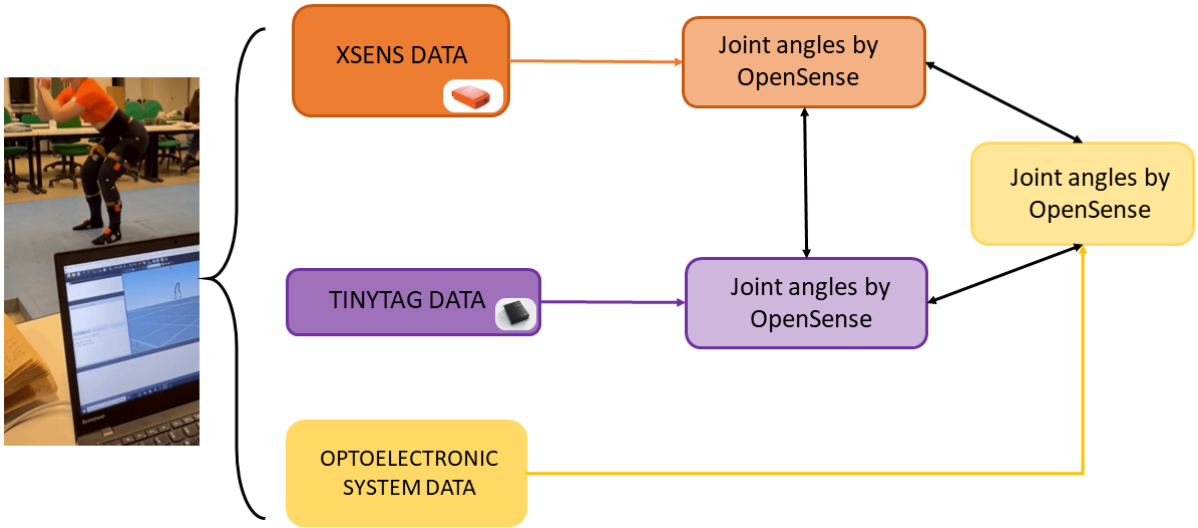

Figure 1.3: Block diagram Phase 1: Validation of experimental IMU in OpenSense. After the data were acquired simultaneously, the IMUs' data, commercial and experimental, were processed through OpenSense while the MOCAP's data were processed through its own software. Subsequently, the kinematic results were compared.

[1] https://taltech.ee/en/environmental-sensing-and-intelligence-group

Phase 2: Creation of a benchmark physiological range on land and in water
A practical application of the developed method is conducted by evaluating joint angles on land and in water, exploiting the TinyTag's main characteristic of being waterproof. Therefore the second milestone of this work demonstrates the reliability of the estimate made through OpenSense in a non-conventional framework. This experimental part of the project involved 15 age and gender-matched healthy subjects, who will be asked to follow a protocol involving five repetitions of four simple exercises commonly used in aquatic physical therapy sessions. The application of the wearable sensor system, inside and outside water, and the kinematic analysis by OpenSense will allow the definition of the physiological ROM of a distinct population (ages between 21-25) performing the selected exercises. This range is useful to evaluate differences occurring when performing similar exercises in water and on the ground[15]. In this way, it would be possible to provide clinicians with a simple assessment tool that will later allow a direct comparison between normal and pathological motion, or predict the effectiveness of different rehabilitation processes.
This second phase is summarized in a schematic way in Figure 1.4.

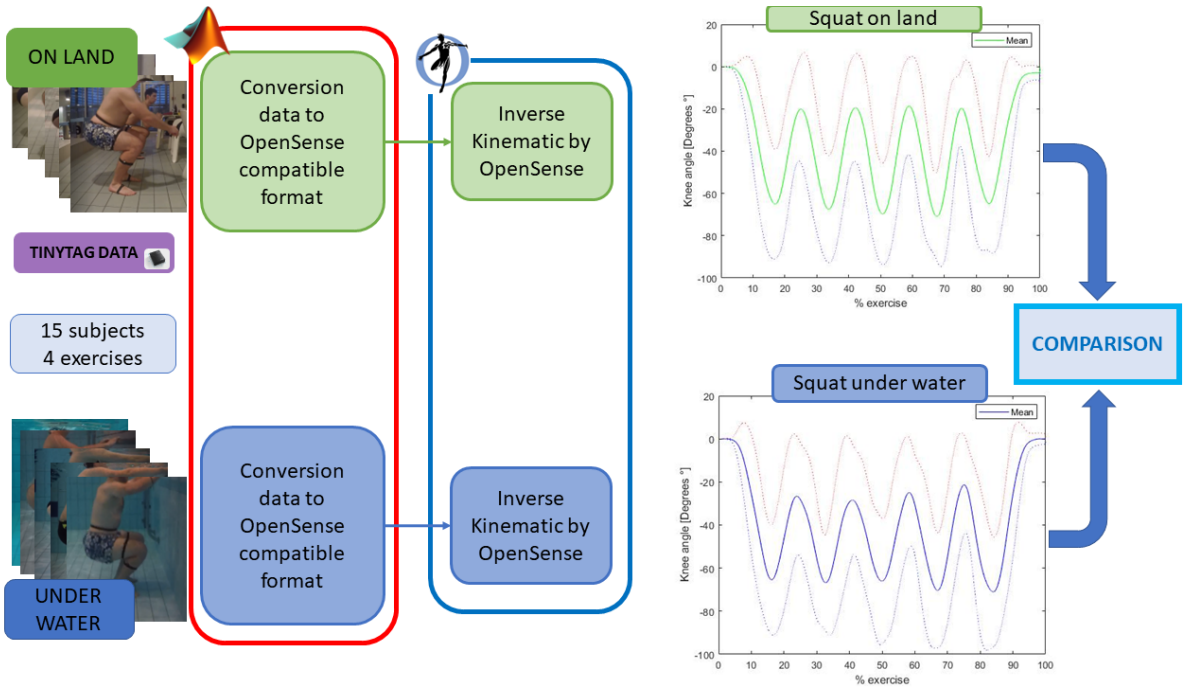

Figure 1.4: Block diagram Phase 2: Creation of a benchmark physiological range on land and in water. TinyTag data were acquired both underwater and on land, inverse kinematics were performed by OpenSense, a normality ROM was established in both environments and finally, a comparison was made to highlight differences and similarities.

1.3. Thesis structure

After the first "Introduction" Chapter, the thesis is structured as follows. In the "State of the Art" (Chapter 2) using the same subdivision of topics introduced, the conducted work will be motivated, by referring to studies already present in the scientific literature, pointing out where this research is positioned and why it is important to be carried out. Specifically, in the kinematic analysis (Section 2.1), the definition of the ROM will be explained. The first sub-section (2.1.1) will be dedicated to the systems currently available for motor assessment, also listing their relative advantages and disadvantages. The second one exploits the need of motor rehabilitation. Instead, in the "OpenSense" Section 2.2, the workflow and the input parameters necessary to obtain a correct inverse kinematic analysis will be explained. The last Section of the "State of the Art" Chapter is dedicated to the "Aquatic environment" (2.3). Firstly, it is introduced how and why water is used in the rehabilitation field and then which methodologies have the possibility of being used in this environment. Chapter 3 "Purpose of the thesis" aims to indicate what objectives the researchers have set themselves. "Materials" (Chapter 4) will instead be devoted to describing all the instrumentation (4.1) and the data processing (4.2) of the research. The first three sub-sections are descriptions of the technologies exploited and of the management of the acquired data. In Chapter 5 "Methods" the experimental part of the study is described in detail. Starting with the preparation of the test subject with the measuring systems, the explanation of the individual exercises performed in which there is a sub-section explaining of each exercise the joint angle taken into account for experimentation and ending with the division of the two phases protocols.In Phase 1 (5.3) and Phase 2 (5.4) Sections, the objectives of the respective phases are initially taken up, while later the implementation is explained in detail, ending with the statistical indexes taken into consideration for the final discussions. In the "Results" Chapter 6, tables and graphs display the obtained outcomes. These elements are the base of the considerations that will then be investigated in detail in the "Discussion" Chapter 7 that analyses, for phase 1, exercise by exercise, how well the OpenSense software using TinyTag as input data is able to calculate kinematic variables. On the other hand, for phase two, in which the physiological ROM is assessed, the two comparisons carried out are distinguished. Lastly, two specific Sections discuss the limitations of the study, distinguishing between the ones related to the instrumentation used and those more properly related to the choices made by the researchers. Which can more easily be changed for future studies.
The last Chapter 8 draws a conclusion of the work carried out and discusses the future implication outcomes on the scientific community by obtaining free virtual biomechanical modeling using only non-invasive wearable sensors.

2 | State of the art

In this chapter, the literature on the topics addressed by this thesis is presented, keeping the same structure as the previous chapter. Starting with the human kinematic (Section 2.1), where the definition of Range Of Motion (ROM) and the importance of rehabilitation will be described in detail. Followed by the main methodologies used for acquiring human motion, detailing their strengths and weaknesses. Proceeding in Section 2.2 with the description of the modeling software implied in this thesis. And finally, the focus is set on the aquatic environment, on the positive aspects of carrying out rehabilitation in a denser fluid than air (Section 2.3.1) and the technologies used to date for functional assessment in water (Section 2.3.2).

2.1. Kinematic analysis

The kinematic analysis aims to describe the motion of a body, its position, velocity and acceleration without reference to the forces causing it [5, 16].
The information on the human body's displacements is usually computed by referring to the anatomical landmarks, such as bone centers of mass or joint centers of rotation [17]. For what concern human motion analysis, the human body is represented, according to a musculoskeletal model, as a chain of rigid bodies, each of them describing a body segment. Depending on the investigation purpose and the chosen degree of precision, the number of considered segments may vary. If interested in the motion of the arm during a certain movement there is no need to consider the entire body [18]. Differently, if the study is focused on the kinematics of the whole body, the model must consider all the segments [19]. The choice of the model needs to be cautious since every added segment raises the possible value of the model and its precision concerning the real-world behavior, but also the complexity of the problem. The ROM is used as a key parameter to assess the functionality of body segments [20] since the values can be used to evaluate the motion ability. The ROM is defined as the possible movement around a specific joint or body part. Numerous articles in the literature kept their focus on defining a range of normality and have established values within which a human movement is considered physiological

for a certain population, defined by age, gender, muscle mass and anatomical differences [21, 22]. Nonetheless, when dealing with human assessments, it is important to be aware of the inter- and intra-subject variability, which respectively are the fluctuations of the parameters occurring between different subjects and among two different trials of the same subject [23].
Being able to quantify the movement range of a joint allows clinicians to verify the patient's health status. For example, if the subject is able to move a certain joint correctly and perform the complete movement, then it means that the rehabilitation process followed or the treatment employed has achieved the desired results. Furthermore, continuous objective follow-up on the improvements of joint angles allows the clinician to acknowledge the recovery process and, if needed, adjust the rehabilitation method session after session. The ROM is usually measured with a manual (shown in Figure 2.1) or an electrical goniometer or inclinometer placed on the body segments of interest. Nonetheless, these

Figure 2.1: An operator using a manual goniometer to evaluate a joint angle

tools are used by a clinician manipulating the goniometer and guiding the performance of the movement, called, in this case, *passive*. The values obtained through these protocols have limited importance since it is not guaranteed that the patient is able to make such movements thanks to their motor skills, but are conveyed acts and therefore subjected to a bias. On the other hand, when the subject is left free to move, the so-called *active* movement would be achieved, thus measuring the actual residual motor capacities.
This measurement bias is addressed by assessing ROM during active motion and in a real-world context, exploiting the other methods to evaluate the human motion (Section 2.1.1).

2.1.1. Measurement techniques

Objective measurement of motion has become of paramount importance since it can assist the clinician in making therapy decisions, usually based only on their experience.
The data provided by these measurements allow the clinician and the subjects, to notice a quantitative improvement in their motor skills, which demonstrates the progress of the performance and can help in better planning the rest of the therapy [24]. For this purpose, there are many methods and tools to capture and quantify human motion commonly employed in both the clinical and sports field. The choice and preference depend highly on the task performed and on the study purpose since each method has advantages and disadvantages.
In the following list are reported the most common technologies, with pros and cons, that deal with the study of body kinematics, such as the trajectories of points, lines, and other geometric objects and their differential properties such as velocity and acceleration. For more information refer to [25].

Optical Methods These are the most common techniques for the evaluation of human kinematics. The imaging system is able to capture the complexity of human movement [17] and consists of the evaluation of images or videos to reconstruct positions and movements with respect to a reference frame in two or three dimensions. Among the optical methods, the one that is generating the highest interest is based only on cameras but the main one and most used, seen as the *gold standard* for human motion measurement is the optoelectronic system (MOCAP) [26]. This method uses an infrared multi-cameras system to estimate the movement of retro-reflective markers placed on the surface of the body in precise anatomical landmarks, according to specific protocols (Figure 2.2).

As an alternative to the use of retro-reflective markers, also called passive markers, some studies have used active ones, i.e. markers characterized by an LED light that makes them more visible to the MOCAP cameras. The results show very reliable accuracy with an average error of 2.509 mm with SD $\pm$ 1.34 mm so, but only when markers and infrared cameras form a 45° angle so a very specific situation [27]. The main problem with both this technology is the fact that the movement needs to be performed inside the range of visibility of the cameras.
In Figure 2.3 the other visual-based option is presented: the marker-less motion caption camera system [28]. This method uses a pattern of near-infrared light cameras to perceive depth which is used to reconstruct a 3D object. No special suits or body stickers need to be worn, which makes the movement freer and easier. But, it needs to be said that the accuracy of this system is still far from being equal to the one of the MOCAP.

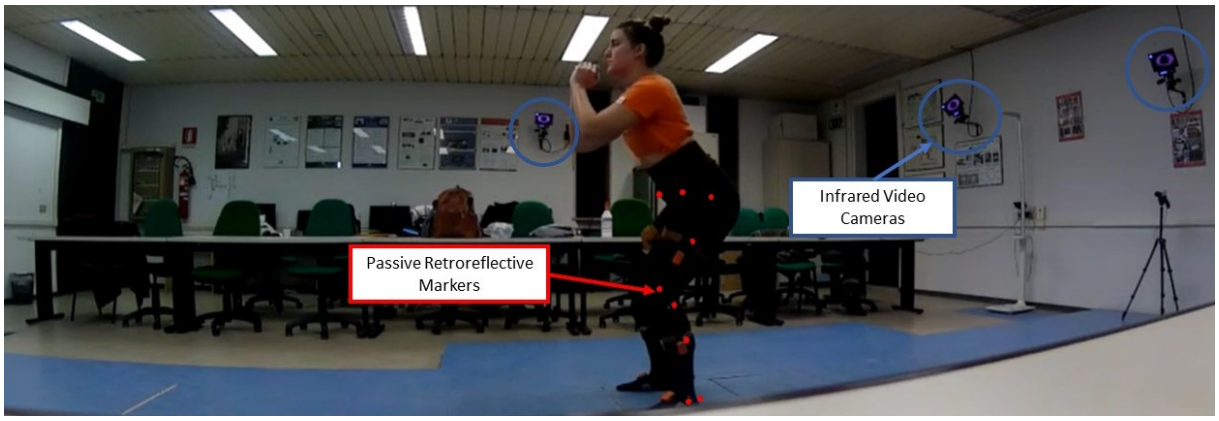

Figure 2.2: Representation of the MOCAP using external markers placed on the body surface

As far as clinical movement analysis applications are concerned, i.e. of patients who have

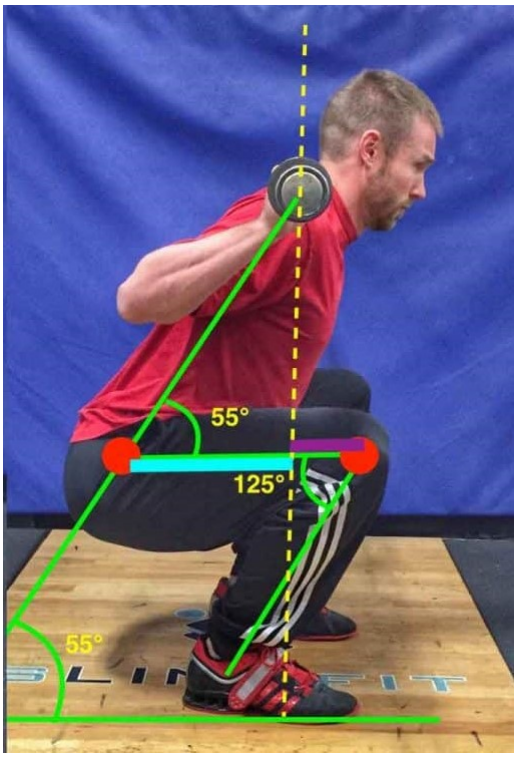

Figure 2.3: Example of markerless human motion capture [2].

motor difficulties and are confined to rehabilitation in a hospital or clinic, the MOCAP is the best and most widely used solution as it is very accurate [29–32].
On the other hand, for applications in the field of sports science, which involves the need to move in large environments, this technology shows all its limitations. In the article "Accuracy of human motion capture systems for sport applications; state-of-the-art review" [33], are distinguished and identified the most suitable measurement systems

for each of the various sports analyzed. Team sports mainly involve large measurement volumes and for these applications, accuracy is not as important as for technical clinical analysis. Therefore, if the entire volume of interest can be recorded by cameras, the markerless systems are the most suitable. To analyze small movements in sports generally requires higher accuracy, therefore can be analyzed into smaller volumes since accuracy is generally inversely proportional to the coverage of a positioning system (i.e. lower accuracy for a larger measurement volume). Smaller volumes can be covered by high-precision MOCAP. Large-volume ones that need to be measured with a high level of accuracy are currently the most critical in terms of measuring kinematics. The most suitable options are IMU (detailed system in the following paragraph), however, these measurement categories often require the development of a suitable algorithm for fusion filtering. Therefore, it can be concluded that there is a gap in the supply of measurement systems for the acquisition of large volumes with high precision [34–36].

Inertial Measurement Units (IMUs) Alternatively to the MOCAP for the study of kinematics, wearable IMU sensors are often used since they have the possibility to be used outside the controlled environment of a laboratory. This crucial aspect opens the doors to new possibilities: firstly, the acquisition can be performed everywhere with the only limit of the life of the batteries; secondly, the patient can be followed and monitored in his daily-life activities where there is no clinician and where he can move naturally, creating, therefore, more realistic data [37]. Thirdly, wearable IMU loggers are less invasive and they are usually more versatile and less expensive than MOCAP. The IMU integrated into these sensors is composed of 3 principal components:

- 3 axes Accelerometer: measure acceleration exploiting the mass-spring-damper system oriented as the axes of their internal reference system. It is usually composed of masses, dampers, elastic components, sensitive components, and adaptive circuits. In the process of acceleration, the sensor is subjected to motion by using Newton's second law, measuring the inertial force on the mass block. According to the different sensitive components of the sensor, common accelerometer sensors can be categorized as capacitive, inductive, strain gauge, piezoresistive and piezoelectric.
- 3 axes Gyroscope: is a device that can measure angular velocity and estimate the orientation of an object along the three axes of its internal reference system. Measured in degrees per second, angular velocity is the change in the rotational angle of the object per unit of time. These sensors can calculate the tilt and lateral orientation of the object whereas an accelerometer can only measure linear motion. Gyroscope sensors are also called Angular Rate Sensors or Angular Velocity Sen-

sors. These sensors are installed in applications where the orientation of the object is difficult to sense by humans.

- 3 axes Magnetometer: measure the intensity and direction of the magnetic field in which the object is located with respect to the Earth's Magnetic field. It can be used to evaluate the direction toward which the sensor is oriented.

Combining the information collected by the described sensing tools it is possible to reconstruct 3-dimensional movements. The fusion of information from accelerometer, gyroscope and magnetometer to estimate IMUs' positions and orientations continues to be one of the most challenging areas of inertial sensor research. The integration of noisy data from accelerations and velocities to orientation and position causes numerous errors including orientation drift that is often difficult to isolate from the rest of the useful information. Solutions can be often found on the market where sensors commercially available include onboard filters and fusion methods. Some of these methods incorporate a very high integration frequency to try to limit noises and errors while other ones give more importance to magnetometer data than the noisier accelerometer and gyroscope data. To perform this data fusion there are different options, the most common are:

1. *Complementary Filter* fuses the accelerometer and integrated gyro data by passing the former through a 1st-order low pass and the latter through a 1st-order high pass filter and adding the outputs [38].

2. *Kalman Filter* [39] is a set of mathematical equations that provides an efficient computational means (recursive) to estimate the state of a process, in a way that minimizes the mean of the squared error. The filter is very powerful as: it supports estimations of past, present, and even future states, and it can do it even when the precise nature of the modeled system is unknown [40].

3. *Mahony Filter* [41] and *Madwick Filter* [42] are: (1) computationally inexpensive, (2) effective at low sampling rates; e.g. 10 Hz, and (3) contain adjustable parameters defined by observable system characteristics. This last filter is the one used in this study.

The applications of these wearable devices in biomechanical motion analysis are multiple: prevention, monitoring, posture control, rehabilitation, kinematic measurement, and more[25]. One of the main features of these integrated IMU devices is that they are very small and certainly non-invasive, nor cumbersome to movement, but two aspects need to be kept in mind: the battery life needs to be suitable for the application and when tied to the body, in most cases by means of elastic bandages, the skin vibration can add

artifacts to the data collected. Of all the commercially available systems, the one built by Xsens© appears to be the most common in human motion tracking studies [3, 43–45]. These sensors have shown high accuracy and promising possibilities in replacing the MOCAP motion analysis. Thanks to the graphical interface and analysis software available upon the license, this system shows a convenient visualization for clinicians, allowing also realtime assessment, which is generally not possible with customized IMUs.
Several articles in the literature have investigated gait analysis by comparing the gold standard and the kinematic analysis performed by Xsens sensors using the software provided by the same manufacturer [3]. Although the results seem reliable, the root mean square error (RMSE) between Xsens and MOCAP data ranged from 2 to 15 degrees in the sagittal plane both for walking and jogging, and the accuracy of fine movements seems not yet to be comparable to that of the MOCAP, hence clinicians could use Xsens IMUs just to assess large abnormalities.
There are two main disadvantages of this commercial wearable sensor system. Firstly, purchasing the equipment is very expensive, considering that the suit and the sensors, including the charging Docking Station and straps for positioning start from 3.750 $[1], whereas the license that allows the graphical visualization of the motion and the kinematic analysis costs around 10.000 $ per year. Secondly, the sensors are not applicable to the aquatic environment. Although the three sensors of acceleration, gyroscope and magnetometer have also been integrated with a barometer and a thermometer, the devices do not have a waterproofing coating to make them water resistant and therefore their application to the study of aquatic motion is not possible.

For completeness following are reported other methods commonly used to acquire the kinematics of objects in motion.

Electrogonionmeter : an electro-mechanical instrument that measures angles of joint movements.

Magnetic systems : ferromagnetic devices placed on the subject, that distort the magnetic field. The distortion points are used to obtain information about the subject's motion.

Acoustic tracking systems : ultrasonic pulse is used to find the location of the body but is highly affected by noise and disturbance.

[1] https://buy.movella.com/mtw-awinda-research-bundle-mtw2-dk-6

It is also worth mentioning the main methods exploitable for the study of the dynamic components of motion, these tools are often used in combination with the ones previously described. To understand the forces and moments that put objects or bodies into motion.

- Force plates: metal plates with load cells at each corner, to measure the magnitude and direction of the forces applied.
- Gait or pressure mat: arrangement of sensors to study the foot contact and the forces exchanged between floor and body.
- Force shoes: soles to sense the distribution of foot pressure.
- Electromyography: the electric signal produced by muscles during contraction is evaluated through surface or intramuscular sensors to monitor their activity.

2.1.2. Rehabilitation

Rehabilitation is a specialized medical field that combines medical therapy and non-pharmacologic interventions with the goals of maximizing function and independence and ameliorating symptoms [46]. Rehabilitation interventions use different methods and are designed to help individuals with the management of their disease. The design of rehabilitation programs is based on the disease state, its severity, the use and type of medications, and on social, psychological, and environmental factors.

ROM is one of the most valid parameters to assess the abnormal status and design the rehabilitation program. Motion therapy aims to restore normal muscular structure and coordinated movements of one or more limbs and, consequently, throughout the body. It is usually performed initially passively and then actively. Nowadays, efforts are being made to integrate Augmented and Virtual Reality into rehabilitation and telerehabilitation to make it more interactive for the patient, but so far there is no relevant scientific evidence that it could replace traditional one but only as an added application. [47]

2.2. OpenSense

In Section 1.1.2 the software OpenSim is presented, but here is presented the toolkit that exploits the features of the software using IMU data instead of data from a MOCAP system. This workflow integrated into OpenSim, called OpenSense [48], allows most of the features and manipulation tools previously described: being an easy-to-use and open-source software for modeling, simulating, controlling, and analyzing the neuromusculoskeletal system. In the next two pages (Table 2.1 and 2.2) are reported the most

relevant papers published about OpenSense.

Source	Aim	Sample size	Systems other than IMUs	Sensor specification	Exercise	Results
Colella et al. [49] 2021	Design of a Battery Assisted Passive Radio-Frequency IDentification (RFID) tag integrated with IMUs	1	IMU integrated with RFIDg	2 torso-pelvis Prototypes Lab	-	The whole system correctly recognizes and reproduces the performed movements.
Slade et al. [50] 2021	Estimation of metabolic energy expenditure in real-time during common activities	24	Smartwatch	2 one leg Prototypes Lab	Walking, running, climbing stairs and biking	Wearable System has a cumulative error of 13% across common activities, significantly less than 42% for a smartwatch and 44% for an activity-specific smartwatch.
Bailey et al. [51] 2021	Validity and sensitivity of an InCap biomechanical model of joint angle variability for gait.	14	Vicon camera MOCAP, force plates	7 lower limbs Xsens Optoelectronic lab	Treadmill gait	RMSD among individual joints (1.7–7.5°). IMU-based joints angle time series were acceptably accurate in most of the joints' movements.
Xuan Teo et al. [52] 2021	Quantify the muscle activities and assess the ergonomics risks during FFB harvesting and LF collection	6	EMG surface electrodes	6 upper limbs and trunk APDM Oil palm plantation	Primary motions during FFB harvesting and LF collection	Concurs with previous qualitative studies for both FFB harvesting and LF collection, confirming the high prevalence of MSD on various parts of the body among harvesters and collectors, mostly lower back.

Table 2.1: This table summarizes information for each OpenSense (year 2021) article. Especially on the aim, the sensor used and the kinematic results obtained. The symbol - means "not specified"

Since the OpenSense tool is relatively new, the studies are very recent, five out of nine used a MOCAP as a reference for comparison and gait is the exercise that has been studied the most. Overall, the results achieved are satisfactory, the tool presents the ability to detect clinically meaningful differences between joint angles[56] and the time series were acceptably accurate in most of the joint movements [51]. However, the restricted number

Source	Aim	Sample size	Systems other than IMUs	Sensor specification	Exercise	Results
Nagaraj et al. [53] 2021	Full-body inverse kinematics and deep learning to estimate physiologically feasible joint angles in real time	-	None	17 full body Xsens Lab	usual tasks	The approach has shown promising results.
Di Raimondo et al [54] 2022	Muskolo skeletal + InCap system validation wrt MOCAP	11	Vicon 3D motion capture	7 lower limbs Xsens Optoelectronic lab	Walking, running, and stair ascent and descent trial	The integrated method reduced the RSME for both the hip and the knee joints below 5°, and no statistically significant differences were found between MoCap and InCap kinematics.
Bian et al. [55] 2022	Integrating a musculoskeletal (MSK) model and artificial neural network	6	Vicon camera MOCAP	7 pelvis, thighs, shanks, and feet Delsys Trigno Avanti Optoelectronic lab	Stand-to-sit-to-stand and walking	MSK-model-based hybrid methods perform better for joint angle estimation. The RMSE between the IMU-based joint angle and marker-based was 7.26°.
Hafer et al. [56] 2022	Sagittal kinematics difference between MoCap and InCap	27	Vicon camera MOCAP, force plates	4 sacrum+ 1 leg APDM Optoelectronic lab	Gait	The tools similarly detected clinically meaningful differences in gait.
Al Borno et al. [48] 2022	Development of an open-source workflow to estimate lower extremity joint kinematics from IMU data	11	MOCAP	8 upper+lower back, legs Xsens Optoelectronic lab	Walking and lower-extremity movements	RMS differences between 3 and 6 degrees. correlation coefficients were moderate to strong (r=0.60–0.87).

Table 2.2: This table summarizes information for each OpenSense (years 2021-2022) article. Especially on the aim, the sensor used and the kinematic results obtained. The symbol - means "not specified"

of physical activities acquired creates a gap in understanding which are the limits of this tool in terms of accuracy in more complex exercises. In only two studies non-commercial

IMUs were used to acquire the motion. More studies need to be done to make the OpenSense workflow more flexible and not chained to commercial sensors. Moreover, all the studies are performed on land in controlled contexts, and no one has studied motion underwater. The functioning of this tool will be discussed in more detail below in Section 4.2.

2.3. Aquatic environment

2.3.1. Rehabilitation in water

The water environment presents unique physical characteristics (mentioned in Section 1.1.3) that modern rehabilitation programs try to exploit to enhance the results without exposing the patients to risks [57]. Water therapy is commonly used in sports medicine for different purposes like endurance training, to improve muscular strength, to promote after-training relaxation and avoiding injuries. Water exercise is also recommended in the rehabilitation field to recover after injury or surgery [58], but also in case of chronic diseases like Parkinson [7], sclerosis [59], heart diseases [60], fibromyalgia [61], osteoarthritis [62], dystrophy [63] hemophilia [64], pulmonary diseases [65] and asthma [66]. In addition, water can help to improve balance disorders [67], pain-related pathologies [68] and even obesity [69]. This wide range of possibilities is given by the fact that it is possible to design an exercise plan according to patients' needs thanks to the simplicity of controlling the body in the water environment. Of course, there are some cases in which water rehabilitation should be avoided, such as severe cardiovascular and cardiopulmonary diseases, chlorine allergy, diabetes, contagious diseases and infections.
Since this study will be focused on the lower limbs, there are specific exercises that are common in water rehabilitation, such as vigorous forward and side-way walking through water reaching the chest with the knees, lower limb cycling exercises with hands-on handrails, climbing up the pool wall with knees and hips flexed, pulling the knees towards the chest, squat, hip abductions, knee and hip flexion-extension exercises and other variations of these exercises [70].

2.3.2. Evaluation of underwater motion

As previously mentioned in Section 1.1.3, is well established that water provides benefits to the body due to the unique characteristics of the fluid. As pointed out in a recent systematic review on underwater motion analysis, it is important to find a way to make measurements in this environment[71], because otherwise, the only way to assess progresses in rehabilitation programs is through questionnaires or the experience of clinicians. In particular, this method is qualitative and even scarcely practical due to the distortion of what the clinician can see underwater from the outside. This distortion is caused by the refraction of light and the movement of water during the exercise.
Nevertheless, the quantification of motion underwater is challenging because of compatibility issues between the water environment and the instrumentation regularly used to

assess motion, especially for the MOCAP, the gold standard. The main problem with this technology, in the aquatic environment, is related to the difficulty for the cameras to track the movement of the markers during motion [9], the presence of water interferes with the transmission and reception of electromagnetic waves between cameras and markers due to the refraction of the different mediums. In addition, the presence of multiple cables, used for the cameras, nearby the pool makes the environment more dangerous. Despite the difficulties that the water environment generates, some studies were conducted on this topic, using other methods.

In most cases, when talking about studies on water rehabilitation, qualitative methods, such as tests and questionnaires were exploited, usually combined with quantitative methods [9]. The common quantitative techniques are electromyography[72], dynamometers, force plates [73], goniometer [74] and methods based on metabolic assessments. However, the main method to overcome the constraints represented by water is the use of wearable inertial systems [9]. The possibility of using this instrumentation outside the control volume of the laboratory allows for broadening the scope of IMUs also in water, once waterproofing is provided. Besides that, technological development also allowed for reducing the size of IMU sensors, which could be a great advantage for their use in a water environment, so that they don't interfere with the freedom of movement without adding weight to drag [75].

3 | Purpose of the thesis

The review of the existing literature on underwater motion analysis and OpenSense software pointed out that the scientific community might benefit from a quick and effective interface and software for visualizing and manipulating data from experimental IMUs on humans. This thesis will attempt at bridging the gap between the valuable characteristics of the IMUs developed by the Tallinn University of Technology (TalTech) and their limited data interpretability. Therefore the main aim of this work is by developing and validating an algorithm, that exploits a virtual model generated by the OpenSim software, using human motion data acquired from IMUs built by TalTech. To validate the reliability and efficacy of the algorithm, two experimental phases are foreseen:

- Phase 1 concerns the validation of the OpenSense model and the developed method driven by TinyTag comparing its performance in evaluating joint angles of lower limbs against the gold standard MOCAP.
- Once this model has been validated, in Phase 2, the main characteristic of these sensors, namely being water-resistant, can be exploited to perform measurements in environments other than those commonly used in motion analysis. To test their reliability, the sensors will be used to perform acquisitions on healthy subjects both in and out of the water, in order to decree a physiological joint angle excursion range of normality for four simple exercises typically used in hydrotherapy.

4 | Materials

4.1. Motion tracking systems

This Section describes in detail the motion analysis systems used in this research.

4.1.1. Optoelectronic System

As a ground-truth reference, the optoelectronic SmartDX 400 system (BTS Bioengineering company, Italy) was used. The experimental tests were conducted in the "Luigi Divieti" Posture and Movement Analysis Laboratory located at the Department of Electronics, Information and Bioengineering of Politecnico di Milano, Italy[1]. As already explained in Chapter 2.1.1, this system is based on the use of infrared cameras capable of tracking the trajectory of retro-reflective markers in a calibrated area. The laboratory has eight

Figure 4.1: 'Luigi Divieti' Posture and Movement Analysis Laboratory and SmartTracker software interface

infrared cameras at 100 Hz pointing at a fairly large controlled volume of a walkway usually used for gait analysis, which also contains two force platforms, which were not used in this study.
Passive markers (plastic spheres covered in reflective material) are placed on the subject

[1] https://www.movlab.polimi.it/en/the-lab/strumentazione/

on anatomical reference points, following the guidelines of a specific protocol, as presented by Davis [76].
The infrared cameras identify and track the markers during the performed tasks allowing the 3D reconstruction by superimposing the information about the positions of the markers given by the preferred protocol. The measurements obtained are very accurate and reliable.
Afterward using specific software, SMART Tracker, it's possible to build a scheme of the body investigated, to estimate different parameters, such as velocity, acceleration, forces, internal joint angles and other kinematic parameters. An example of a reconstructed body by the software is shown in Figure 4.1.
As mentioned, since the retro-reflective markers are positioned on precise locations of the body surface, making the method non-invasive, the software is also able to evaluate the exact center of rotation of the joints using the anthropometric characteristics of the subject as input. Thanks to its accuracy, the MOCAP is considered the perfect way to investigate human motion. On the other hand, this cumbersome system cannot be used outside the laboratory, since the cameras and the equipment are very difficult to move and the data acquired can be susceptible to interferences and environmental settings.

4.1.2. Xsens

The commercial MTw Awinda IMUs used for the validation phase are shown in Figure 4.2, they are provided by the Xsens company, an industry leader in the designing, manufacturing and marketing of wearable devices capable of making real-time biomechanical measurements. The technical datasheet of the devices is reported below in Table 4.1[2].
The output data of these IMUs are characterized by being already strongly filtered to obtain a smooth signal for visualization's sake, but that may cause the loss of some information about the actual recorded data values.

Figure 4.2: Xsens device and the USB-pen drive license

Together with the inertial sensors, it's possible to purchase the license for the Xsens

[2]https://www.movella.com/products/wearables/xsens-mtw-awinda

Tracker Placement	Velcro straps
Latency	30 ms
Dimensions	47 × 30 × 13 mm
Weight	16 g
Operating temperature range	0 °C to 50 °C
Working frequency	100 Hz
Dynamic accuracy (roll/pitch)	0.75 deg RMS
Static accuracy (roll/pitch)	0.5 deg RMS
Full scale	± 2000 deg/s | ± 160 m/s2 | ± 1.9 Gauss

Table 4.1: Technical Data-sheet MTw Awinda Xsens devices

software (MVN), whose interface is shown in Figure 4.3 capable of providing information about the kinematics of the body parts, estimating essential data such as the joints' angles, the center of mass position, acceleration, and others, similarly to the MOCAP.

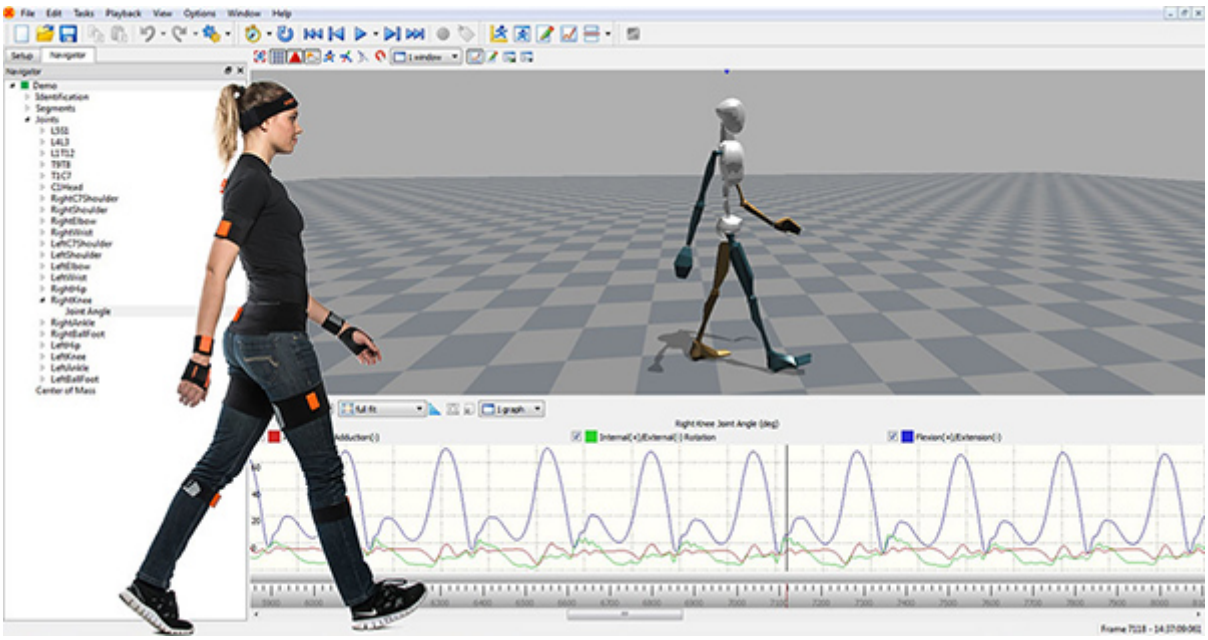

Figure 4.3: Example of Xsens MVN software interface [3]

4.1.3. TinyTag

The IMU sensors *TinyTag* were designed and manufactured by the Environmental Sensing and Intelligence Group of Tallinn University of Technology (Tallinn, Estonia). Each sensor includes a 9-axis, BMX160 IMU sensor (on the left of Figure 4.4), developed by Bosch (Germany) [77], an on-board microSD to store the recorded data, a temperature sensor, a time clock, a magnetic switch and a battery. The IMU, sampling at 100 Hz, provides precise acceleration (m/s^2), angular rate (°/s) and geomagnetic measurement (μT) in the

directions of its reference system. For this study, the sensitivity of the device, i.e. the smallest displacement value that the instrument can detect, was set as high as possible so that the slightest motor movement including any vibrations of the subject could be analyzed. However, this means that the output signals from the sensors are affected by a very high level of noise, which is why the data processing phase was essential to better interpret the data collected and the results obtained. In Table 4.2 the main characteristics of the BMX160 IMUs are reported.
There are two versions of the TinyTag sensors (reported on the right in Figure 4.4), one [3] a slightly bigger than the other[4], the main difference is the size as the sensing components are the same, one is 55 mm x 13 mm x 14 mm, with a weight of 9 ± 0.3 g (upper right in Figure 4.4), while the other one is 33.9 mm x 7.75 mm x 5.90 mm with a weight of 1.2 g (bottom right in Figure 4.4). Resuming both sensors are small enough to not interfere with the movements of the subjects once attached to the body. The battery consists of rechargeable Lithium-Polymer with a lifetime of 4 hours of continuous use. The smaller version has a shorter battery life and includes two LEDs that could be used to align multiple sensors or to study the motion with a camera-based system.

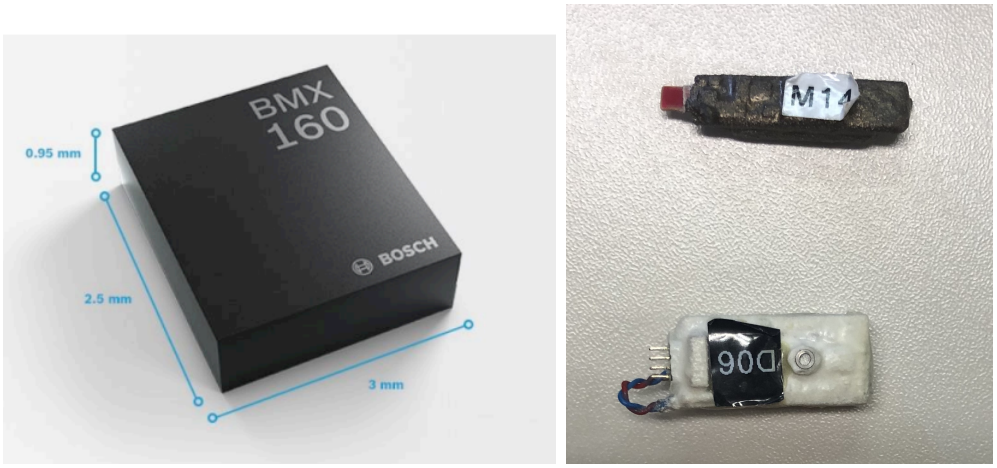

Figure 4.4: IMU BMX160 with its dimensions, on the left, and the two versions of TinyTag sensors, on the right

After the true experimental phase, the sensors can be connected to the computer using a user-friendly micro-USB connection and are detected as a USB drive. The temperature supported by the devices is in the range of -40 °C to 85 °C (-40 °F to 185 °F), but for measurements in water, it is advisable to maintain a temperature around 20°C. In addition, the sensors have integrated temperature and pressure detectors. The sensors are turned on and off using a magnet and have a blue light-emitting diode (LED) that

[3]https://biorobotics.pages.taltech.ee/backpack/en/specifications/
[4]https://biorobotics.pages.taltech.ee/microtag/en/specifications/

Dimensions	2.5 x 3.0 mm^2
Supply voltage	1.71 - 3.6 V
Consumption	1585 μA
Acceleration and gyroscope resolution	16 bits
Acceleration range	$\pm$2 - $\pm$16 g
Acceleration resolution range	0.000061g - 0.00049 g
Gyroscope measurements range	125 - 2000 °/s
Gyroscope measurements resolution	0,06 - 0,004 °/s
Magnetic field range	$\pm$1150 - $\pm$2500 μT
Magnetic resolution	0.3 μT

Table 4.2: Technical Data-sheet IMU unit in Tinytag devices

flashes to signify that the sensors are on.

4.2. Data processing

This sub-section will explain in detail the data processing procedures required for the calculation of the joint angles. For all the systems for motion analysis used in this thesis, for both the validation and experimental phases, it will be explained how the raw data was manipulated to remove the noise and be compatible with the input format required by the OpenSense workflow. It's afterwards specified how the inverse kinematic analysis was carried out by the open-source software in order to calculate the joint angles of interest. All three systems, Xsens IMU, Tinytag IMU and the MOCAP use a sampling frequency of 100 Hz during the acquisition of the data, therefore no resampling is needed. All codes mentioned in the following paragraphs are available on the GitHub repository (Appendix: A).

- Optoelectronic measurement system (MOCAP)

After the subject has performed the movement equipped with the passive retro-reflective markers, the data recorded containing the 3D position of each marker over the whole experiment are saved in *.trc* files. For MOCAP data processing the licensed software from BTS are used. The file is imported into the SMART Tracker (Version: 1.10.469.0) software. The Davis protocol for the tracking procedure with a label associated with each marker is followed frame by frame throughout the recording to ensure that the movement is correctly recognised. This step is one of the most time-consuming when using this method for motion analysis and, if a mistake is made, it could affect the entire results and data analysis. After this step, SMART Analyzer software is used to perform inverse kinematics. An ad-hoc protocol (Appendix B) was created, that involves interpolating the traces of individual markers and filtering them with a smoothing filter using a triangular

window(the length of the window is *(2 x Filter Order chosen)+1*) so that there are no more discontinuities if markers were not visible in all frames during acquisitions and the noise fluctuations are removed. The anatomical internal center of instantaneous rotation, distinguished from the superficial one identified by the markers, was identified for each joint (ankle, knee and hip) using the anthropometric measures of the subjects analyzed. Particularly the subject leg length (LL) in mm is needed to calculate the distance between the inner center of rotation of the hip joint and the superficial one, using the formula below:

$$\begin{cases} HJCx = 11 - 0.063LL \\ HJCy = 8 + 0.086LL \\ HJCz = -9 - 0.078LL \end{cases} . \tag{4.1}$$

The Posterior- anterior direction (Hip Joint Center x), the Medial- lateral direction (Hip Joint Center y) and the Inferior- superior direction (Hip Joint Center z) are evaluated to better recognize the center of joint rotation and finally, the joint angles of interest were estimated and reported as graphs.

- Xsens

Regarding the Xsens IMUs, the company provides, along with the set of wearable sensors, a USB stick containing the license for the software (MVN Analyze) developed by the company itself. The sensors are synchronized and calibrated by the MVN software following a procedure that involves standing still and then walking for a few seconds. As this study focuses on the open-source OpenSim software's ability to perform inverse kinematics, the Xsens data of quaternion orientations[5] were saved in Excel and made compatible with the OpenSense format via MATLAB code (Appendix A) and then processed following the OpenSense tutorial. The other features, such as kinematics estimation, given by the license of the company were not used or taken into consideration.

-TinyTag

As mentioned the sensors built by TalTech University are equipped with an internal memory capable of saving the data of the accelerometer, gyroscope and magnetometer from the moment it is switched on to the moment it is switched off, without fusing the information to get the orientation. Following step by step what was done to the raw sensor data. First, a calibration of the gyroscope, accelerometer and magnetometer was performed. Each logger was placed on a flat surface and kept still for a while along the three main

[5]Unit quaternions, known as versors, provide a convenient mathematical notation for representing spatial orientations and rotations of elements in three-dimensional space. Specifically, they encode information about an axis-angle rotation about an arbitrary axis [78].

axes of the IMU reference system. When still, the accelerometer should measure only acceleration of gravity on one axes and null on the others while the gyroscope should be silent. In this way, stationary acceleration ad angular rotations biases were assessed, taken into account and removed. Finally, the magnetometer calibration reduced the error introduced by both the hard iron effects and the soft iron effects.
The synchronization was done by placing all 7 required sensors inside a metallic coil and supplying the coil with an electrical impulse so that it is recorded by TinyTag's magnetometer before every acquisition, which then allows the sensors to be synchronized during post-processing.
Then a third-order Savitzky-Golay polynomial filter was applied with a window size of 71 samples, chosen on the basis of literature research in this field [48]. This made the raw data smoother and less affected by noise.
The software OpenSense needs as input data the orientation of the sensors with quaternion format, at this point the information is still divided into the data from the three sensors. To get the quaternions starting from the data a fusion algorithm is needed. Several fusion methods were tried in this study (previously mentioned in Section 2.1.1) but the results that led to the highest reliability were those obtained using the Madgwick filter sensor fusion algorithm [42].
It was decided to split the acquired signal first into the individual performed exercises and then into the individual repetitions of these to mitigate the errors introduced by the gyroscope low-frequency bias (i.e. drift), which was reduced by resetting the fusion algorithm at every repetition. At the end of the script, tables containing all the orientations of the IMUs over time described by quaternions were saved.

- OpenSense
As explained in Chapter 2.2, this project will focus on studying the inverse kinematics calculated by the software with IMUs data as input.
The IMUs sensors are placed:

- One sensor on the pelvic area

Note: This sensor in OpenSense software is called the *basic IMU* because all the orientations of the other IMUs refer to the relative orientation of the one in the pelvic zone.

- Two on the thighs
- Two on the shanks
- Two on both feet

In this way, it's possible to perform the inverse kinematics on the model built by OpenSense as shown in Figure 4.5.

For both Xsens and TinyTag sensor data, manipulations were made to make them com-

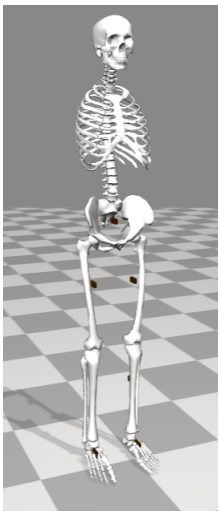

Figure 4.5: IMU sensors showed on OpenSense software as orange boxes

patible with the APDM format readable from the tutorial code of the OpenSense workflow provided by the software developers. The data of each trial and exercise recorded were converted into tables containing the sampling frequency expressed in Hz, the temporal instants, and for each body district sensor used, the four quaternions columns.
The MATLAB R2022a tutorial code, reported below in list 4.1, is structured as follows: after the import of the OpenSim libraries into MATLAB (line 2), then for each experimental trial dataset (line 4) organised in a table is created a storage *.sto* file which links the name of each experimental IMU sensor with the virtual sensors placed on model bone segments in the chosen OpenSim model.

Listing 4.1: Tutorial code for creating the *.sto* file

```
1 % Import the OpenSim libraries
2 import org.opensim.modeling.*;
3 % Define the trial name. The table with the IMUs quaternion
     for the single exercise
4 trialName = 'Squat_Subj1.csv';
5 % Create an APDMDataReader and supply the settings file that
     maps IMUs to your model
6 apdmSettings = APDMDataReaderSettings('Settings_OUR_IMUs.xml'
     );
7 myAPDMDataReader = APDMDataReader(apdmSettings);
```

```
% Read the quaternion data and write it to a STO file for use
    in OpenSense workflow
tables = myAPDMDataReader.read( trialName );
quaternionTable = myAPDMDataReader.getOrientationsTable(
   tables);
STOFileAdapterQuaternion.write(quaternionTable,  strrep(
   trialName,'.csv', '_orientations.sto') );
```

Moving to the OpenSim (Version 4.3, USA) environment, the `3DGaitModel2392.osim` model is chosen. It contains all the information needed for the biomechanical description of the human body, including body segments, kinematic constraints (joints, 23 DOF) and dynamic constraints(i.e.76 muscles).
The whole workflow shown in Figure 4.6 summarizes all the passages to obtain a virtual twin of the motor movement through OpenSense workflow.
A calibration procedure of the model is demanded to register the IMU to the corresponding body segment, by reading the *.sto* file. It calculates the rotational transformation from the IMU coordinate system to the corresponding body segment coordinate system of the model (usually in a rotation matrix, Euler angle, or quaternions).
The *basic IMU*, always recognized as the one positioned on the pelvic area, and its heading direction, which may vary according to the plane in which the specific exercise is performed, were indicated using the *IMU Placer* tool of OpenSense. Since all the reference frames are deducted from the pelvis IMU it is of crucial importance. At this point, it is possible to access the `"IMU Inverse Kinematic Tool"`, which from the input .sto file recognizes the sensors and the total duration time of the exercise and as output returns a *.mot* file, which contains all the motor information (position over time of the body segments). At the end of this procedure, OpenSim can be used to its full potential in order to obtain kinematic variables or predict movements for example with blocked DOF or even when the muscle length is abnormal.

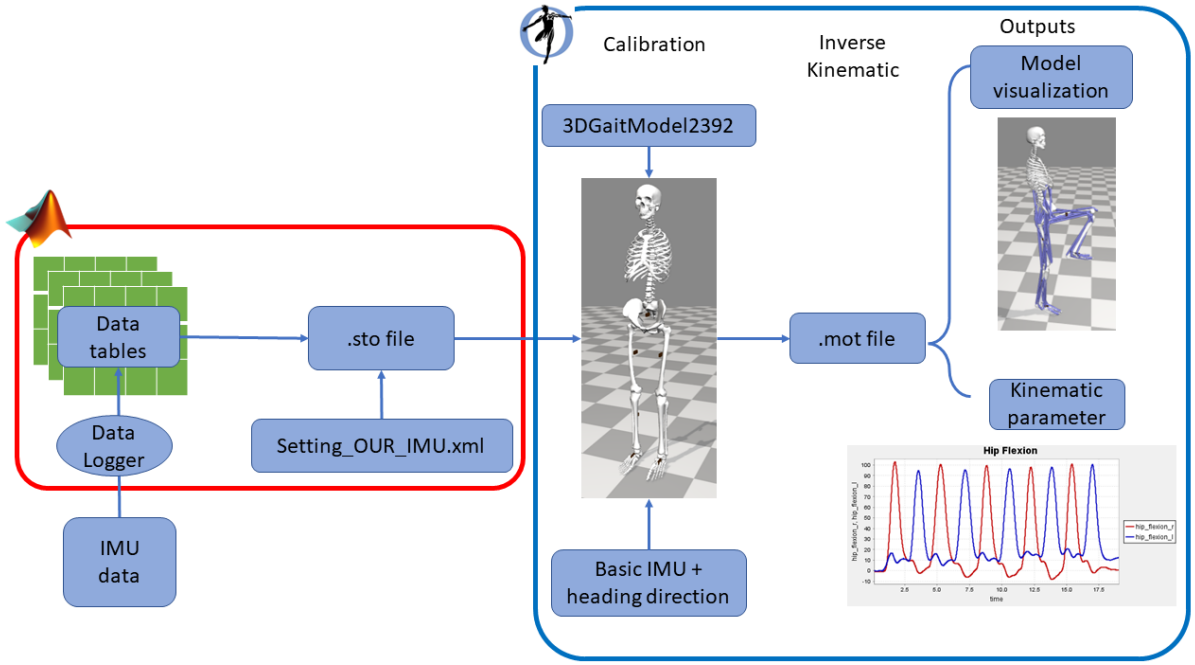

Figure 4.6: Workflow followed by this thesis to realize the virtual model based on IMU's measurement through OpenSense

5 | Methods

5.1. Subject preparation and positioning protocol

Prior to any data collection, the subjects were prepared wearing IMU sensors and or without the MOCAP markers, depending on the phases of the investigation. In Phase 1, all three motion capture systems are used, in Phase 2, only TinyTag but the anatomical positions chosen are the same. In the positioning phase, knowing the reference frame of the sensors is essential to ensure consistent placement of the IMU devices, in Figure 5.1 is reported the two Tinytag sensors and the Xsens IMUs ref frame, it's crucial that all the sensors are placed in the same way so that all the reference frames are oriented in the same direction. For this study, Velcro strips of the same size but of different lengths according to the circumferences of the body segments of the various subjects were used to fix the TinyTag sensors.

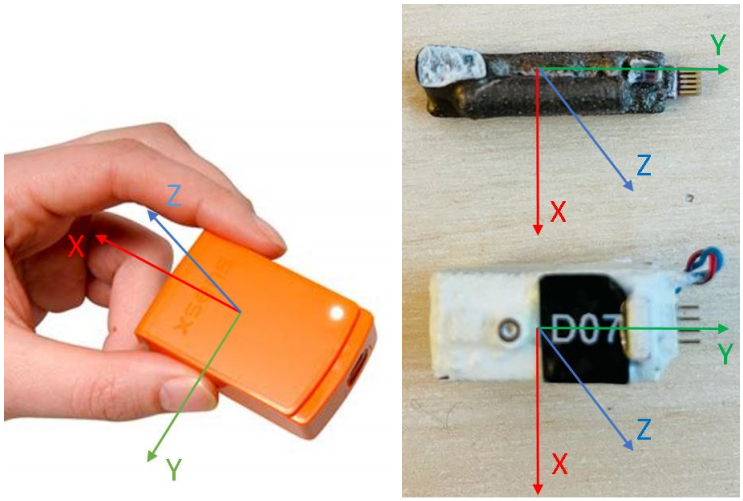

Figure 5.1: Reference frame of Xsens (left) and both TinyTag (right) sensors are shown

For both sets of IMU devices, the positioning is the same, following the outwalk protocol [48], seven sensors (Figure 5.2) are needed to describe the lower limbs kinematics and conduct the analysis of inverse kinematics would through OpenSense. The exact positioning of the sensors is described from top to bottom, laterally on the two legs, centered

approximately at height of each segment's center of mass.
Regarding the MOCAP in this study, Davis's protocol is used [76], exploiting twenty-two markers and showed in Figure 5.2. It is the most widely used protocol in gait analysis, it focuses more on the lower body but allows also the study of trunk displacement.

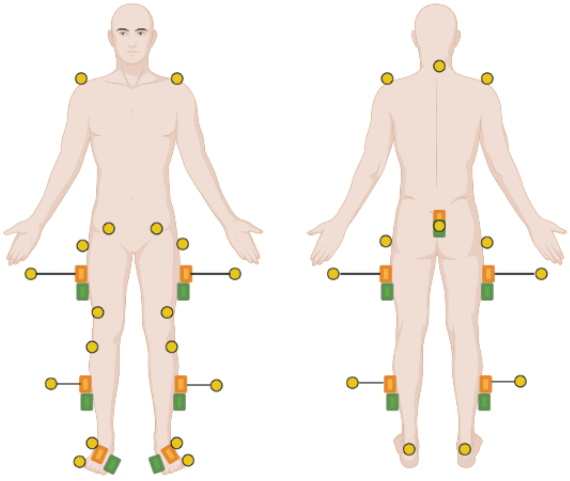

Figure 5.2: IMU sensors (orange boxes Xsens and green boxes TinyTag) and retro-reflective markers (yellow dots) placement on the subject. Frontal view on the left and posterior view on the right

5.2. Exercises

In this study, the focus is on the variation of the lower limbs' joint angles during exercises. The performed exercises are chosen among the most common activities in rehabilitation processes. All the exercises are performed with the intensity and ROM chosen by the subjects and no directions are given in that sense. The exercises of interest are four and are described below.

Squat (S)

From a standing position, with feet parallel and approximately at shoulder distance, the hip is lowered and raised. During the descent phase, the hip and knee joints flex while the ankles dorsiflex; conversely, the hip and knee joints extend and the ankle joint plantar-flexes when standing up. The hands can be on the waist or with the arm flexed in front of the body and for a correct motion the knee shouldn't go ahead of the feet. Motor exercise is shown in Figure 5.3 and takes place mainly on the sagittal plane.

Frontal leg swing (FLS)

In standing position, one leg moves away from the midline of the body in the frontal plane, keeping the knee extended and then returns to the standing position, the hip joint has an

Figure 5.3: Squat exercise performed

abduction and then adduction movement while the knee and ankle stay still (Figure 5.4). The plane of interest of this movement is the frontal one.

Figure 5.4: Frontal leg swing performed

Knee to chest (KTC)

From standing position, the hip of one leg is flexed raising the knee towards the chest, while the knee is flexed to keep the foot parallel to the floor, then returns to starting position. In this exercise, the ankle joint is not involved and the exercise takes place on the sagittal plane. Motor exercise is shown in Figure 5.5

Figure 5.5: Knee to chest performed

Heel to hamstring (HTH)

The exercise is composed of the full flexion of the knee starting from standing position,

until the foot reaches the closest possible position near the gluteus and then returns to the standing position, keeping the hip locked (Figure 5.6). The hip and ankle joints are kept at rest and the motion involves the sagittal plane.

Figure 5.6: Heel to hamstring performed

5.2.1. Joint angles

A joint angle is defined as the angle between two body segments linked by a joint on a defined plane. The figures specify the sign convention considered in this work.

Knee flexion/extension angle
The knee angle is defined as the angle on the sagittal plane between a spatial vector joining the lateral malleolus and fibula head and a spatial vector spanning from the lateral femoral epicondyle to the great trochanter [79]. This specific angle was considered the focus of the analysis of the **Squat** and **Heel To Hamstring** exercises with the convention in Figure 5.7.

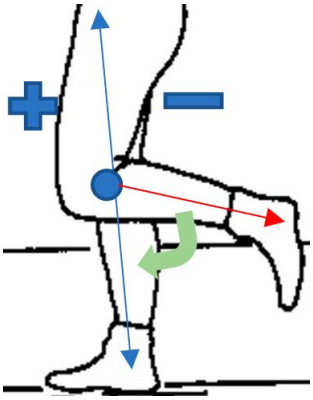

Figure 5.7: Schematic definition of the knee angle of flexion/extension

Hip flexion/extension angle
The hip flexion/extension angle is defined as the angle on the sagittal plane between the

vertical line going from the hip instantaneous center of rotation to the foot in standing position (blue in Figure 5.8) and the same line (in red) during the motion from the head of the femur and the foot. This instead is related to the exercise of **Knee To Chest**.

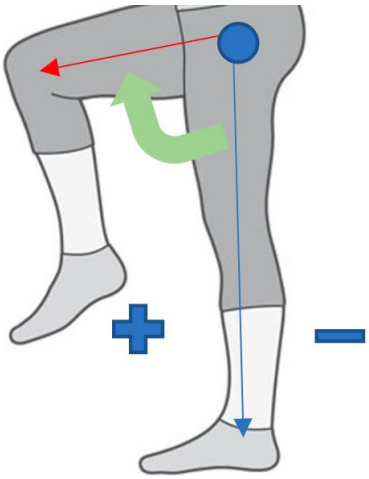

Figure 5.8: Schematic definition of hip flexion/extension angle

Hip adduction/abduction angle

The hip adduction/abduction angle is defined as the angle on the frontal plane between the vertical line going from the hip's instantaneous center of rotation and the foot in the standing position (blue in Figure 5.9) to the same line during the movement (in red) from the head of the femur to the foot. The **Frontal Leg Swing** exercise involves most this defined angle .

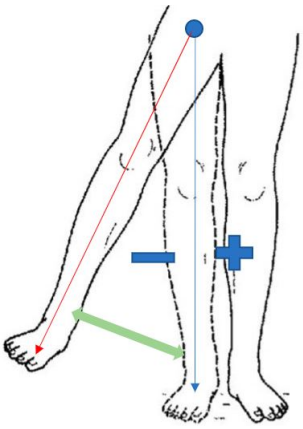

Figure 5.9: Schematic definition of hip abduction/adduction angle

5.3. Phase 1: Validation trial

This chapter will explain the first part of the thesis project concerning, the validation of the OpenSim tool. The validation study is, more in detail, a performance correlational study intended to establish the relationship between the results obtained from two, or more, instruments in order to assess their interchangeability and often to assess the reliability and trustworthiness of a newly developed method.

5.3.1. Test protocol

To carry out the validation study, the above-described methods for motion capture were compared recording the same motor task and measuring the same motor parameter: the joint angle of interest. The main comparison was made between the accuracy of the joint angles estimated by OpenSense when driven by TinyTag sensors against the gold standard MOCAP, in addition, since the OpenSense tool was developed and tested so far exploiting Xsens data, it has been decided to consider a further validation including the estimates of the joint angle patterns obtained by OpenSense when receiving as input data from commercial Xsens sensors(Figure 5.10). According to existing literature, this method is considered by the developers of OpenSim to be reliable. [48].

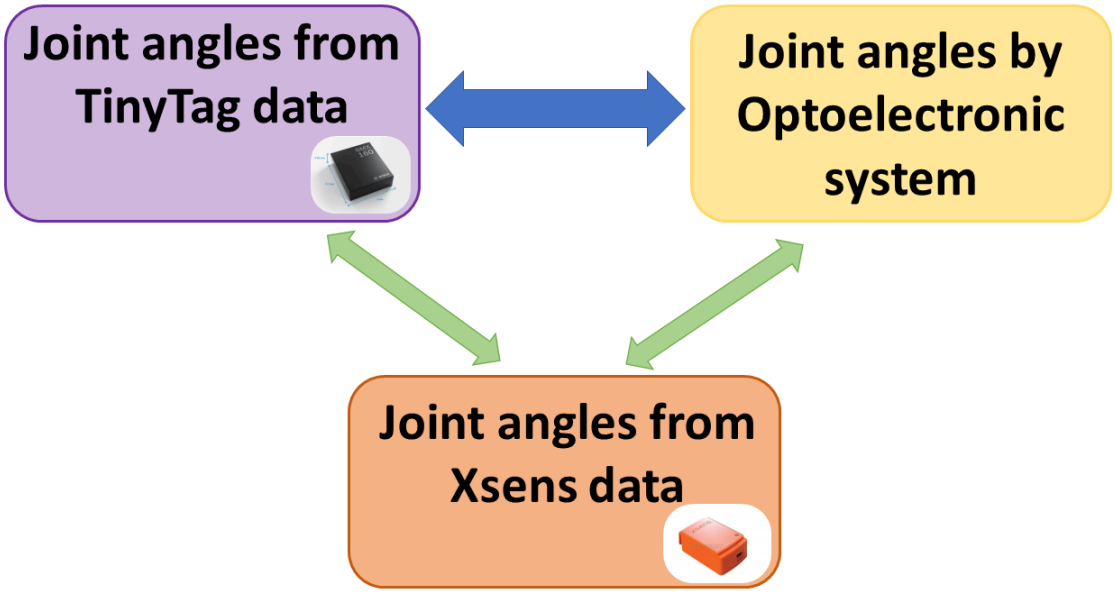

Figure 5.10: Scheme of the three-way comparison for phase validity

The validation test was conducted in the "Luigi Divieti" Posture and Movement Analysis Laboratory of Politecnico di Milano (Italy) and involved the participation of two subjects

(24 years old) dressed in comfortable clothes. Each session consists of five Squats, ten Frontal Leg Swings(five per leg), ten Knee To Chest (five per leg) and ten Heel To Hamstring (five per leg). Each subject performed twelve sessions, for a total of twenty-four sessions obtained. The protocol also included the use of one video camera (GoPro HERO 5)[1] that framed the subject during the execution of movements for reference and to make a visual comparison between the real movement and the one reproduced by the virtual model.

5.3.2. Experimental protocol

1. Anthropometric measurements were acquired for both subjects (Leg length).
2. The MOCAP is calibrated.
3. The retro-reflective markers are placed on the subject as reported in section 5.1.
4. The Xsens IMUs are placed on the subject (Section 5.1).
5. The Xsens system is calibrated following the instructions of the company's software MVN.
6. The TinyTag IMUs are turned by a magnet on and synchronized with the electromagnetic impulse of the coil, then placed on the subject using velcro straps (Section 5.1).
7. The GoPro camera is turned on and the recording is started.
8. The subject performs a single squat for synchronization between the three motion capture systems.
9. The 4 exercises are performed, with 10 seconds of rest between each exercise.
10. All the IMU sensors are removed and turned off.
11. All the markers are removed from the subject.

The next Figure 5.11 shows a detailed block diagram of the data processing phase from raw data to the indices analyzed in this phase of the thesis, specifying the software used.

5.3.3. Statistical analysis

The first step is the synchronization of all measurement systems by identifying the first isolated squat and cutting all signals by starting them at the maximum acceleration

[1] https://productz.com/en/gopro-hero5/p/BLqDG

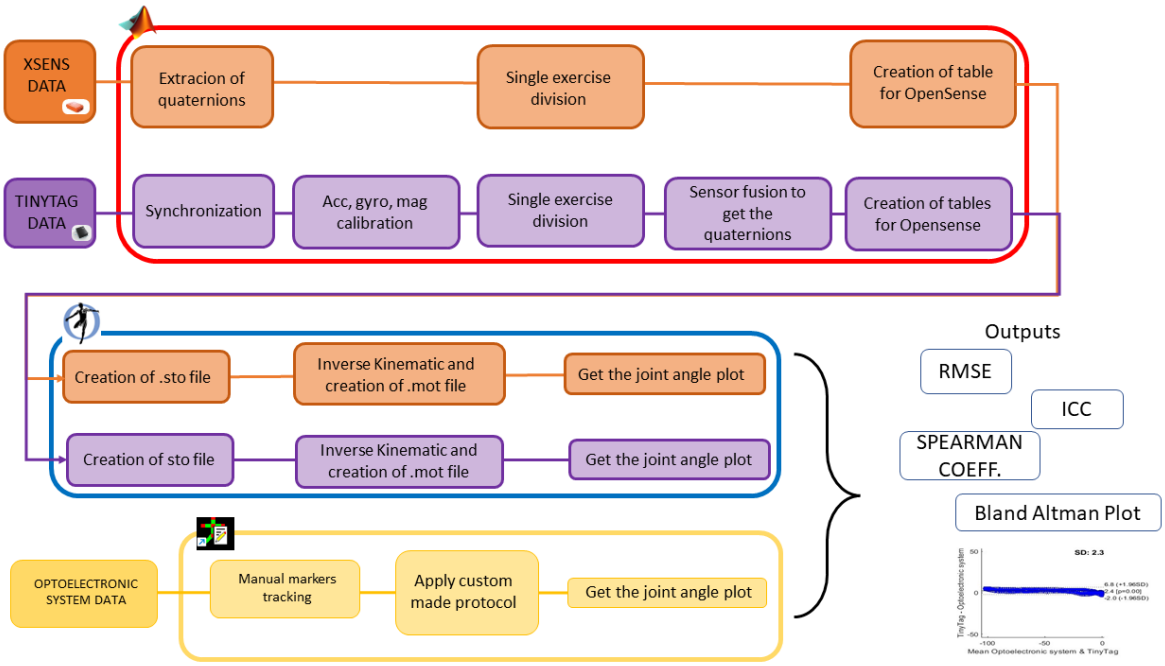

Figure 5.11: Block diagram Phase 1, all the passages step by step explained in the text are shown

measured. All the statistical analysis is then performed on MATLAB R2022a through custom codes reported in Appendix A. From the processing of the data (Section 4.2) the joint angles are obtained and the statistical analysis is performed over these data. Various indexes are considered:

- **Root Mean Squared Error (RMSE)**: evaluates the distance point by point between two estimates graphs of the joint angles over time. It is one of the main outcomes in validation studies [80, 81] and it is defined as follows:

$$RMSE = \sqrt{\frac{1}{n}\sum_{i=1}^{n}(d_i - f_i)^2} \tag{5.1}$$

- **Spearman's correlation coefficient (rho)**: is a non-parametric measure of correlation. It assesses how well varying from -1 to 1 the relationship between two variables can be described using a monotonic function. While Pearson's correlation assesses linear relationships, Spearman's correlation assesses monotonic relationships whether linear or not without assuming that data are normally distributed. If there are no repeated values, a perfect Spearman correlation of +1 or -1 occurs when each of the variables is a perfect monotone function of the other [82].

- **Intraclass Correlation Coefficient (ICC)**: is used to measure the reliability of ratings in studies where there are two or more raters. The value of an ICC can range from 0 to 1, with 0 indicating the absence of reliability among raters and 1 pointing out perfect reliability among raters. For this study the *Two-way mixed effects model* was chosen: this model assumes that a group of k fixed raters is randomly selected from a population and then used to rate each result. *Absolute Agreement*: as the relationship of interest concerning if different judges assign the same score to the same measurement. Finally, as the type, the *Single rater*, since the ratings from a single rater were used as the basis for actual measurement [83].
- **Bland-Altman plot**: is used to visualize the differences in measurements between two instruments or measurement techniques. It is often used to assess how similar a new instrument or technique is at measuring something compared to the ones currently being used. The x-axis of the plot in Figure 5.12 displays the average

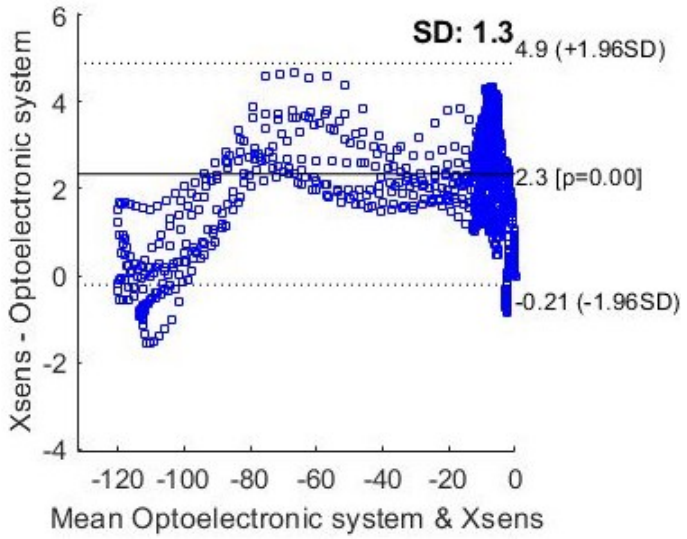

Figure 5.12: Example of Bland Altman plot [4]. In this case, it shows the differences between MOCAP and Xsens assessments data (represented as blue blocks) reporting also: the value of the Standard Deviation of the difference, the Bias of the two measurements tools and the Confidence interval

measurement between the ones made by the two instruments while the y-axis reports the difference between them. Three lines are also shown in the plot: the average difference between measurements of the two instruments (called bias), the upper limit of the 95% confidence interval for the average difference, and the lower limit of the 95% confidence interval for the average difference, estimated as bias ± 1.96 Standard Deviation (SD) of differences [4].

5.4. Phase 2: Physiological ROM assessment

For the second phase concerning the identification of an underwater physiological Range of Motion by the TinyTag sensor system, twenty-five people were recruited. Approval to the Estonian Research Ethics Committee of National Institute for Health Development[2] had to be obtained. The document of approval can be found in Appendix C.
Moreover, an informed consent (Appendix D) was signed and an anonymous questionnaire (Appendix D) was filled out by each participant.

5.4.1. Test protocol

Twenty-five healthy young adults were recruited, whose characteristics are reported in Table 5.1) and after providing consent to serve as participants in the study, they filled out an anonymous questionnaire (Appendix D).

	Number of participants	**Age (years)**	**Height (cm)**	**Weight(Kg)**
All	25	22.4 (± 1.71)	176 (± 7.76)	70.16 (± 10.4)
Male	14	22.70 (±1.84)	181 (± 6.30)	75.64 (± 8.81)
Female	11	22.09 (± 1.64)	171 (± 5.42)	63.18 (± 7.94)

Table 5.1: Participants recruited for Phase 2, physiological ROM assessment. Mean ± SD

All the participants attended two testing sessions, one land-based and one water-based, both with identical testing protocols and occurring within one week's distance. Both sessions took place in the Õismäe Leisure Centre mall[3] (Tallinn, Estonia), in the municipal swimming pool. The pool has 6 lanes of 25m, but only one was used in the study, with depth spanning from 110 to 180cm, allowing all subjects to have the water just above the pelvic zone. The on-land protocol was first performed by the pool and then entered and performed the second underwater session. During this second experimental phase of the thesis, only TinyTag sensors were used to record motion in the two environments. Additionally, a waterproof video camera (GoPro Hero5) for reference was used, which always guarantees the anonymity of the subject. In order to capture each participant's natural technique and ROM, and to ensure consistency between environments, no instructions were provided concerning foot positions or the excursion to express in the exercises.

[2]https://en.tai.ee/en/about-us/tallinn-medical-research-ethics-commitee
[3]https://www.tallinn.ee/en/services/oismae-swimming-pool

5.4.2. Experimental protocol

The protocol performed point by point is given below, the underlined parts refer only to the session performed in water.

1. The subject is asked to wear a swimsuit.
2. The TinyTag sensors are turned on using a magnet and synchronized using an electromagnetic impulse given by a metallic coil.
3. The sensors are placed on the subject using velcro straps (Section 5.1).
4. ONLY IN THE UNDER-WATER CASE: The subject enters the pool and grabs the metallic bar on the pool wall to ensure stability.
5. ONLY IN THE ON LAND CASE: The subject grabs a chair to ensure stability.
6. The waterproof camera recording starts.
7. The 4 exercises are performed, with 10 seconds of rest between each exercise.
8. ONLY IN THE UNDER-WATER CASE: The subject exits the pool.
9. All the IMUs are removed from the subject and turned off.

5.4.3. Statistical analysis

The statistical analysis is performed on MATLAB R2022a through custom codes reported in Appendix A.

After estimating in OpenSense the joint's angles as in Section 4.2, the excursion of the performed ROM in each repetition is calculated as the difference between the starting position and the position of the completed exercise before returning to the starting pose (Figure 5.13).
Per exercise, the mean and standard deviation of these ROM are evaluated and used to:

- Assess differences between on-land and underwater movements;
- Draw summarizing graphs of the physiological ROM expressed;
- Analyze differences between male and female subjects.

The differences are analysed through descriptive statistics and visualization. Lastly, since each exercise was repeated in time, to take into account fatigue and better assess land-water differences, the ROM for each repetition was compared using violin plots [84].

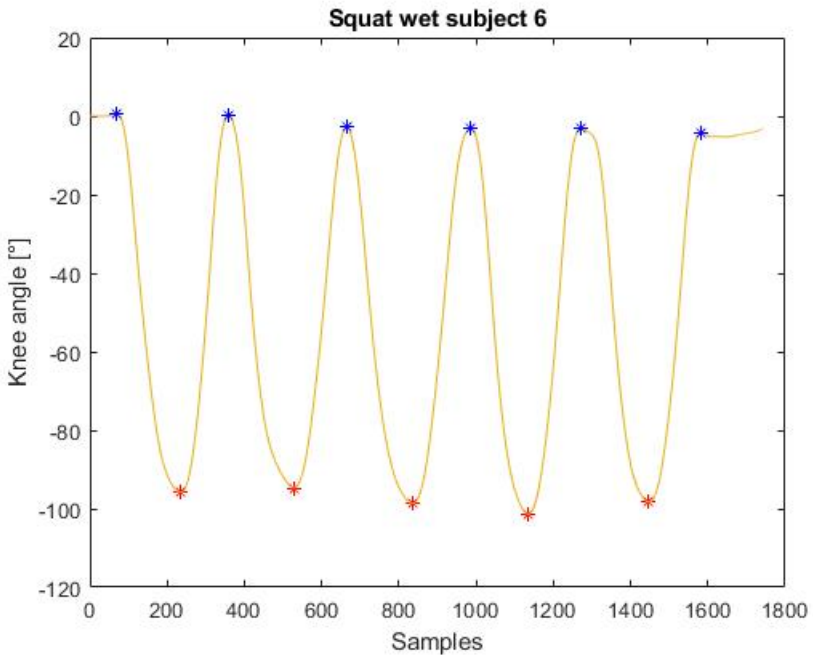

Figure 5.13: Example of excursion of the knee angle, measured during S, where the stars represent the beginning and the maximum ROM reached in each repetition.

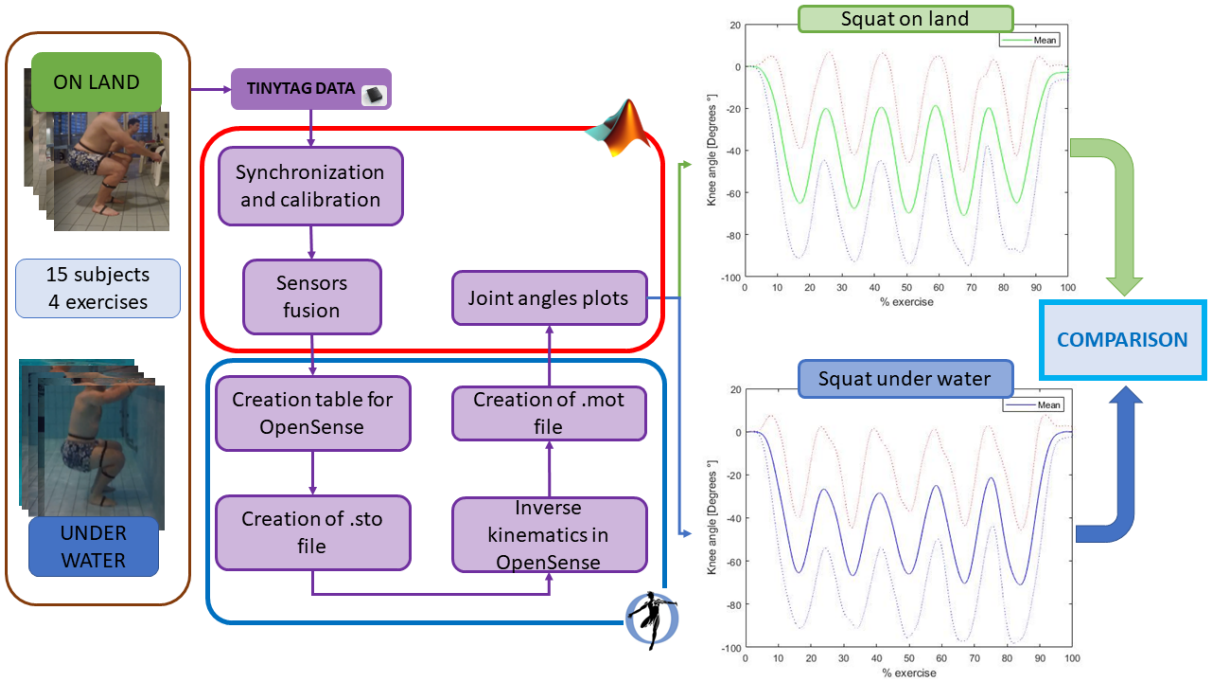

Figure 5.14: Block diagram Phase 2: Creation of a benchmark physiological range on land and in water. TinyTag data were acquired both in-water and out-of-water and converted, inverse kinematics were performed by OpenSense, joint angles were extracted, and finally, a comparison was made to highlight differences and similarities.

6 | Results

In this chapter, the obtained results are displayed distinguishing between the two research phases conducted.

6.1. Phase 1 results

Phase 1 of this thesis foresees the comparison of the three motion capture systems used when assessing the same kinematic metric. The estimates made by OpenSense when driven by the prototype IMU sensors from TalTech (1) or by commercial Xsens devices (2) have been compared against the results obtained from MOCAP. Finally (3) the outcomes of OpenSense when driven by the two IMU methods are confronted. The number of subjects and their characteristics are shown in Table 6.1, considering that each participant performed the protocol twelve times the total number of sessions obtained is twenty-four. However, five of these were discarded due to problems during acquisition, resulting in a

Number of participants	Age (years)	Height (cm)	Weight(Kg)
2	24 (±0)	176 (±4)	72.5 (±7)

Table 6.1: Useful participants characteristics used for phase 1 statistical analysis

total of nineteen sessions used for statistical analysis of all the comparisons between the measurement systems. The parameters estimated during phase 1, previously described in Section 5.3.3, are reported here with the relevant study results. The indexes were estimated on the angle of interest of each exercise (specified in Section 5.2.1) considering the entire joint angle estimate of the task (all the repetitions together) made through SMART Analyzer or OpenSense.

6.1.1. Optoelectronic system - TinyTag comparison

Below the Table 6.2 with all the results obtained from the first comparison, which aims to validate the method proposed by this study for the analysis of motor kinematics is reported.

	S	FLS	KTC	HTH
RMSE [°]	2.52 (±1.222)	10.40 (±5.397)	5,03 (±2.035)	8.20 (±2.89)
Spearman coefficient [Adim]	0.98 (±0.016)	0.71 (±0.201)	0.85 (±0.085)	0.75 (±0.11)
ICC [Adim]	0.99 (±0.01)	0.58 (±0.170)	0.93 (±0.06)	0.88 (±0.112)
Bias [°]	-0.80 (±2.797)	-2.21 (±6.592)	4.82 (±2.845)	10.7 (±10.58)

Table 6.2: Table of indexes regarding the comparison between the MOCAP and the TinyTag data. Notes: The values presented are Mean (±SD)

- **RMSE**

The main output used to establish the measurement validity of the TinyTag sensor with respect to the MOCAP is the RMSE. After a careful literature review, it was concluded that joint angles of less than 5° can be considered a good level of mean square error in the study of motion analysis [85, 86]. Regarding the Squat and the Knee To Chest exercises the RMSE is around 5° respectively of knee and hip angle. Focusing on the Frontal Leg Swing and Heel To Hamstring the error is more than twice the acceptable one.

- **Spearman**

To check the distribution of the data obtained for all three measurement systems, the Kolmogorov-Smirnov statistical test was performed and it was obtained, with a high statistical significance ($p < 0.05$), that was not normally distributed. For this reason, it was decided to investigate their monotonic correlation via Spearman's non-parametric coefficient. The coefficients reported for each exercise show a strong correlation, higher than 0.75, between the results obtained with MOCAP and TT. The lowest value is the hip adduction/abduction angle in FLS presenting also the higher standard deviation, meaning the presence of some data perfectly correlated.

- **ICC**

The ICC focuses on the absolute agreement between the measurement tools. This parameter for the S and the KTC exercises seems to be highly correlated between one tool or another. For the HTH the result may still be considered acceptable because over the 0.75 threshold. The FLS shows a very low value of ICC and at the same time, the range described by the standard deviation is limited.

- **Bland-Altman plot**

In validation studies on measuring methods, the Bland-Altman plot seems to be the most widely used as it succeeds quantitatively and visually in giving an idea of the comparison of the two methodologies estimating the same phenomena. In particular, reference is made to the variable *bias* that defines the average of the difference of the measurements

obtained with the two systems. In literature, a bias of less than 10° indicates that the two measurement systems are able to provide similar analysis [85].
Defining the bias as *gold standard - new* a positive value means that the proposed method overestimates the assessment while a negative bias indicates that the measure is underestimated. In this case, for all exercises, it appears that the bias value is very small, especially in the S exercise where it reaches the lowest value, which means that the OpenSense estimate of the joint angle is very similar to the optoelectronic one. An exception is observed for the knee angle during the HTH exercise, as in this case, the value 10.7° is very close to the acceptable threshold.
In the following page, Bland-Altman plots of the comparison between TinyTag and MOCAP are reported showing for each exercise the repetition with smaller and bigger RMSE and therefore better and worse measurement bias.

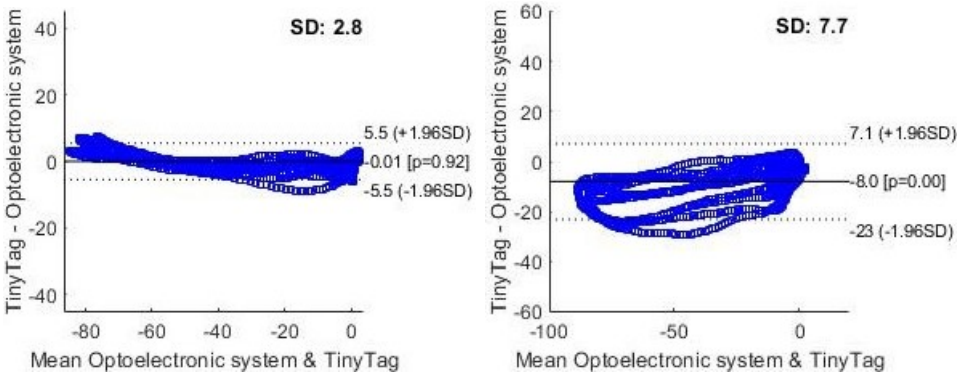

Figure 6.1: BlandAltman plots of the S exercise with lower RMSE on the left and higher RMSE on the right.

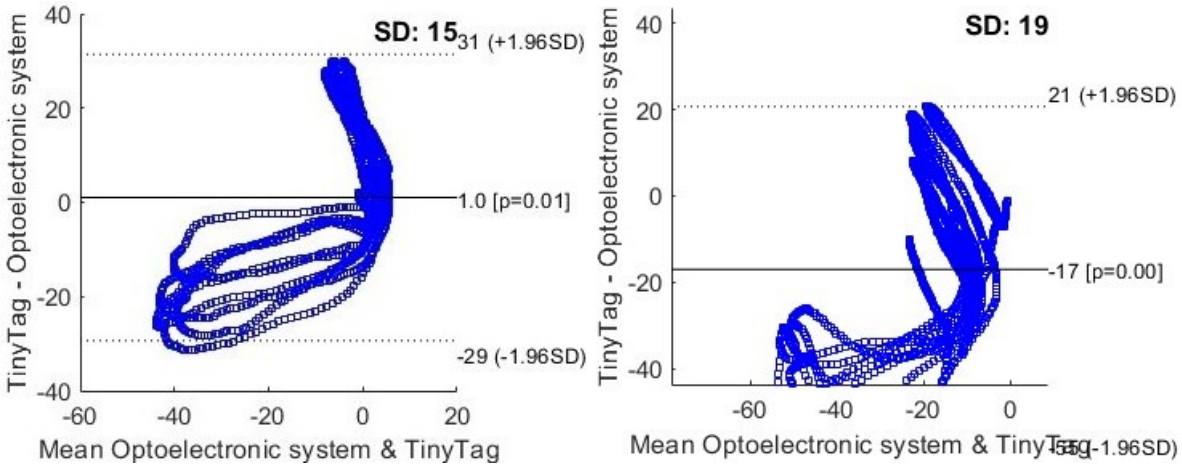

Figure 6.2: BlandAltman plots of the FLS exercise with lower RMSE on the left and higher RMSE on the right.

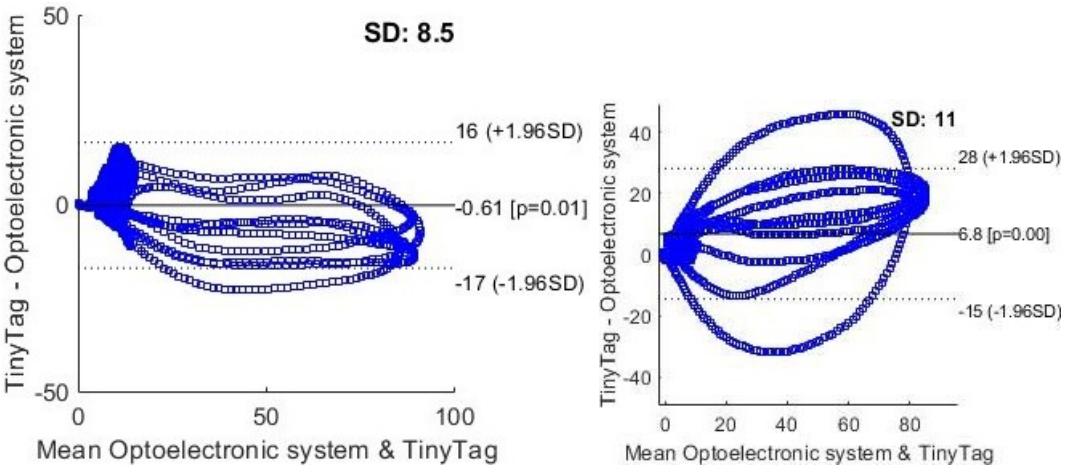

Figure 6.3: BlandAltman plots of the KTC exercise with lower RMSE on the left and higher RMSE on the right.

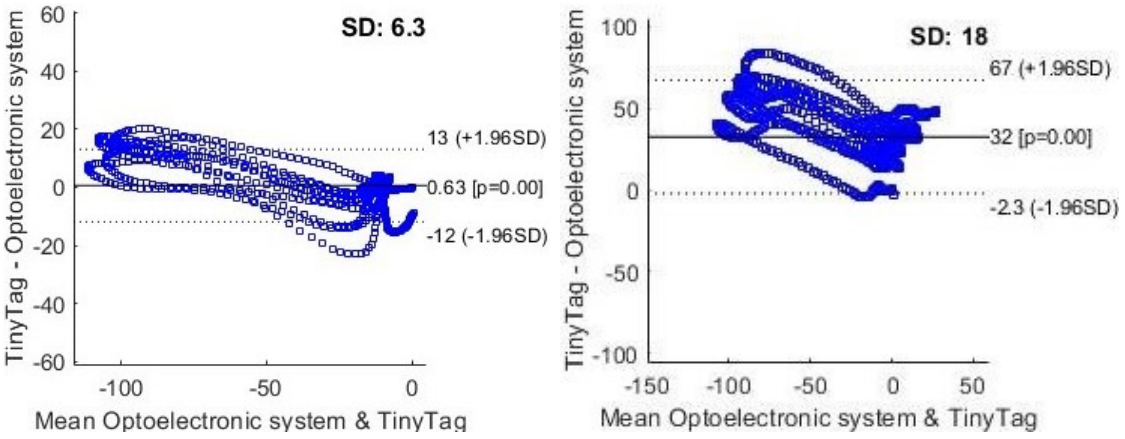

Figure 6.4: BlandAltman plots of the HTH exercise with lower RMSE on the left and higher RMSE on the right.

6.1.2. Optoelectronic system - Xsens comparison

In Table 6.3, the second comparison of this research is studied, comparing the results obtained from the inverse kinematics performed by OpenSense with the input data of the Xsens sensors against the optoelectronic system for all indices analysed. In addition, a

	S	**FLS**	**KTC**	**HTH**
RMSE [°]	1.07 (±0.813)	2.52 (±0.976)	2.62 (±3.481)	1.56 (±0.561)
Spearman [Adim]	0.99 (±0.006)	0.95 (±0.011)	0.94 (±0.04)	0.98 (±0.01)
ICC [Adim]	0.99 (±0.006)	0.91 (±0.06)	0.97 (±0.06)	0.99 (±0.06)
BIAS [°]	-0.10 (±2.627)	-2.39 (±2.714)	-3.36 (±2.003)	0.20 (±2.456)

Table 6.3: Comparison between Xsens data and MOCAP. All the indexes chosen for the study relative to each exercise are reported. Notes: The values presented are Mean (±SD)

representation through a bar plot reporting means and standard deviations is done to interpret better the numbers obtained in 6.1.1 and 6.1.2 to set side by side the validation indexes for TinyTag and Xsens.

From the graph 6.5 is clear that for two exercises, the S and the KTC, the RMSE is similar between the two comparisons, but in the FLS and HTH, a higher error is computed by the TinyTag sensors with respect to the one made by Xsens sensors. As can be seen in the plot, Spearman's coefficient values are very similar for all the exercises, except for the FLS where the TinyTag sensors show a lower value with respect to the Xsens comparison. The ICC values are very similar for all the exercises, except for the FLS where the TinyTag sensors show a lower correlation with the gold standard with respect to the Xsens comparison. Lastly, the bias for the Bland-Altman plot in the S exercise is low while for the FLS and KTC, the biases are similar in the two comparisons. But, when it comes to HTH the bias of the Xsens is almost 0, instead for the TinyTag is very high (around 11°).

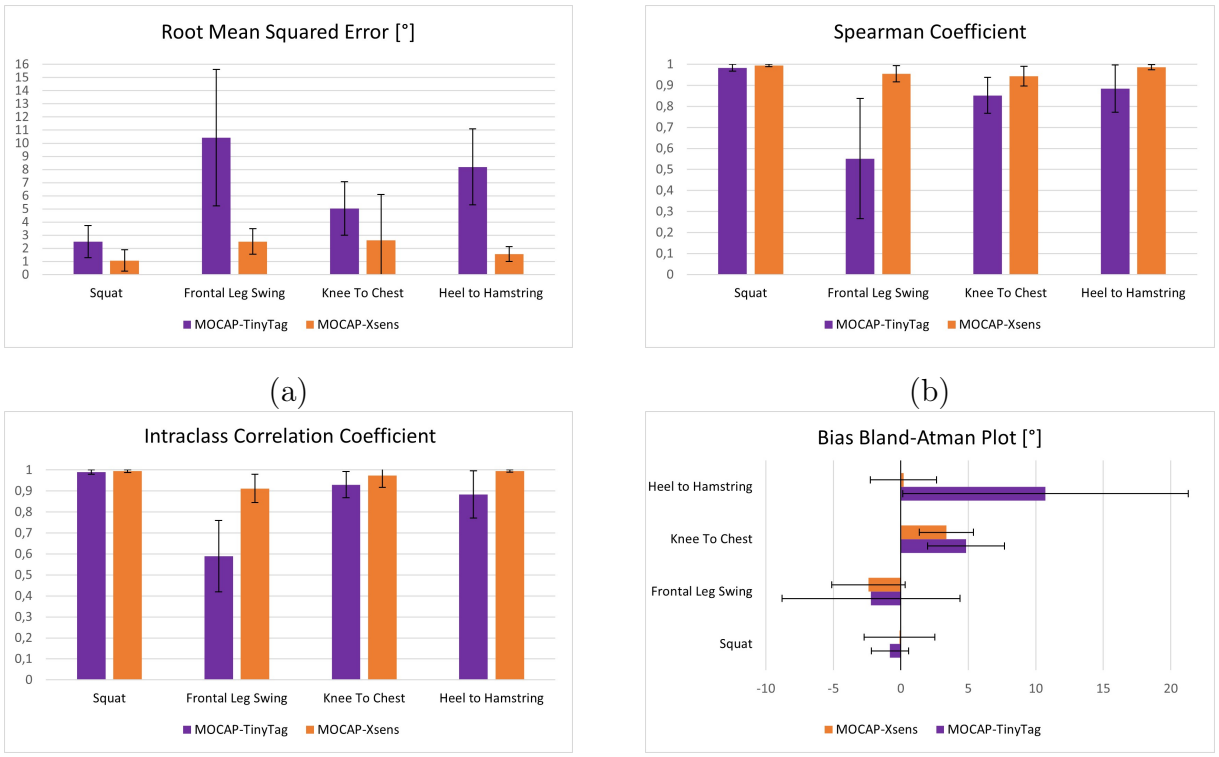

Figure 6.5: Subplot of Barplot showing the results obtained from the comparison between the MOCAP, the gold standard, and the two IMUs on which this study focuses. Specifically, the figure is divided as follows: (a) RMSE; (b) Spearman Coefficient; (c) ICC; (d) Bias of Bland-Altman Plot

6.1.3. Xsens - TinyTag comparison

Following the validation of the sensors from the Tallinn University of Technology against the MOCAP, this thesis set out to integrate a further comparison of the inverse kinematics calculated by the OpenSense software driven by the sensors built by the company Xsens or by TinyTag. From the results obtained (Table 6.4), it can be seen that for almost all

	S	FLS	KTC	HTH
RMSE [°]	2.54 (±1.416)	10.4 (±5.396)	4.62 (±2.155)	8.31 (±2.928)
Spearman [Adim]	0.98 (±0.016)	0.54 (±0.303)	0.90 (±0.086)	0.75 (±0.131)
ICC [Adim]	0.98 (±0.014)	0.64 (±0.217)	0.97 (±0.023)	0.85 (±0.118)
BIAS [°]	-0.53 (±4.143)	0.180 (±7.770)	1.33 (±3.097)	10.6 (±10.5)

Table 6.4: Comparison between Xsens data and TinyTag data of all the indexes chosen for the study relative to each exercise. Notes: The values presented are Mean (±SD)

the indexes, the values lie exactly in the middle of the two comparisons previously made. For the S and KTC exercise the difference is low, but for the HTH is around 8°, and for FLS is around 10°. The Sperman and the ICC indexes reflect the same behavior as the RMSE. Instead, the bias of the BlandAltmann detects some interesting facts: in the FLS the bias is low, which means that the RMSE is due to other causes, instead in the HTH the bias is very high and that could be the cause of the high RMSE.

6.2. Phase 2 results

In the second phase, an analysis of the ROM expressed in the four exercises is done. The excursion of the ROM is evaluated as described in Section 5.4.3, therefore as the difference between the starting position and the maximum joint angle performed. Of all the 25 subjects acquired, only 15 subjects (7 females and 8 males) were used in the statistical analysis due to defects in the data, caused by misplacement or corruption in one of the two sessions (underwater or on land).

The main purpose of this phase is the definition of physiological ROM for the exercises

	Number of participants	Age (years)	Height (cm)	Weight(Kg)
All	15	22.33 (± 1.49)	175.33 (± 8.61)	69.33 (± 10.4)

Table 6.5: Useful participants characteristics used for phase 2 statistical analysis

selected in healthy young adults and the comparison between the ROM measured on land and in water as environments where the exercises are performed (Section 6.2.1). Another Section (6.2.2) is related to the possible difference between males and females.

6.2.1. Underwater - On land comparison

For each performed exercise, the physiological ROM was estimated by observing the excursion (max to min) of the whole task considering separately the five repetitions and calculating mean and standard deviation.
In Appendix E are reported the tables (Table E.1 and E.2) with the values of the excursion for the four exercises for all the involved subjects on land and underwater while their overall average and standard deviation and the results are reported in Table 6.6. The difference in degrees observed between the exercise performed underwater and on land is reported in the last column represented also as a percentage of the ROM.

	UNDER WATER	ON LAND	DIFFERENCE
S [°]	83.03 (±12.27)	81.80 (±12.07)	1.23(1.5%)
FLS [°]	48.91 (±10.82)	44.30 (±13.62)	4.61(10.1%)
KTC [°]	94.57 (±15.45)	84.69 (±9.63)	9.88(11.1%)
HTH [°]	110.49 (±9.08)	98.29 (±9.42)	12.2(11.8%)

Table 6.6: Table with the mean values and std of the excursion in the 4 exercises above all the 15 subjects measured with TinyTag sensors.

As can be seen in Table 6.6, the S exercise doesn't seem to suffer from any influence by the environment. Also for the FLS only a small difference is noticed, instead for the last two exercises a bigger difference is measured. However, in all the tasks, when the exercise is performed underwater the ROM is always larger than the one executed on land.
To better understand the differences and similarities between the executions measured in the two environments, a violin plot [84] showing the distribution of excursions is reported for each exercise considering separate left and right lower limbs (except for S) and showing for each repetition land (Green) and water (Blu) measures. Concerning the S exercise (Figure 6.6), all repetitions show a consistency in the distribution of results which does not seem to show significant differences. In the FLS violin plot (Figure 6.7), the measurements in water for both limbs are more dispersed than the median value of those on land. This observation can be extended to the KTC exercise (Figure 6.8) where for the left leg, for example, there is a 20° difference between the median of water and on land. In the last HTH exercise (Figure 6.9) for both the left and right limbs, the excursions achieved on land are different from those measured in water by a minimum of 9° to a maximum of 20°, therefore they show wide variability.

Finally, we report the plots of the physiological ROM as the average (full line) and standard deviation (dashed lines) of all the behaviors (on land and in water) of the subjects distinguishing between right and left lower limb/ joint and considering the exercise in its

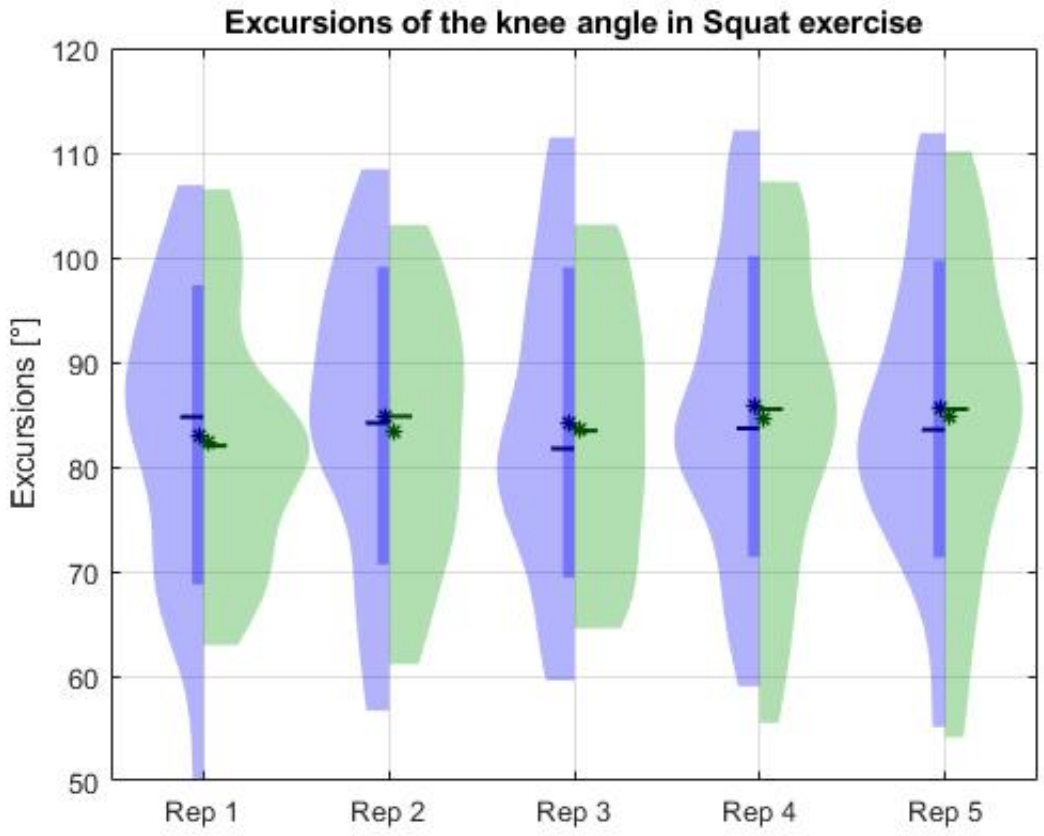

Figure 6.6: Violin plot of the S exercise knee angle excursions for each repetition (x-axis), in blue is the underwater distribution, in green is the one on land measured with TinyTag sensors.

entirety with the 5 repetitions and normalizing over it (expressed in % of the exercise). Also from the graphic representation of the ROM, as previously observed through the tables, the excursions into the water appear to be greater in almost all the exercises. Particularly visible in the last exercise KTC, in both the limbs shown in Figures 6.16 (left side) and 6.15 (right side).

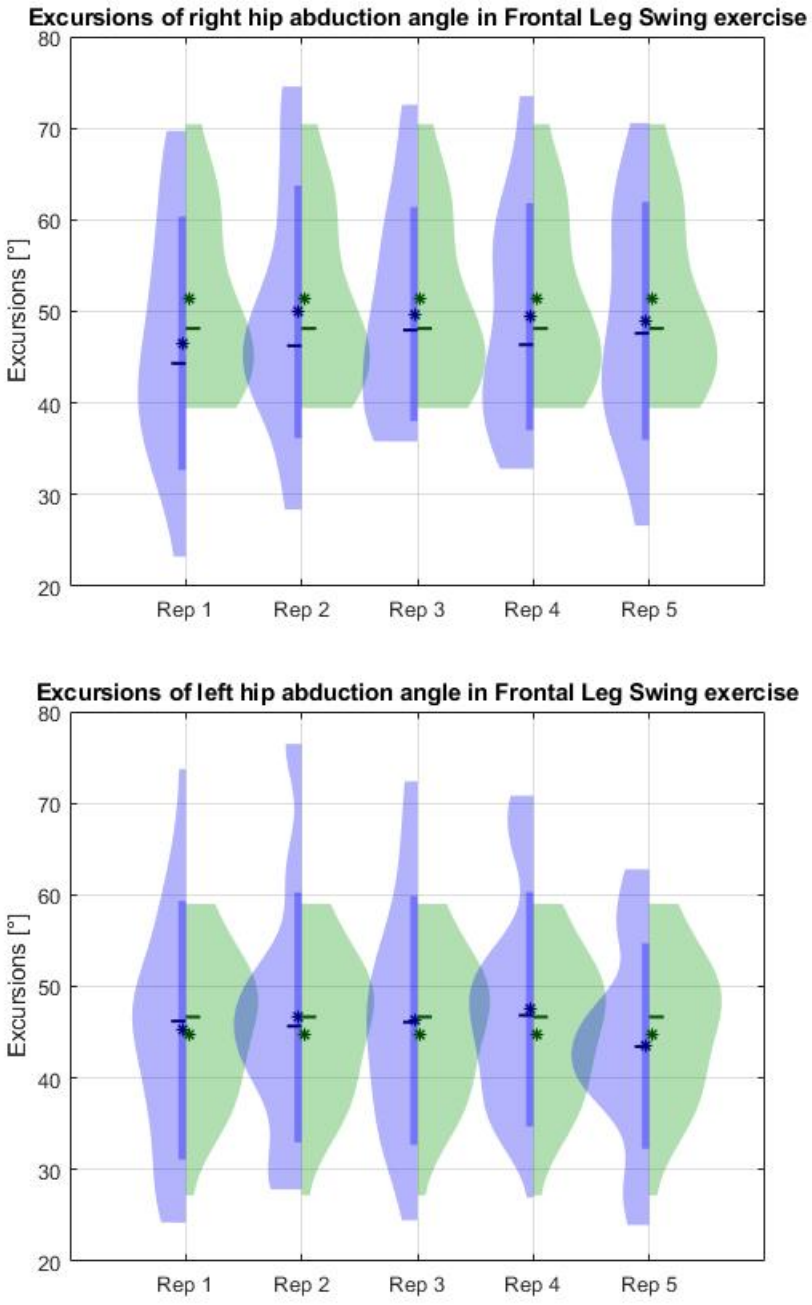

Figure 6.7: Violin plots of the FLS exercise hip abduction angle excursions for each repetition (x-axis), in blue is the underwater distribution, in green is the one on land measured with TinyTag sensors.

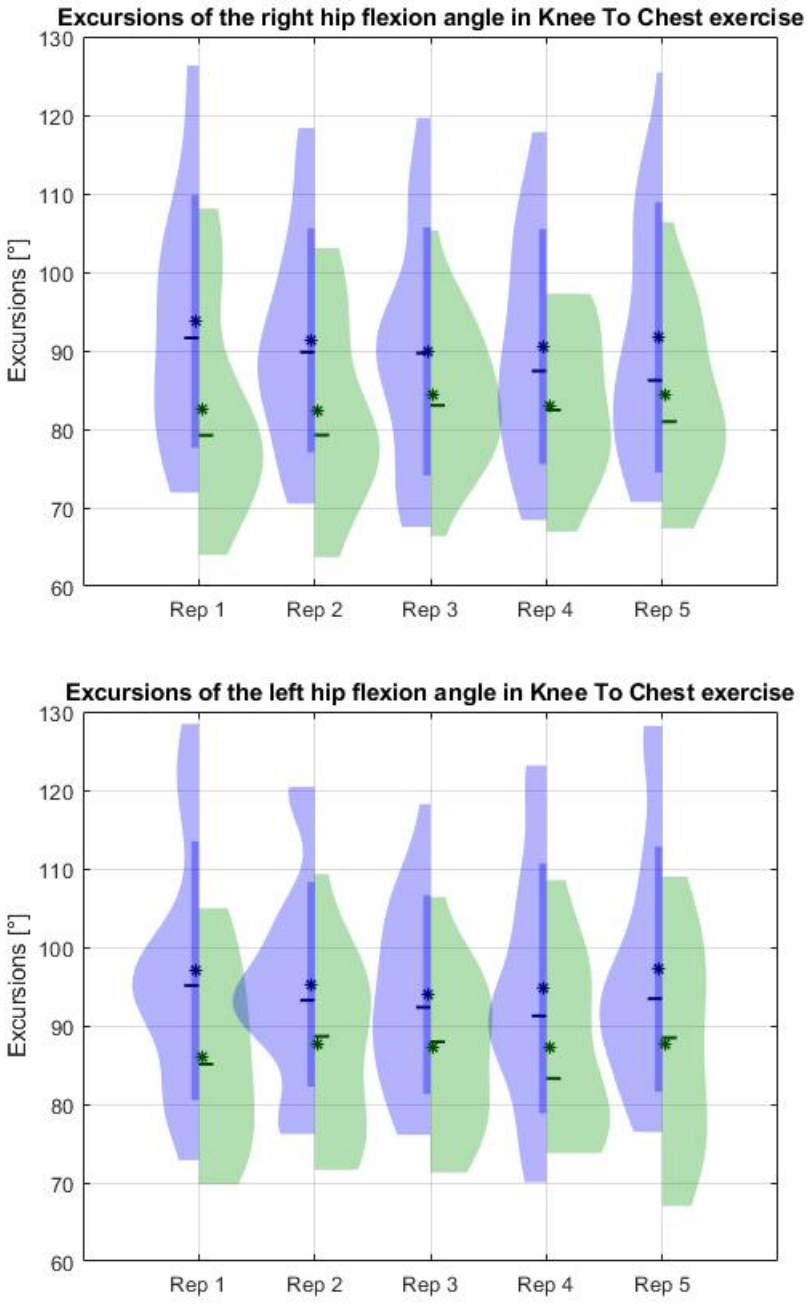

Figure 6.8: Violin plots of the KTC exercise hip flexion angle excursions for each repetition (x-axis), in blue is the underwater distribution, in green is the one on land measured with TinyTag sensors.

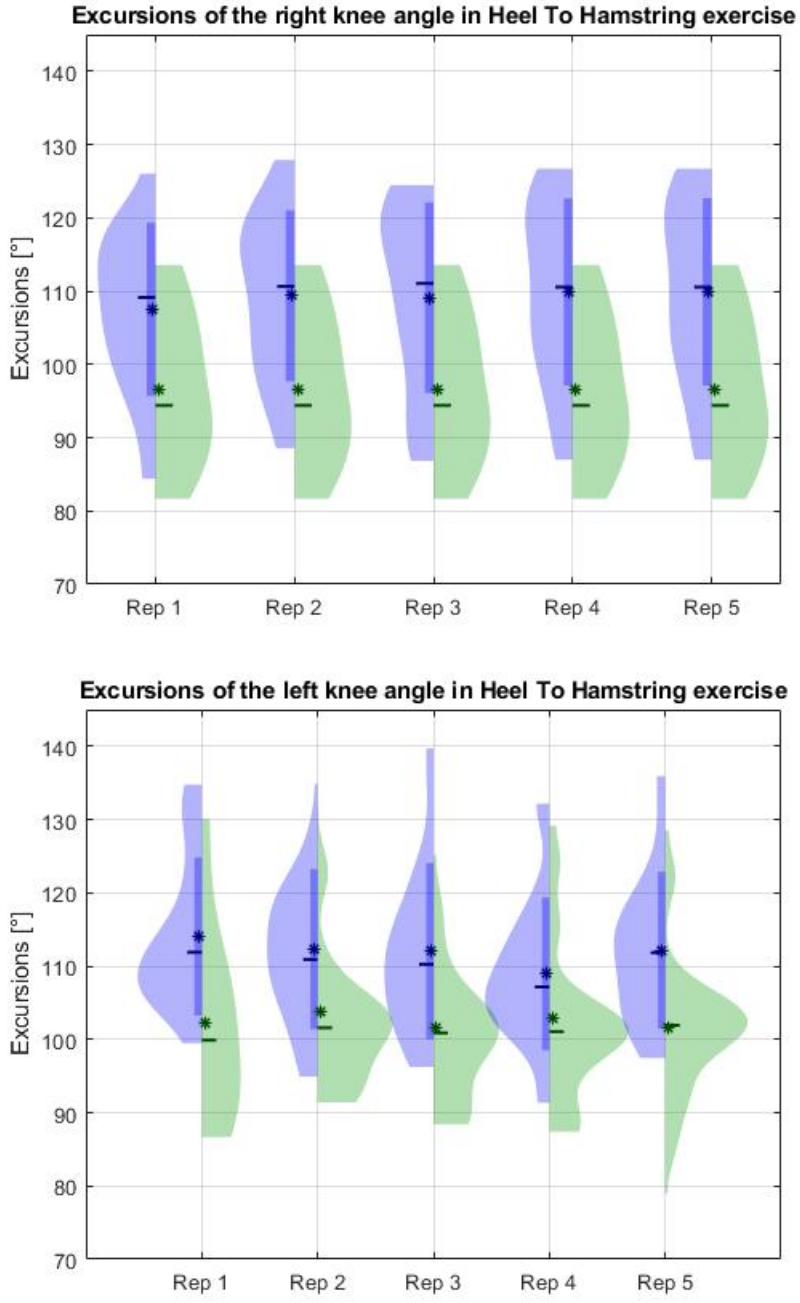

Figure 6.9: Violin plots of the HTH exercise knee flexion angle excursions for each repetition (x-axis), in blue is the underwater distribution, in green is the one on land measured with TinyTag sensors.

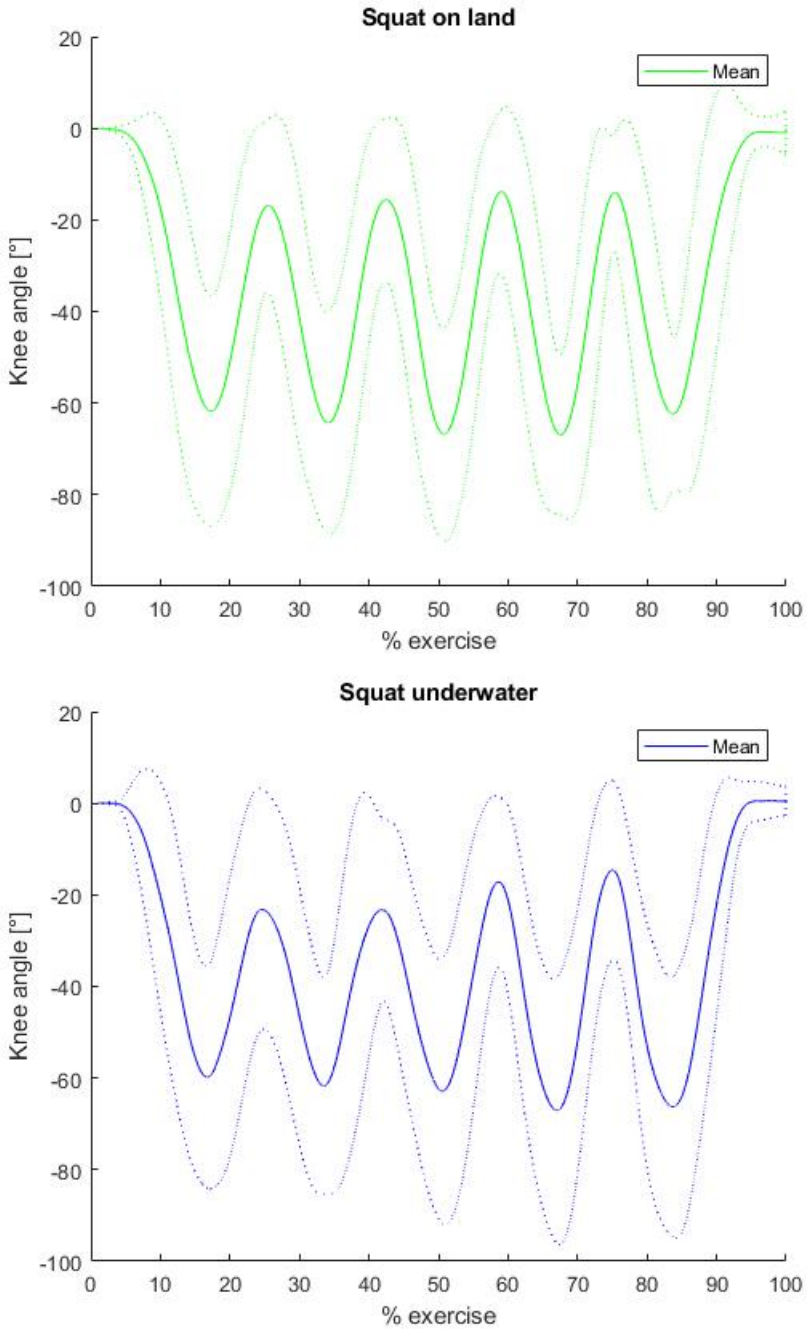

Figure 6.10: Physiological ROM of the S exercise with the std reported as dotted lines, in blue is the underwater distribution, in green is the one on land measured with TinyTag sensors.

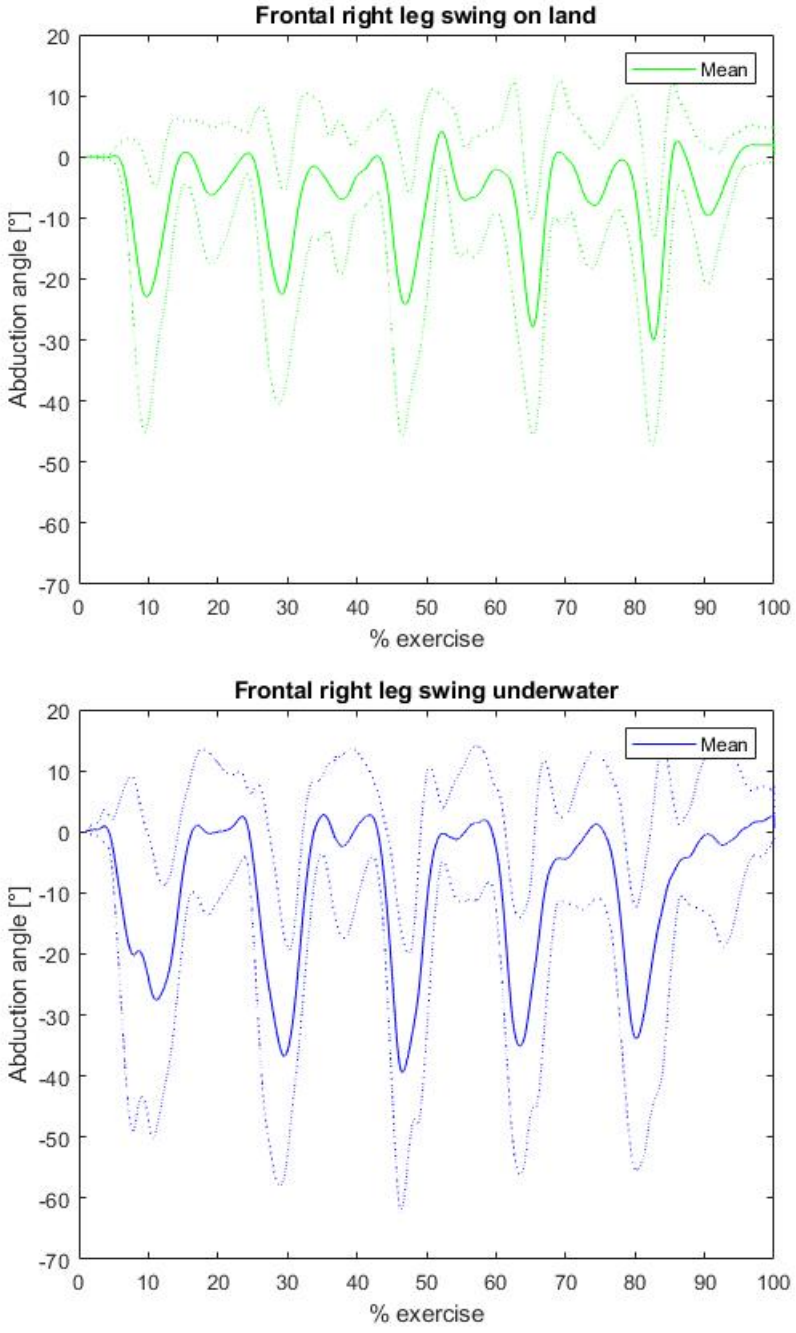

Figure 6.11: Physiological ROM of the right FLS exercise with the std reported as dotted lines, in blue is the underwater distribution, in green is the one on land measured with TinyTag sensors.

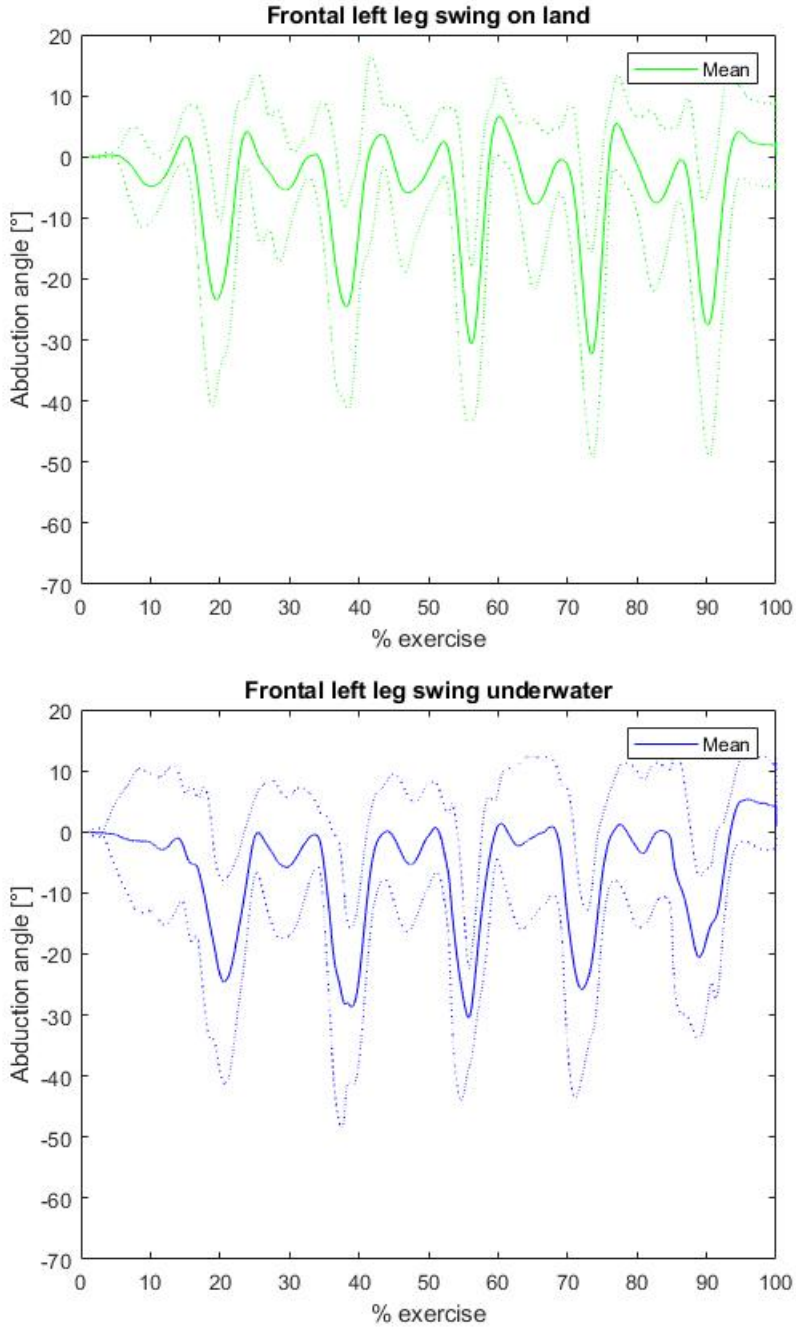

Figure 6.12: Physiological ROM of the left FLS exercise with the std reported as dotted lines, in blue is the underwater distribution, in green is the one on land measured with TinyTag sensors.

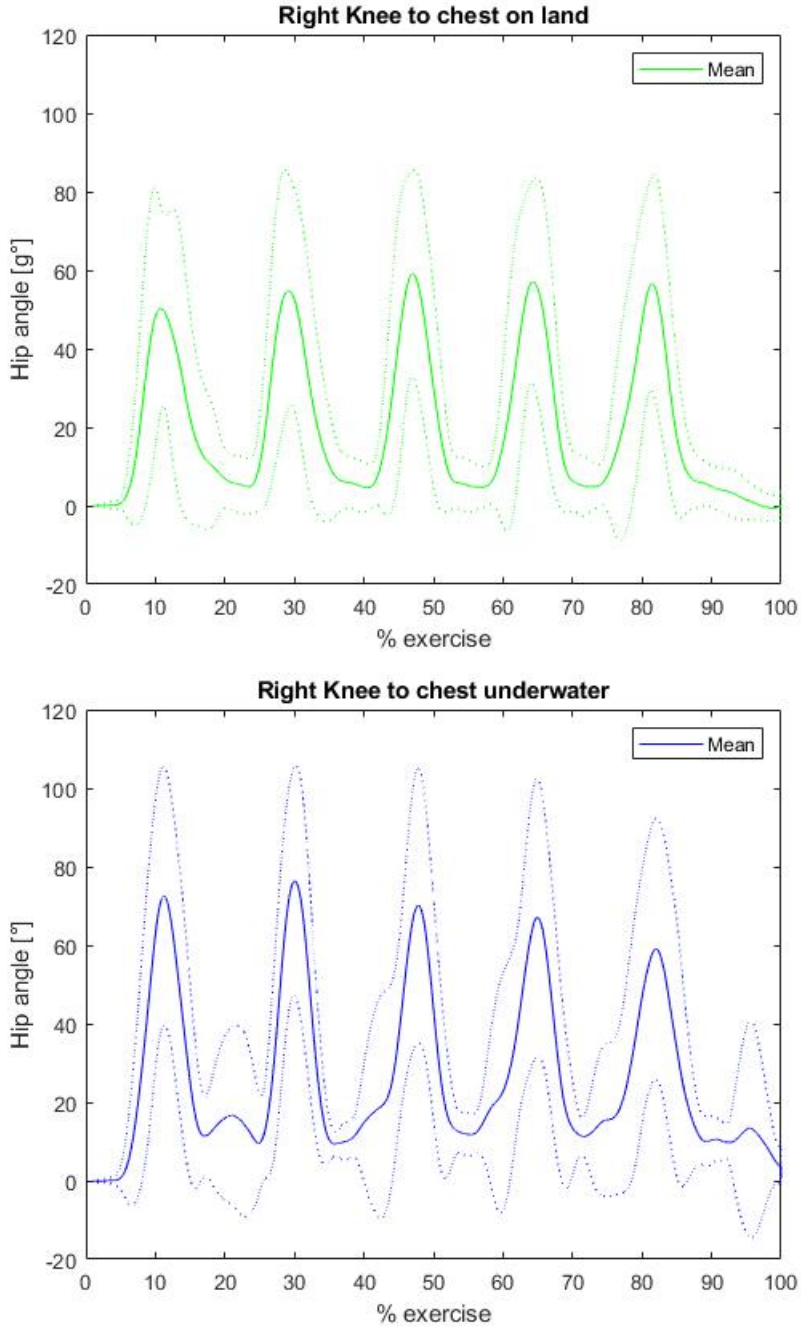

Figure 6.13: Physiological ROM of the right KTC exercise with the std reported as dotted lines, in blue is the underwater distribution, in green is the one on land measured with TinyTag sensors.

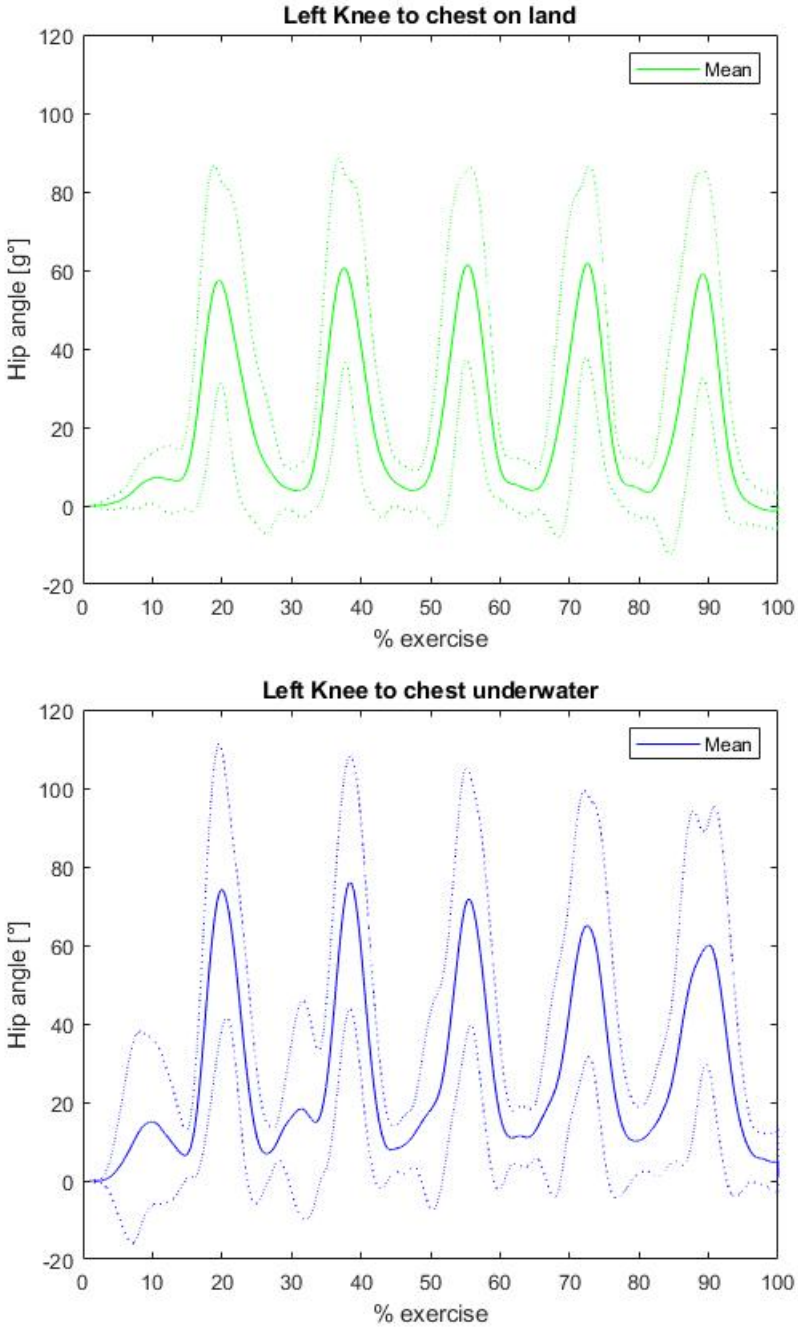

Figure 6.14: Physiological ROM of the left KTC exercise with the std reported as dotted lines, in blue is the underwater distribution, in green is the one on land measured with TinyTag sensors.

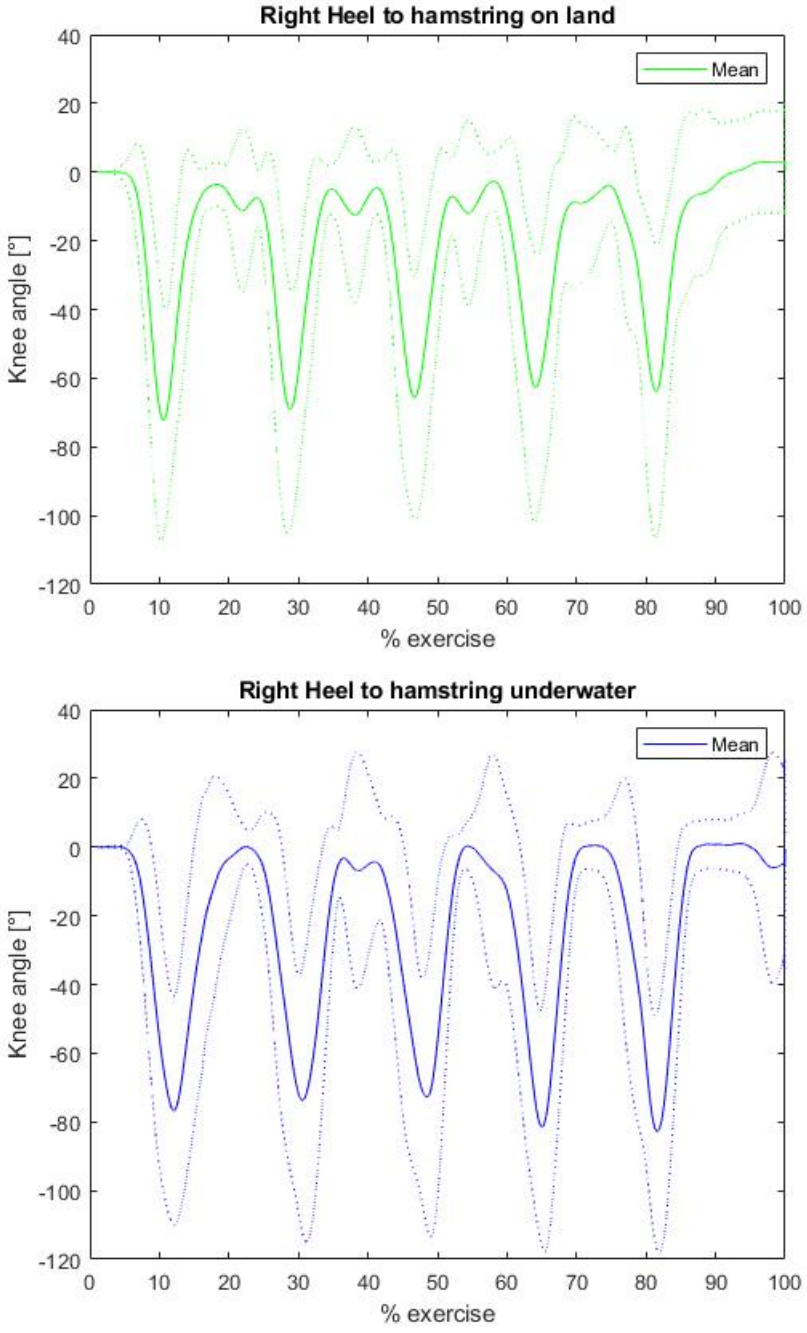

Figure 6.15: Physiological ROM of the right HTH exercise with the std reported as dotted lines, in blue is the underwater distribution, in green is the one on land measured with TinyTag sensors.

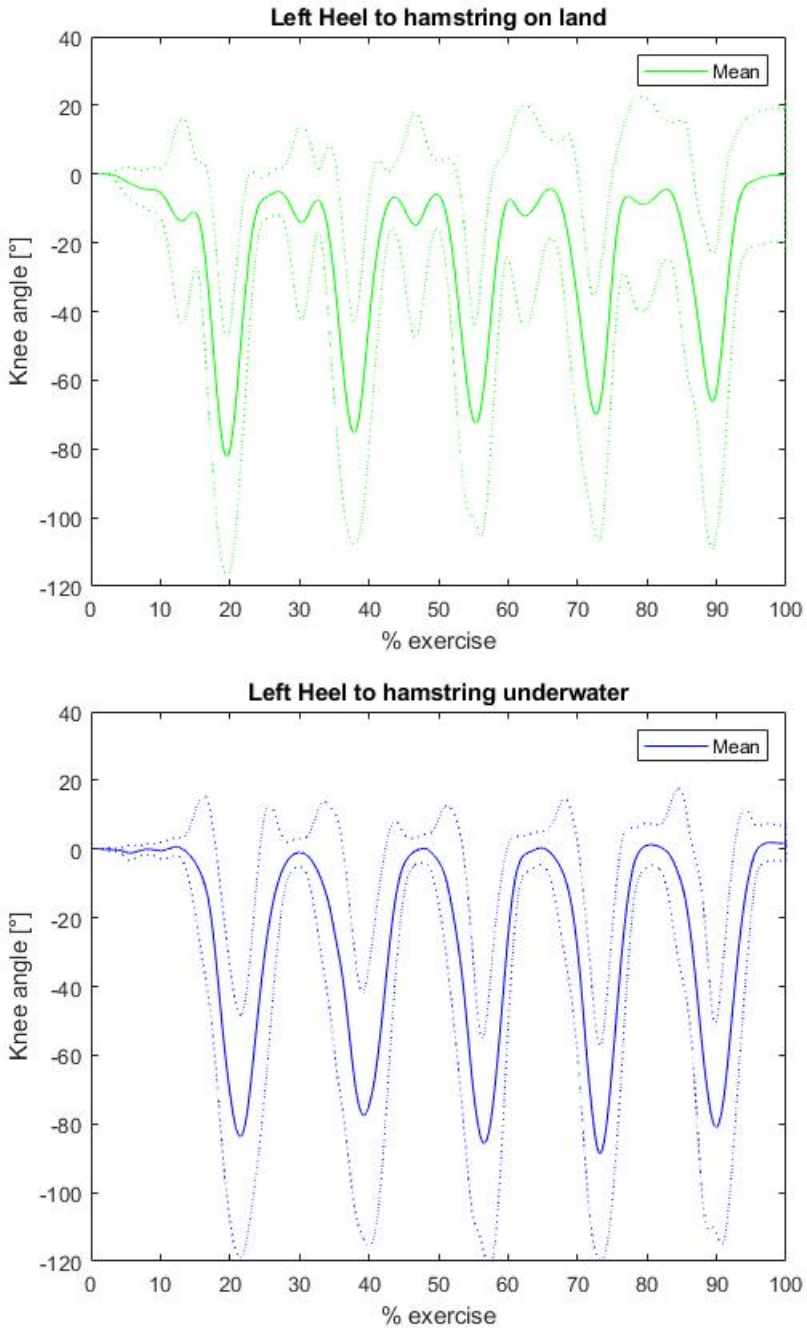

Figure 6.16: Physiological ROM of the left HTH exercise with the std reported as dotted lines, in blue is the underwater distribution, in green is the one on land measured with TinyTag sensors.

6.2.2. Males - Females comparison

To further investigate the physiological ROM, male and female ROM presented in the previous section were considered separately, regardless of the measurement environment. In Table 6.7 are reported the results.

	MALE	FEMALE	DIFFERENCE
S [°]	84.89 (±12.00)	79.59 (±11.73)	5.3(6.4%)
FLS [°]	43.88 (±13.50)	49.71 (±10.41)	-5.83(-12.4%)
KTC [°]	93.03 (±13.02)	85.74(±13.68)	7.29(8.1%)
HTH [°]	105.04 (±9.19)	103.65 (±11.74)	1.39(1.3%)

Table 6.7: Table with the mean values and SD of the excursion in the 4 exercises divided by gender measured with TinyTag sensors.

As can be seen in Table 6.7, female subjects performed a larger ROM only for the S, but in general, a big difference between the two genders is not appreciable, with a maximum value of difference equal to 7.29° for KTC.

7 | Discussion

The discussion chapter is divided into the two phases to be clearer in the exposition.

7.1. Phase 1

This first phase is focused on the validation of the inverse kinematic analysis performed by the OpenSim software with the inertial sensor information, comparing it to the one performed by the MOCAP, the gold standard for motion analysis. As this study is based on performing simple motor exercises, this section will be divided to analyse each and discuss the results obtained.

7.1.1. Squat

This is a very slow and controlled exercise and allowed all three measuring systems to follow the variations in knee angle, the focus of the analysis on this task, thus revealing a perfect concordance between all the results obtained. The RMSE of the TinyTag system compared to the MOCAP is around 2,5° with a very low standard deviation making the two measurements comparable. All the other indexes are excellent (Section 6.1.1), both correlation coefficients are near to the unity which implies a high level of concordance and the bias of the difference is almost zero. This can be visualized in Figure 6.1 where the Bland-Altman plot gives an idea of the good correlation. Indeed, all the measures even in the worst case obtained are in a range very small.
Additionally, the Xsens system works well, with an even lower error, close to 1°, and perfect correlation indexes. Therefore both approaches can be used to successfully analyze the movement as shown in Figure 7.1.

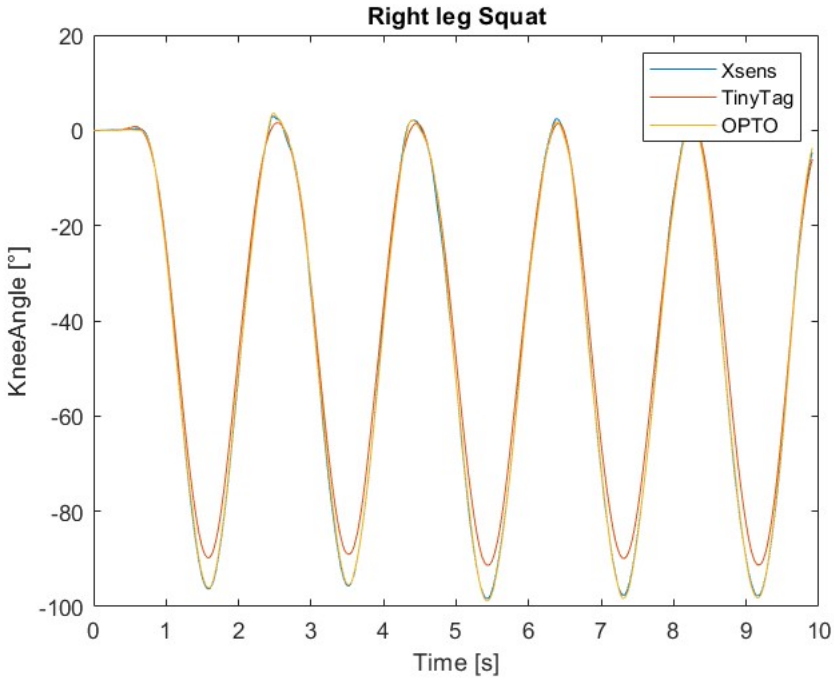

Figure 7.1: Graph of right leg Squat comparison for the three measurements systems

7.1.2. Frontal leg swing

For FLS the joint of interest was the hip abduction/adduction on the frontal plane. Both the systems, but especially the TinyTag, seem not capable of acquiring the movement in a correct way with respect to the MOCAP, as can be seen by the values of the statistical indexes like the value of RMSE, around 10° for TinyTag or the mean bias of the Bland-Altman plot equal to 2.4° for Xsens. This limitation can be seen also in a visual way in Figure 7.2, showing how neither of the IMU systems is equal to the MOCAP trajectory. The cause of this error is, probably, related to the software OpenSense itself, since even

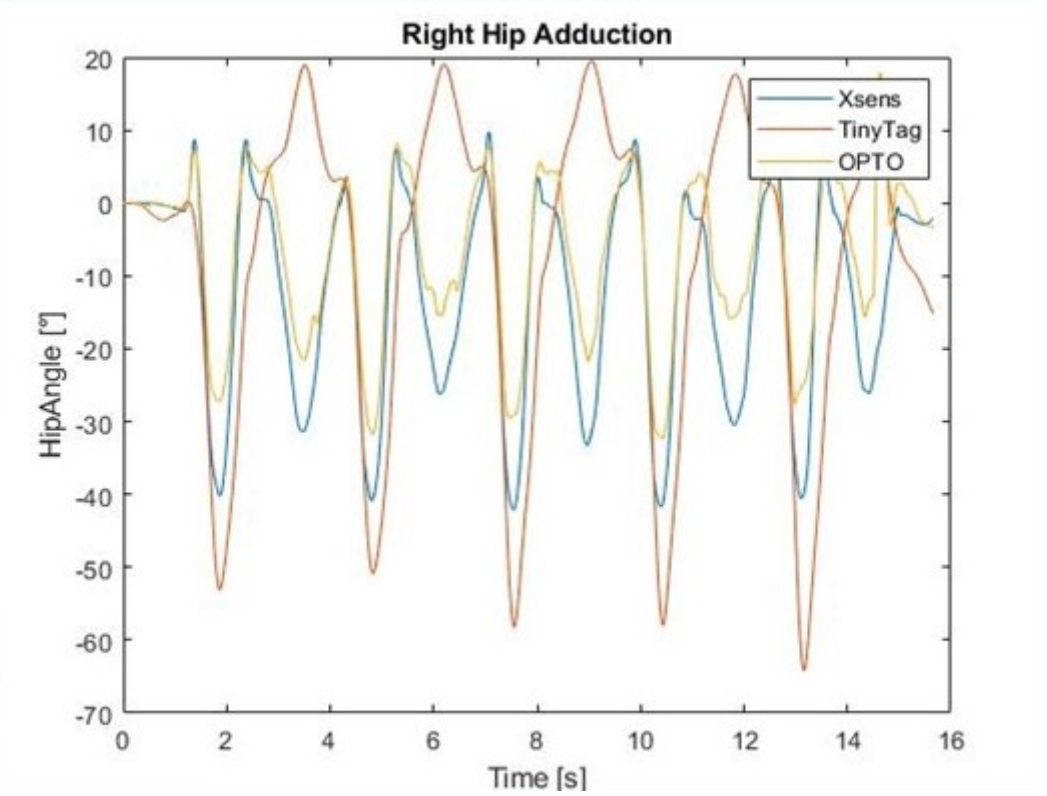

Figure 7.2: Example of the abduction angle in the FLS captured by the 3 systems.

the Xsens IMUs, which should be accurate [48], don't follow the behaviour of the MOCAP. The difference in measuring could be related to the fact that this movement is the only one that lays on the frontal plane, while the other studied angles are on the sagittal plane. For the TinyTag, it is observed an incorrect evaluation of the excursion made and also, in some cases like in Figure 7.2, a wrong interpretation of the movement, resulting in an opposite behaviour of the joint angle plot.

In the **second phase** of this study, it was also noticed that a small number of subjects showed a different ROM behavior in the FLS exercise. When the abduction angle was plotted for most of the subjects the graph look like the one on right in Figure 7.3, very

close to the one observed by MOCAP during the validation, but for some other subjects it had a different trend: the one in the left side of Figure 7.3.

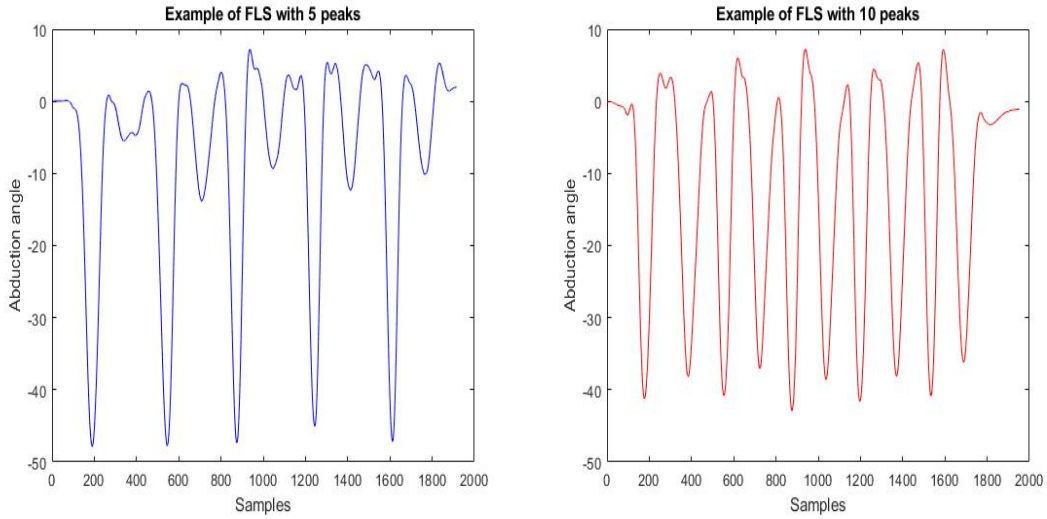

Figure 7.3: Example of graphs of the FLS exercise with 5 (left) and 10 valleys (right).

As can be seen, there are double the valleys on the right side of the Figure. The explanation is to be searched inside the values of the abduction angle itself and in the video recorded. In every case similar to the left image in Figure 7.3 the subject involved an inclination of the pelvis when abducting the leg, in order to achieve a larger ROM, instead, when the subject didn't involve the tilting of the pelvis, the graph is with 5 valleys as on the right in Figure 7.3.

7.1.3. Knee to chest

For KTC the joint considered is the hip and its flexion/extension on the sagittal plane. In this exercise, the RMSE of the TinyTag sensors (around 5°) and the correlation indexes (>0.85) are still acceptable, even though they are not ideal. The bias of the Bland-Altman (average of 4.82°) suggests that the problem could be related to a systematic difference between the two systems.
Regarding the Xsens sensors, the accuracy is higher than TinyTag but there is still a bias (average of -3.36°) in the Bland-Altman plot that suggests that there could be a disagreement like in the TinyTag.
As shown in the example data in Figure 7.4, the two IMUs systems, have two different trends. The TinyTag underestimates the excursion performed, while the Xsens overestimates the ROM of the joint. The MOCAP is usually in the middle between the two IMUs systems.

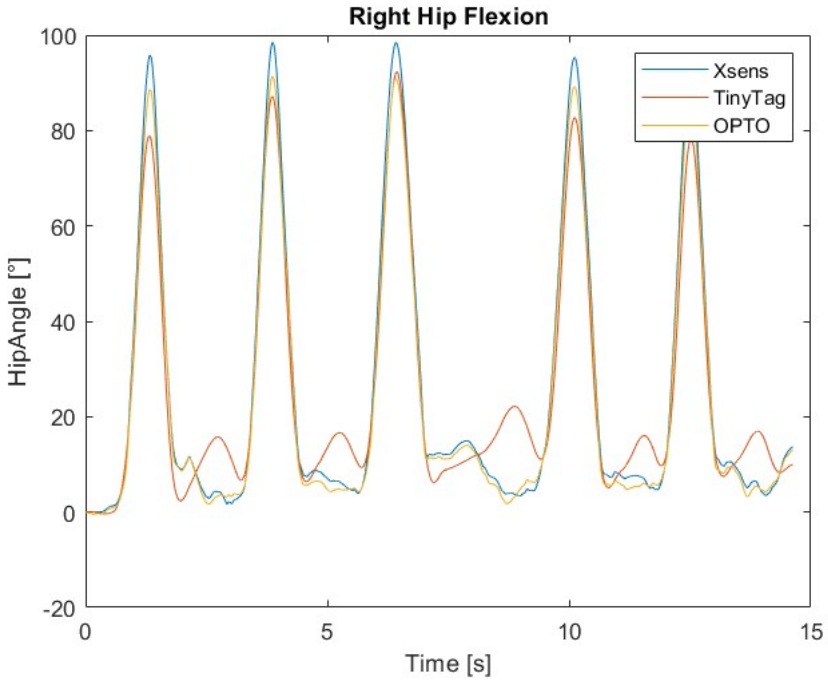

Figure 7.4: Graph of right leg KTC comparison for the three measurements systems

7.1.4. Heel to hamstring

In this exercise the same angle of the S exercise is analyzed, the knee angle, obtained from the knee flexion/extension on the sagittal plane. But the results are not similar between the two tasks.
The exercise of the HTH suffers from the drift, an error summation over time of the gyroscope and the magnetometer that cause the shift of acquired data [87]. The presence of the drift is appreciable from the indexes estimated, in particular from the bias in the Bland-Altman plots (around 10.7°) and from Figure 7.5, which shows an example data of the exercise where the knee angle is assessed by the three motion capture systems.

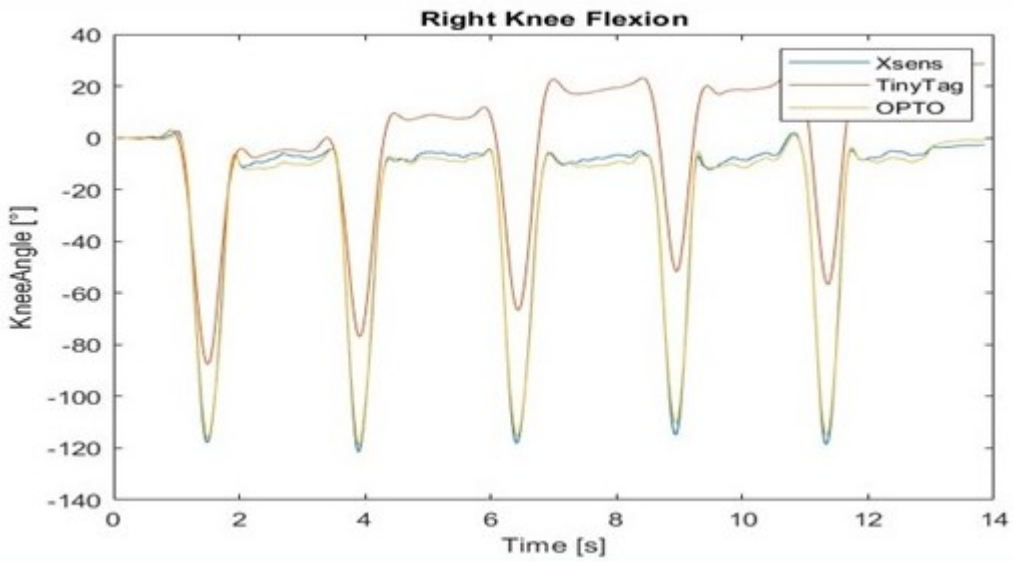

Figure 7.5: Effect of the drift in the HTH exercise

The possible causes of the drift are multiple:

- Electromagnetic field sources: the laboratory, where the validation phase took place, is filled with technologies and this environment, full of variable electromagnetic fields, can affect the data acquired by the magnetometer. In fact, the drift is lower in the data collected during the phase 2 exercise (Figure 6.15) because it was performed inside a pool without considerable external electromagnetic fields.
- Dynamics of the exercise: HTH is a highly dynamic exercise and it has been proven that this kind of movement tends to be harder to investigate via IMU, especially with a frequency of acquisition equal to 100Hz [33]. To examine this issue and demonstrate that out of the four exercises analyzed, this is the most dynamic one the maximum acceleration was calculated and displayed in Table 7.1. The values are obtained as the average of the maximum acceleration referring to the marker

located on the foot captured by the MOCAP during Phase 1 among all the sessions.

	S	FLS	KTC	HTH
Acc [m/s2]	4.443	4.011	11.768	19.400

Table 7.1: Maximum acceleration obtained from MOCAP for each exercise where can be seen how the HTH has the higher value.

- Time: According to the protocol presented in Section 5.4.1, HTH is the last exercise performed and since the error of the drift is a summation over time, it has the biggest impact on this exercise. To prove that, another acquisition was made, doing this exercise as first and the results (Figure 7.6) showed how there is almost no drift effect, but simply fluctuations of the measurement.

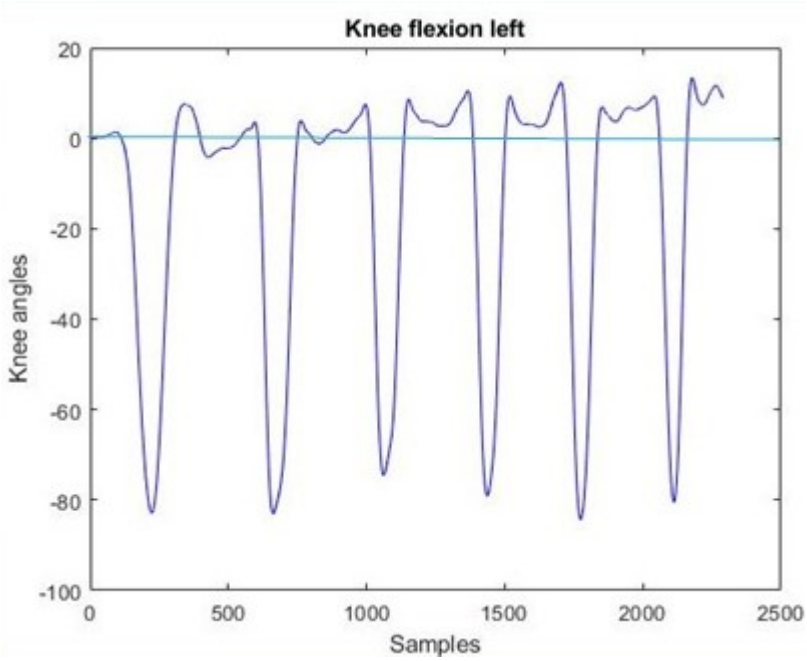

Figure 7.6: Results of the knee angle when HTH is the first exercise, with less drift shown.

For what concerns the Xsens, they showed overall good results for the HTH exercise, with an average RMSE equal to 1.56° and good values in all the correlation indexes.
Phase 1 showed how the new method is able to well follow the motion when it's controlled and when the duration of the acquisition is kept low. But it highlighted also the limitation on the frontal plane and on the long duration of acquisition.

7.2. Phase 2

The aim of phase 2 of the thesis is to establish the joint angle range, common to the entire recruited population, by analysing the previously described exercises both in and out of the water. The performed movements are commonly used in water rehabilitation, and therefore, the results obtained in this thesis could be used as a discriminating parameter to assess if the execution by a subject is pathological or not, according to its resemblance with the patterns defined

7.2.1. Underwater- On land comparison

In Table 6.6 are reported the mean values of ROM over the four exercises in the two environments. It can be seen that the excursion is higher underwater with respect to the one on land, in particular, in the exercise where the balance is given by only one foot, like FLS, KTC and HTH. This aspect is crucial because the water environment helps the subject in maintaining balance, allowing a more controlled exercise performance with a larger ROM (difference of $> 10\%$).
Talking about the S, the difference between the two environments is minimal (around 1°). This could be due to the depth of the pool, which for shorter subjects, would force them to put their heads under the water to perform the entire movement. Since the instruction was to perform the movement freely, some of them decided not to put their head in the water, limiting the expressed ROM. This aspect could explain why the S is the only exercise where there is no major difference between the execution in the two environments.
Considering possible applications in rehabilitation processes, it can be said that the FSL, KTC and HTH exercises should be taken into serious consideration since, in water, a higher ROM is allowed and the fluid has a double effect: it helps maintain balance and enhance the muscles involvement by adding more resistance to the movement. Both these features are very positive in the rehabilitation process where the aim is to try to stimulate the body without taking risks of any kind.
From the violin plots, some interesting facts can be analysed. In the graph of the S exercise (Figure 6.6) the water distribution grows with the repetitions, in fact, in the first rep the distribution is similar to the one on land, but then with the gaining of confidence also the ROM becomes larger. A similar discussion can be said on the FLS exercise, but rather than that instead, Figure 6.7 shows a difference in behaviours on land: the excursion of the left leg is smaller than the one of the right leg. About the KTC exercise (Figure 6.8), no difference between the left and right limb is noticed, but an important

gap between water and land is shown, in fact, all the repetitions underwater have larger ROM than the ones on land. Finally, in the HTH exercise, there is a similarity with the case of KTC, as can be seen in Figure 6.9, the water distribution has higher values than the one on land.

7.2.2. Males - Females comparison

Regarding the comparison between ROM of males and females, no significant differences are underlined. Table 6.7 reported the angles analysed reached by both genders and also their differences. In the HTH the difference of 1,39 is irrelevant, instead for the KTC the males seem to be able to carry their thighs higher than females, thanks perhaps to the superior strength of the femoral muscles. This consideration can also be motivated by the results obtained from the questionnaire (reported in Appendix D) submitted to the subjects, which show that most male participants have on average a higher number of workouts per week than female participants (Table 7.2).

	Number of partecipants	**Number of workouts per week**
All	15	1,86 (± 0,91)
Male	8	2,1 (± 0,64)
Female	7	1,57 (± 1,1)

Table 7.2: Number and number of weekly workouts of the subjects recruited for physiological ROM assessment

In contrast, the exercise of FLS shows that females achieve a greater abduction angle than males, which could be explained by the former's greater elasticity and flexibility. As these reflections refer to very low numbers, they cannot be defined as statistically relevant for all the young adult population as they could be limited mainly to the subjects recruited for the experiment.

7.3. Technical limitations and challenges

This section will explain the limitations faced with the measuring instruments used in this study and also those relating to OpenSim open-source software.

7.3.1. Optoelectronic system limitations

Starting from the **MOCAP**, being the gold standard method implies that it's the most accurate system in the research field, but the limitations of its reliability are important.

First of all, as mentioned before, it can be used only in a controlled laboratory environment hence the water environment and all experiments on water rehabilitation are excluded. Secondly, focusing on the steps followed in this project:

- Prior to beginning the experiment, it was necessary to take anthropometric measurements of the test subjects, a step that is not required when using inertial sensors;
- Marker positioning phase is crucial for accurate measurements, requires the person to wear only underwear and is time-consuming.
- During data processing, in the frame-by-frame marker tracking phase, besides being a very time-consuming step (around 30 minutes for each subject's repetitions), it is possible that this period is further increased by the fact that not all markers were visible in some frames and a relabelled process was needed. In the motor exercises of S and HTH there was the possibility that the subject's own body covered the markers on the pelvis and great trochanter and thus made it more difficult to associate the labels useful for the Smart Anlayser protocol.

7.3.2. IMUs systems limitations

Moving to the **Xsens IMUs system**, the sensors themselves are not too large or heavy to disturb the movement of the subject, but the bands, supplied by the manufacturer, can be cluttered. Moreover, it happens frequently that, during the performance of exercise, the software gives communication problems caused by loss of calibration and the entire session needed to be re-performed. This problem is probably due to the presence of many sources of electromagnetic fields in the laboratory where validation experiments were carried out, which may cause misreading from the magnetometer, constraining the XSense fusion algorithm.

About the **TinyTag IMUs system**, it must always be taken into account that the smaller, and therefore less invasive, and more sensitive the sensors, the shorter the battery life. This is why the duration of the battery must be taken into account when designing the experimental protocol with this measurement system. Another limit is the impossibility of having measurements for biomechanical applications in real-time, to solve this a radio module should be added. The sensor does not provide feedback regarding its status, other than that of being on or off, so any problems with signal acquisition can only be detected once data are imported into the computer. Furthermore, unlike commercially available sensors, TinyTags require manual calibration and synchronisation, which was done by means of a coil using the magnetometer signal, as well as the fusion of information between the accelerometer, magnetometer and gyroscope, which was done by the researchers of

this study.

When using IMU sensor-based systems for biomechanical measurements, it is also important to emphasize the importance of the environment surrounding the analyzed subject with regard to magnetic disturbances. The acquisitions took place in the motion analysis laboratory for the validation study, as it required the MOCAP. The quality of the acquired data and consequently the results obtained appeared to be highly affected by disturbances related to unwanted ferromagnetic sources. In the second phase of experimentation, on the other hand, both sessions were conducted in the swimming pool, which had very few computers and electronic equipment, so the data seemed to be cleaner from this issue.

7.3.3. OpenSense limitations

Concerning the OpenSense workflow with inertial sensor signals as input, this study pointed out a strong restriction, regardless of the commercial or prototypical nature of the IMUs. The virtual model created to mimic the performed movements seems to be unable to display displacements of the pelvis in any direction but only rotation around its own axis. This was discovered when the S exercise was studied, which involves lowering the pelvis in the posterior direction and then returning to the standing position with both feet fixed to the ground. In this case, the skeleton shown by the open-source software was capable of performing the correct movement with the correct knee angle excursion, but the visualisation was incorrect as it involved bringing the knees closer to the chest instead of lowering the pelvis to the floor, as shown in Figure 7.7.
In addition to that the limit on following movements on the frontal plane, already presented in Section 7.1.2 could be linked to the same issue of the translation of the pelvis that instead of being seen as in the MOCAP it is transformed in an unrealistic tilting of the pelvis itself.

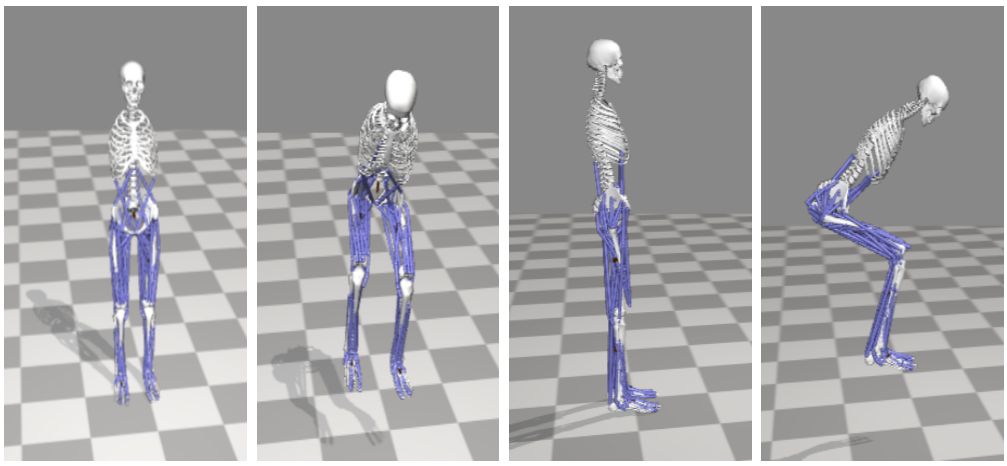

Figure 7.7: OpenSense digital twin of the S exercise. Frontal standing view(left border); Frontal S view(left); Lateral standing view (right); Lateral S view (right border)

7.4. Limits of the study

This section is about the actual limitations of this study that could possibly be improved in future trials to achieve better results. Certainly, to obtain a statistically relevant validation study, more than two subjects are necessary. In this study, the focus was on the OpenSense workflow's ability to correctly calculate kinematic variables using different IMU sensor prototypes than those already tested, and apply such technology and method to the water environment, this could also be done involving a smaller number of participants. A similar comment can be made for the second phase, in which a true physiological range can only be defined if thousands of subjects are recruited. This study, therefore, aims to be a starting point for future studies that can enlarge the pool of subjects recruited and achieve even better results.

Another limitation is the misplacement of TinyTags during both phases. These sensors are very small, which is a huge advantage for patient measurements because they do not create clutter, but at the same time make them very difficult to hold firmly on the body surface. For this study, Velcro strips of the same size but of different lengths according to the circumferences of the body segments of the various subjects were used. The researchers did the positioning manually at the beginning of each session for each subject. Although an attempt was made to follow a unique methodology, ensuring consistency, this step may have influenced the measurement of a slightly different signal between the subjects but also of the same subject in the two sessions. Moreover, relative motion between the sensor and the body (skin friction) and displacement of the sensor in time added even more variability. In the future, the participant could be equipped with a wetsuit with compartments where to place the sensors; this would mitigate the problem.
Among the above-mentioned problems of the second phase (Section 7.2) was the excessive height of the pool water, which for the S exercise limited the movement performed by some subjects. In a subsequent study, it could be decided to use rehabilitation pools and adjust them according to the height of the subject.

8 | Conclusions and future developments

Inertial measurement systems (IMUs) are the most promising devices for human motion capture thanks to their possibility to be used in all kinds of environments, without interfering with the motion of the body. Unfortunately, commercial systems that provide also a visualization tool for the recorded data are usually quite expensive and there is no simple method to visualize the data acquired by experimental IMUs.
This study aims to demonstrate whether it is possible to obtain a simple and straightforward visualization of IMU data free of charge and easy to understand for clinicians. In particular, the main objective is to validate a new algorithm of motion analysis based on waterproof prototypical IMUs (TinyTag) developed by TalTech University. This method uses open-source software (OpenSense) for visualization and computation of kinematic parameters to be used to set a benchmark physiological Range Of Motion (ROM) of lower limbs for underwater rehabilitation exercises.
In the **first phase** of validation, the results showed the qualities of the TinyTag system in measuring the knee angle in the Squat (S) and hip angle in Knee-to-chest exercises (KTC), but they also underlined the flaws of this method to assess the knee angle in the Frontal-leg-swing (FLS) and hip angle in Heel-to-hamstring (HTH) exercises.
For the S and KTC motions, the new system could replace the gold standard for the acquisition and evaluation of inverse kinematics with an acceptable error of less than 5° on average. But the FLS exercise suffers from two defects: the main plane of the exercise is the frontal one, instead, most of the time the interest is on the sagittal plane and the impossibility of pelvis translation by OpenSense, causing a difference with respect to the optoelectronic system. This observed error highlighted the limitation of the software OpenSense, because, even the already validated Xsens IMU showed this error, therefore is not about the sensors.
For what concerns the HTH, the discrepancy is clear and the reason is to be ascribed to the effect of the drift in the raw data of the TinyTag. This phenomenon causes a summation over time that ultimately creates a difference in the results. For what concerns the

HTH, the misrepresentation is clear and the reason is to be ascribed to the effect of the drift in the raw data. This phenomenon causes a summation over time that ultimately creates a difference in the results.
However, the Tinytag could be appropriately utilized to measure the change in large motion or gait abnormalities in settings where an optoelectronic system was not practical or accessible. For future studies, it could be interesting to look for a better way to reduce the drift effect, so that the duration of the acquisition can be longer. From the visualization point of view, in the S exercise, OpenSim has proven to be unreliable as a graphical display method, and the optoelectronic system is preferred because of model constraints, that lock the pelvis in the same location, therefore are the legs that ascend instead of the pelvis that goes down. Next studies could integrate the possibility of creating a musculoskeletal model *.osim* consisting of a kinematic chain referring to feet fixed to the ground allowing the pelvis movement.

About **second phase**, the results showed that the joint ROM measured in the water is larger than the one on land, especially in the exercises where the balance is borne by only one foot, such as FLS, KTC and HTH. Only in the S exercise, no difference has been noticed, but this is probably due to the depth of the pool, which forced the subjects to put their head underwater to fully implement the motion, therefore most of the partecipants decided to reduce the ROM in order to have their head always out of the water.
As already seen from other studies water has beneficial effects on the subject and improves the quality of movement by unloading the weight on the joints and ensuring safety and balance. These aspects summed with the larger ROM and higher resistance on the muscles give these exercises some very interesting features, that should be taken into serious consideration in the rehabilitation processes.
A subsequent study could exploit other features of OpenSense to study the difference in stretching of muscles during similar motor exercises in water and on land, using a larger population sample. Moreover, the method could be used in a rehabilitation context to measure the progress or monitor the situation at different time stamps.

Bibliography

[1] S. L. Delp, F. C. Anderson, A. S. Arnold, P. Loan, A. Habib, C. T. John, E. Guendelman, and D. G. Thelen, "Opensim: Open-source software to create and analyze dynamic simulations of movement," *IEEE Transactions on Biomedical Engineering*, vol. 54, pp. 1940–1950, 2007.

[2] "How markerless motion capture analysis is changing musculoskeletal recovery, performance and health," 2020.

[3] P. Das, B. Massingil, W. Hoogstra, E. A. Jesser, and Y. Lee, "Quantifying concurrent validity of gait kinematics provided by xsens mvn imu system," *Abstracts of the 27th Annual Meeting of the GCMAS*, 2022.

[4] S. Möller, B. Debrabant, U. Halekoh, A. K. Petersen, and O. Gerke, "An extension of the bland–altman plot for analyzing the agreement of more than two raters," *Diagnostics*, vol. 11, 2021.

[5] H. S. Singer, J. W. Mink, D. L. Gilbert, and J. Jankovic, "Chapter 5 - motor assessments," in *Movement Disorders in Childhood (Second Edition)* (H. S. Singer, J. W. Mink, D. L. Gilbert, and J. Jankovic, eds.), pp. 57–66, Boston: Academic Press, second edition ed., 2016.

[6] R. R. Inawat, *Kinematic analysis of the glenohumeral joint: A comparison of post-operative rotator cuff repair patients and controls*. PhD thesis, Marquette University, 2014.

[7] A. Mooventhan and L. Nivethitha, "Scientific evidence-based effects of hydrotherapy on various systems of the body," *North American journal of medical sciences*, vol. 6, no. 5, p. 199, 2014.

[8] A. Demeco, A. de Sire, N. Marotta, A. Palumbo, G. Fragomeni, V. Gramigna, R. Pellegrino, L. Moggio, A. Petraroli, T. Iona, T. Paolucci, and A. Ammendolia, "Effectiveness of rehabilitation through kinematic analysis of upper limb functioning in wheelchair basketball athletes: A pilot study," *Applied Sciences*, vol. 12, p. 2929, Mar 2022.

[9] C. Monoli, J. F. Fuentez-Pérez, N. Cau, P. Capodaglio, M. Galli, and J. A. Tuhtan, "Land and underwater gait analysis using wearable imu," *IEEE Sensors Journal*, vol. 21, no. 9, pp. 11192–11202, 2021.

[10] A. Seth, M. A. Sherman, J. A. Reinbolt, and S. L. Delp, "Opensim: a musculoskeletal modeling and simulation framework for in silico investigations and exchange.," *Procedia IUTAM*, vol. 2, pp. 212–232, 2011.

[11] "Opensense - kinematics with imu data."

[12] L. Torres-Ronda and X. S. i del Alcázar, "The properties of water and their applications for training," *Journal of human kinetics*, vol. 44, p. 237, 2014.

[13] M. Cortesi, A. Giovanardi, S. Fantozzi, D. Borra, and G. Gatta, "Aquatic therapy after anterior cruciate ligament surgery: A case study on underwater gait analysis using inertial and magnetic sensors," *Int. J. Phys. Ther. Rehabil*, vol. 2, 2016.

[14] F. Routhier, N. C. Duclos, É. Lacroix, J. Lettre, E. Turcotte, N. Hamel, F. Michaud, C. Duclos, P. S. Archambault, and L. J. Bouyer, "Clinicians' perspectives on inertial measurement units in clinical practice," *PLoS One*, vol. 15, no. 11, p. e0241922, 2020.

[15] I. Gasparini, "Development of a protocol based on inertial sensors for underwater rehabilitation," Master's thesis, Politecnico di Milano, 2021.

[16] K.-N. An and E. Chao, "Kinematic analysis," in *Biomechanics of the wrist joint*, pp. 23–36, Springer, 1991.

[17] D. A. Winter, *Biomechanics and motor control of human gait: normal, elderly and pathological*. 1991.

[18] M. Salim, H. Lim, M. Salim, and M. Baharuddin, "Motion analysis of arm movement during badminton smash," in *2010 IEEE EMBS Conference on Biomedical Engineering and Sciences (IECBES)*, pp. 111–114, 2010.

[19] N. Hesse, S. Pujades, J. Romero, M. J. Black, C. Bodensteiner, M. Arens, U. G. Hofmann, U. Tacke, M. Hadders-Algra, R. Weinberger, *et al.*, "Learning an infant body model from rgb-d data for accurate full body motion analysis," in *International Conference on Medical Image Computing and Computer-Assisted Intervention*, pp. 792–800, Springer, 2018.

[20] J. Soucie, C. Wang, A. Forsyth, S. Funk, M. Denny, K. Roach, D. Boone, and H. T. C. Network, "Range of motion measurements: reference values and a database for comparison studies," *Haemophilia*, vol. 17, no. 3, pp. 500–507, 2011.

[21] P. Kouyoumdjian, R. Coulomb, T. Sanchez, and G. Asencio, "Clinical evaluation of hip joint rotation range of motion in adults," *Orthopaedics & Traumatology: Surgery & Research*, vol. 98, no. 1, pp. 17–23, 2012.

[22] A. Gupta, B. Fernihough, G. Bailey, P. Bombeck, A. Clarke, and D. Hopper, "An evaluation of differences in hip external rotation strength and range of motion between female dancers and non-dancers," *British Journal of Sports Medicine*, vol. 38, no. 6, pp. 778–783, 2004.

[23] J. Loudon, S. Bell, and J. Johnston, "The clinical orthopedic assessment guide," 1998.

[24] J. S. Dufek, B. T. Bates, H. Davis, and L. Malone, "Dynamic performance assessment of selected sport shoes on impact forces.," *Medicine and science in sports and exercise*, vol. 23, no. 9, pp. 1062–1067, 1991.

[25] M. Akhtaruzzaman, A. A. Shafie, and M. R. Khan, "Gait analysis: Systems, technologies, and importance," *Journal of Mechanics in Medicine and Biology*, vol. 16, no. 07, p. 1630003, 2016.

[26] Topley, Matt, Richards, and J. G, "A comparison of currently available optoelectronic motion capture systems," *Journal of Biomechanics*, vol. 106, p. 109820, 2020.

[27] I. Stanić, D. Borojevic, and V. Zanchi, "Human kinematics measuring using a high speed camera and active markers," 2009.

[28] Y. Sekiguchi, T. Kamiyama, T. Hashimoto, and N. Kikuchi, "Development of markerless motion measurement system using stereo camera for squat exercise," *The Proceedings of JSME annual Conference on Robotics and Mechatronics (Robomec)*, 2021.

[29] D. Suvapun, P. Sorachaimetha, T. Junsa-ard, D. Sittakornkovit, P. Onmanee, P. Rimchala, S. Sukhonthan, and J. Pipitpukdee, "The evaluation of sirindhorn national medical rehabilitation centre guideline for prosthetic knee testing," in *Proceedings of the 5th International Conference on Rehabilitation Engineering & Assistive Technology*, pp. 1–4, 2011.

[30] I. Loiret, N. Rapin, C. Villa, X. Bonnet, N. Martinet, H. Pillet, and J. Paysant, "Visual gait analysis pocket-sized tool for rehabilitation of lower limb amputees," *Annals of Physical and Rehabilitation Medicine*, vol. 60, pp. e37–e38, 2017.

[31] I. Loiret, V. Sanamane, A. Touillet, N. Martinet, J. Paysant, C. Fournier-Farley, and A.-G. François, "Assessment of multigrip prosthetic hand by a crossover longitudinal study," *Annals of Physical and Rehabilitation Medicine*, vol. 60, p. e34, 2017.

[32] R. Klotz, B. Colobert, M. Botino, and I. Permentiers, "Influence of different types of sockets on the range of motion of the hip joint by the transfemoral amputee," *Annals of physical and rehabilitation medicine*, vol. 54, no. 7, pp. 399–410, 2011.

[33] E. van der Kruk and M. M. Reijne, "Accuracy of human motion capture systems for sport applications; state-of-the-art review," *European Journal of Sport Science*, vol. 18, no. 6, pp. 806–819, 2018. PMID: 29741985.

[34] S. Zihajehzadeh, D. Loh, T. J. Lee, R. Hoskinson, and E. J. Park, "A cascaded kalman filter-based gps/mems-imu integration for sports applications," *Measurement*, vol. 73, pp. 200–210, 2015.

[35] S. Bichler, G. Ogris, V. Kremser, F. Schwab, S. Knott, and A. Baca, "Towards high-precision imu/gps-based stride-parameter determination in an outdoor runners' scenario," *Procedia Engineering*, vol. 34, pp. 592–597, 2012.

[36] M. Kim, C. Park, and J. Yoon, "The design of gnss/imu loosely-coupled integration filter for wearable epts of football players," *Sensors*, vol. 23, no. 4, p. 1749, 2023.

[37] Nasrabadi, A. M, Eslaminia, A. R, Bakhshayesh, P. R, Ejtehadi, Mehdi, A. L, and B. S, "A new scheme for the development of imu-based activity recognition systems for telerehabilitation," *Medical Engineering & Physics*, vol. 108, p. 103876, 2022.

[38] R. E. Mahony, T. Hamel, and J. M. Pflimlin, "Complementary filter design on the special orthogonal group so(3)," *Proceedings of the 44th IEEE Conference on Decision and Control*, pp. 1477–1484, 2005.

[39] J. L. Roux, "An introduction to kalman filter," 2003.

[40] G. Welch and G. Bishop, "Welch & bishop , an introduction to the kalman filter 2 1 the discrete kalman filter in 1960," 1994.

[41] R. E. Mahony, T. Hamel, and J. M. Pflimlin, "Nonlinear complementary filters on the special orthogonal group," *IEEE Transactions on Automatic Control*, vol. 53, pp. 1203–1218, 2008.

[42] S. Madgwick, "An efficient orientation filter for inertial and inertial / magnetic sensor arrays," 2010.

[43] A. I. Cuesta-Vargas, A. Galán-Mercant, and J. M. Williams, "The use of inertial sensors system for human motion analysis," *Physical Therapy Reviews*, vol. 15, no. 6, pp. 462–473, 2010.

[44] M. Schepers, M. Giuberti, G. Bellusci, *et al.*, "Xsens mvn: Consistent tracking of human motion using inertial sensing," *Xsens Technol*, vol. 1, no. 8, 2018.

[45] T. Liu, Y. Inoue, K. Shibata, and K. Shiojima, "A mobile force plate and three-dimensional motion analysis system for three-dimensional gait assessment," *IEEE Sensors Journal*, vol. 12, no. 5, pp. 1461–1467, 2011.

[46] M. D. Iversen, "38 - introduction to physical medicine, physical therapy, and rehabilitation," in *Kelley's Textbook of Rheumatology (Ninth Edition)* (G. S. Firestein, R. C. Budd, S. E. Gabriel, I. B. McInnes, and J. R. O'Dell, eds.), pp. 528–539, Philadelphia: W.B. Saunders, ninth edition ed., 2013.

[47] W. Kim, S. Cho, J. Ku, Y. Kim, K. Lee, H.-J. Hwang, and N.-J. Paik, "Clinical application of virtual reality for upper limb motor rehabilitation in stroke: Review of technologies and clinical evidence," *Journal of Clinical Medicine*, vol. 9, 2020.

[48] M. A. Borno, J. J. O'Day, V. Ibarra, J. J. Dunne, A. Seth, A. Habib, C. F. Ong, J. L. Hicks, S. D. Uhlrich, and S. L. Delp, "Opensense: An open-source toolbox for inertial-measurement-unit-based measurement of lower extremity kinematics over long durations," *Journal of NeuroEngineering and Rehabilitation*, vol. 19, 2021.

[49] R. Colella, M. R. Tumolo, S. Sabina, C. G. Leo, P. Mincarone, R. Guarino, and L. Catarinucci, "Design of uhf rfid sensor-tags for the biomechanical analysis of human body movements," *IEEE Sensors Journal*, vol. 21, no. 13, pp. 14090–14098, 2021.

[50] S. P, K. MJ, D. SL, and C. SH, "Sensing leg movement enhances wearable monitoring of energy expenditure," *Nature Communications*, vol. 12, p. 4312, 07 2021.

[51] B. CA, U. TK, N. J, and G. RB, "Validity and sensitivity of an inertial measurement unit-driven biomechanical model of motor variability for gait," *Sensors(Basel)*, vol. 21, p. 7690, 11 2021.

[52] T. YX, C. YS, G. D, G. AA, N. SG, and T. S, "Quantification of muscles activations and joints range of motions during oil palm fresh fruit bunch harvesting and loose fruit collection," *Scientific Reports*, vol. 11, p. 15020, 07 2021.

[53] D. Mathighatta Nagaraj, D. Werth, and R. Dobinson, "Towards kinematically constrained real time human pose estimation using sparse imus," 01 2021.

[54] G. Raimondo, B. Vanwanseele, A. van der Have, J. Emmerzaal, M. Willems, B. Killen, and I. Jonkers, "Inertial sensor-to-segment calibration for accurate 3d joint angle calculation for use in opensim," *Sensors*, vol. 22, p. 3259, 04 2022.

[55] Q. Bian, D. E. Shepherd, and Z. Ding, "A hybrid method integrating a musculoskeletal model with long short-term memory (lstm) for human motion prediction," in *2022 44th Annual International Conference of the IEEE Engineering in Medicine Biology Society (EMBC)*, pp. 4230–4236, 2022.

[56] J. F. Hafer, J. A. Mihy, A. Hunt, R. F. Zernicke, and R. T. Johnson, "Imu-derived kinematics detect gait differences with age or knee osteoarthritis but differ from marker-derived inverse kinematics," *medRxiv*, 2022.

[57] M. Łyp, R. Kaczor, A. Cabak, P. Tederko, E. Włostowska, I. J. Stanisławska, J. Szypuła, and W. Tomaszewski, "A water rehabilitation program in patients with hip osteoarthritis before and after total hip replacement," *Medical Science Monitor : International Medical Journal of Experimental and Clinical Research*, vol. 22, pp. 2635 – 2642, 2016.

[58] G. Asimenia, M. Paraskevi, S. Polina, B. Anastasia, T. Kyriakos, and G. Georgios, "Aquatic training for ankle instability," *Foot & ankle specialist*, vol. 6, no. 5, pp. 346–351, 2013.

[59] A. Amedoro, A. Berardi, A. Conte, E. Pelosin, D. Valente, G. Maggi, M. Tofani, and G. Galeoto, "The effect of aquatic physical therapy on patients with multiple sclerosis: a systematic review and meta-analysis," *Multiple sclerosis and related disorders*, vol. 41, p. 102022, 2020.

[60] D. Teffaha, L. Mourot, P. Vernochet, F. Ounissi, J. Regnard, C. Monpère, and B. Dugué, "Relevance of water gymnastics in rehabilitation programs in patients with chronic heart failure or coronary artery disease with normal left ventricular function," *Journal of cardiac failure*, vol. 17, no. 8, pp. 676–683, 2011.

[61] J. G. McVeigh, H. McGaughey, M. Hall, and P. Kane, "The effectiveness of hydrotherapy in the management of fibromyalgia syndrome: a systematic review," *Rheumatology international*, vol. 29, no. 2, pp. 119–130, 2008.

[62] S. Rewald, I. Mesters, P. Emans, J. Arts, A. Lenssen, and R. De Bie, "Aquatic circuit training including aqua-cycling in patients with knee osteoarthritis," *J Rehabil Med*, vol. 47, pp. 376–381, 2015.

[63] A. V. S. Ferreira, P. S. A. Goya, R. Ferrari, M. Durán, R. V. Franzini, F. A. Caromano, F. M. Favero, and A. S. B. Oliveira, "Comparison of motor function in patients with duchenne muscular dystrophy in physical therapy in and out of water: 2-year follow-up," *Acta Fisiátrica*, vol. 22, no. 2, pp. 51–54, 2015.

[64] S. Von Mackensen, B. Eifrig, D. Zäch, J. Kalnins, A. Wieloch, and W. Zeller, "The impact of a specific aqua-training for adult haemophilic patients–results of the watercise study (wat-qol)," *Haemophilia*, vol. 18, no. 5, pp. 714–721, 2012.

[65] J. Perk, L. Perk, and C. Bodén, "Cardiorespiratory adaptation of copd patients to physical training on land and in water," *European Respiratory Journal*, vol. 9, no. 2, pp. 248–252, 1996.

[66] M. Lomax, "Airway dysfunction in elite swimmers: prevalence, impact, and challenges," *Open Access Journal of Sports Medicine*, vol. 7, p. 55, 2016.

[67] C. E. Booth, "Water exercise and its effect on balance and gait to reduce the risk of falling in older adults," *Activities, adaptation & aging*, vol. 28, no. 4, pp. 45–57, 2004.

[68] E. Ortega, J. García, M. Bote, L. Martín-Cordero, Y. Escalante, J. Saavedra, H. Northoff, and E. Giraldo, "Exercise in fibromyalgia and related inflammatory disorders: known effects and unknown chances," *Exerc Immunol Rev*, vol. 15, no. 15, pp. 42–65, 2009.

[69] K. Wadell, "Water-based exercise is more effective than land-based exercise for people with copd and physical comorbidities," *Journal of Physiotherapy*, vol. 60, no. 1, pp. 57–57, 2014.

[70] M. Łyp, R. Kaczor, A. Cabak, P. Tederko, E. Włostowska, I. Stanisławska, J. Szypuła, and W. Tomaszewski, "A water rehabilitation program in patients with hip osteoarthritis before and after total hip replacement," *Medical science monitor: international medical journal of experimental and clinical research*, vol. 22, p. 2635, 2016.

[71] M. DA, N. HP, and M. JE, "The use of wearable sensors in human movement analysis in non-swimming aquatic activities: A systematic review.," *Int J Environ Res Public Health*, vol. 24, p. 16, 2019.

[72] T. Pöyhönen, H. Kyröläinen, K. L. Keskinen, A. Hautala, J. Savolainen, and E. Mälkiä, "Electromyographic and kinematic analysis of therapeutic knee exercises under water," *Clinical Biomechanics*, vol. 16, no. 6, pp. 496–504, 2001.

[73] O. A. Donoghue, H. Shimojo, and H. Takagi, "Impact forces of plyometric exercises performed on land and in water," *Sports health*, vol. 3, no. 3, pp. 303–309, 2011.

[74] H. A. Meijer, M. Graafland, M. C. Obdeijn, M. P. Schijven, and J. C. Goslings, "Validity and reliability of a wearable-controlled serious game and goniometer for

telemonitoring of wrist fracture rehabilitation," *European Journal of Trauma and Emergency Surgery*, vol. 48, no. 2, pp. 1317–1325, 2022.

[75] D. A. Marinho, H. P. Neiva, and J. E. Morais, "The use of wearable sensors in human movement analysis in non-swimming aquatic activities: A systematic review," *International Journal of Environmental Research and Public Health*, vol. 16, 2019.

[76] R. B. Davis III, S. Ounpuu, D. Tyburski, and J. R. Gage, "A gait analysis data collection and reduction technique," *Human movement science*, vol. 10, no. 5, pp. 575–587, 1991.

[77] "Bosch, "small , low power 9-axis sensor"," tech. rep.

[78] "Quaternions and spatial rotation."

[79] L. Kocsis, R. Kiss, and Z. Knoll, "Biomechanical models and measuring techniques for ultrasound-based measuring system during gait," *Periodica Polytechnica, Mechanical Engineering*, vol. 48, pp. 1–14, 01 2004.

[80] J. Ghattas and D. N. Jarvis, "Validity of inertial measurement units for tracking human motion: a systematic review.," *Sports biomechanics*, pp. 1–14, 2021.

[81] K. Dahl, K. Dunford, S. Wilson, T. Turnbull, and S. Tashman, "Wearable sensor validation of sports-related movements for the lower extremity and trunk," *Medical Engineering Physics*, pp. 144–150, 2020.

[82] MacFarland, T. W., Yates, and J. M., *Spearman's Rank-Difference Coefficient of Correlation*, pp. 249–297. Cham: Springer International Publishing, 2016.

[83] T. K. Koo and M. Y. Li, "A guideline of selecting and reporting intraclass correlation coefficients for reliability research.," *Journal of chiropractic medicine*, vol. 15 2, pp. 155–63, 2016.

[84] M. Yi, "A complete guide to violin plots," 2021.

[85] C. Z. Y. Choo, J. Y. Chow, and J. Komar, "Validation of the perception neuron system for full-body motion capture," *PLoS ONE*, vol. 17, 2022.

[86] M. M. Liu, W. Herzog, and H. H. Savelberg, "Dynamic muscle force predictions from emg: an artificial neural network approach," *Journal of Electromyography and Kinesiology*, vol. 9, no. 6, pp. 391–400, 1999.

[87] J. Zhao, "A review of wearable imu (inertial-measurement-unit)-based pose estimation and drift reduction technologies," in *Journal of Physics: Conference Series*, vol. 1087, p. 042003, IOP Publishing, 2018.

A | Appendix A: MATLAB codes

This is the Github link: https://github.com/Filippo-Motta/OpenSense-fromexperimental-IMU to the repository with the codes used in the thesis.

B | Appendix B: SmartAnalyzer Protocol

Here is the SMART Analyser protocol created by the researchers to calculate joint angles from the *.trc* file containing the optoelectronic system's retro-reflective marker traces.

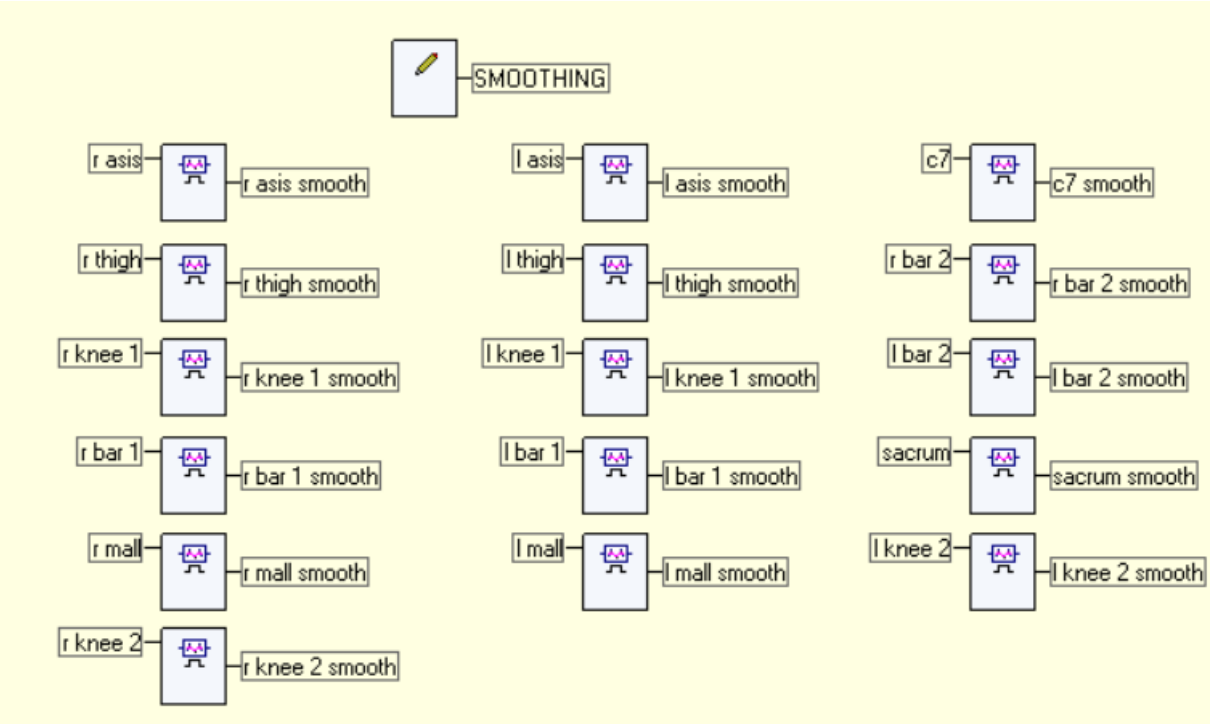

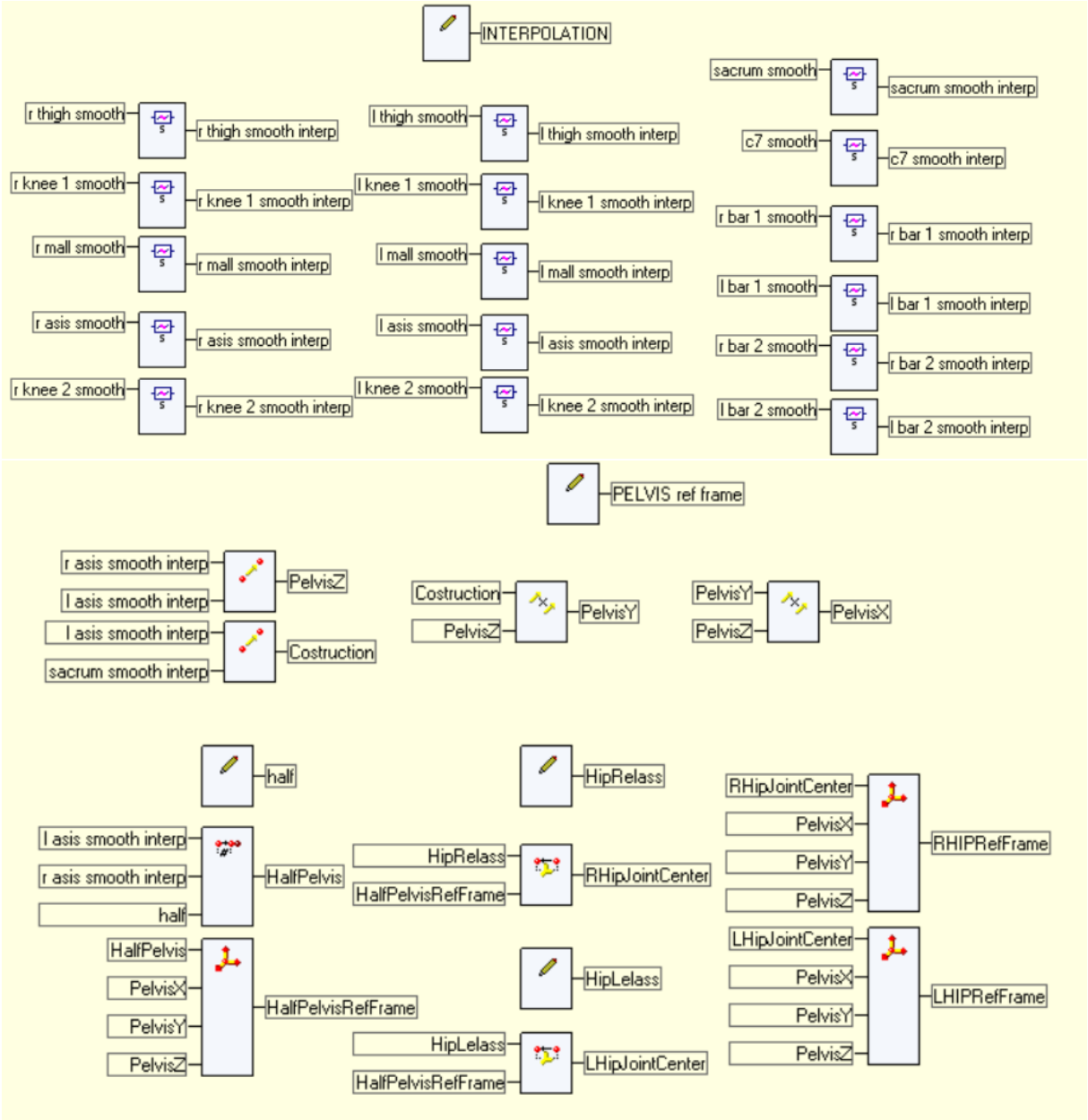
INTERPOLATION
r thigh smooth
r thigh smooth interp
r knee 1 smooth
r knee 1 smooth interp
r mall smooth
r mall smooth interp
r asis smooth
r asis smooth interp
r knee 2 smooth
r knee 2 smooth interp
l thigh smooth
l thigh smooth interp
l knee 1 smooth
l knee 1 smooth interp
l mall smooth
l mall smooth interp
l asis smooth
l asis smooth interp
l knee 2 smooth
l knee 2 smooth interp
sacrum smooth
sacrum smooth interp
c7 smooth
c7 smooth interp
r bar 1 smooth
r bar 1 smooth interp
l bar 1 smooth
l bar 1 smooth interp
r bar 2 smooth
r bar 2 smooth interp
l bar 2 smooth
l bar 2 smooth interp
PELVIS ref frame
r asis smooth interp
l asis smooth interp
PelvisZ
l asis smooth interp
sacrum smooth interp
Costruction
Costruction
PelvisZ
PelvisY
PelvisY
PelvisZ
PelvisX
half
l asis smooth interp
r asis smooth interp
half
HalfPelvis
HalfPelvis
PelvisX
PelvisY
PelvisZ
HalfPelvisRefFrame
HipRelass
HipRelass
HalfPelvisRefFrame
RHipJointCenter
HipLelass
HipLelass
HalfPelvisRefFrame
LHipJointCenter
RHipJointCenter
PelvisX
PelvisY
PelvisZ
RHIPRefFrame
LHipJointCenter
PelvisX
PelvisY
PelvisZ
LHIPRefFrame

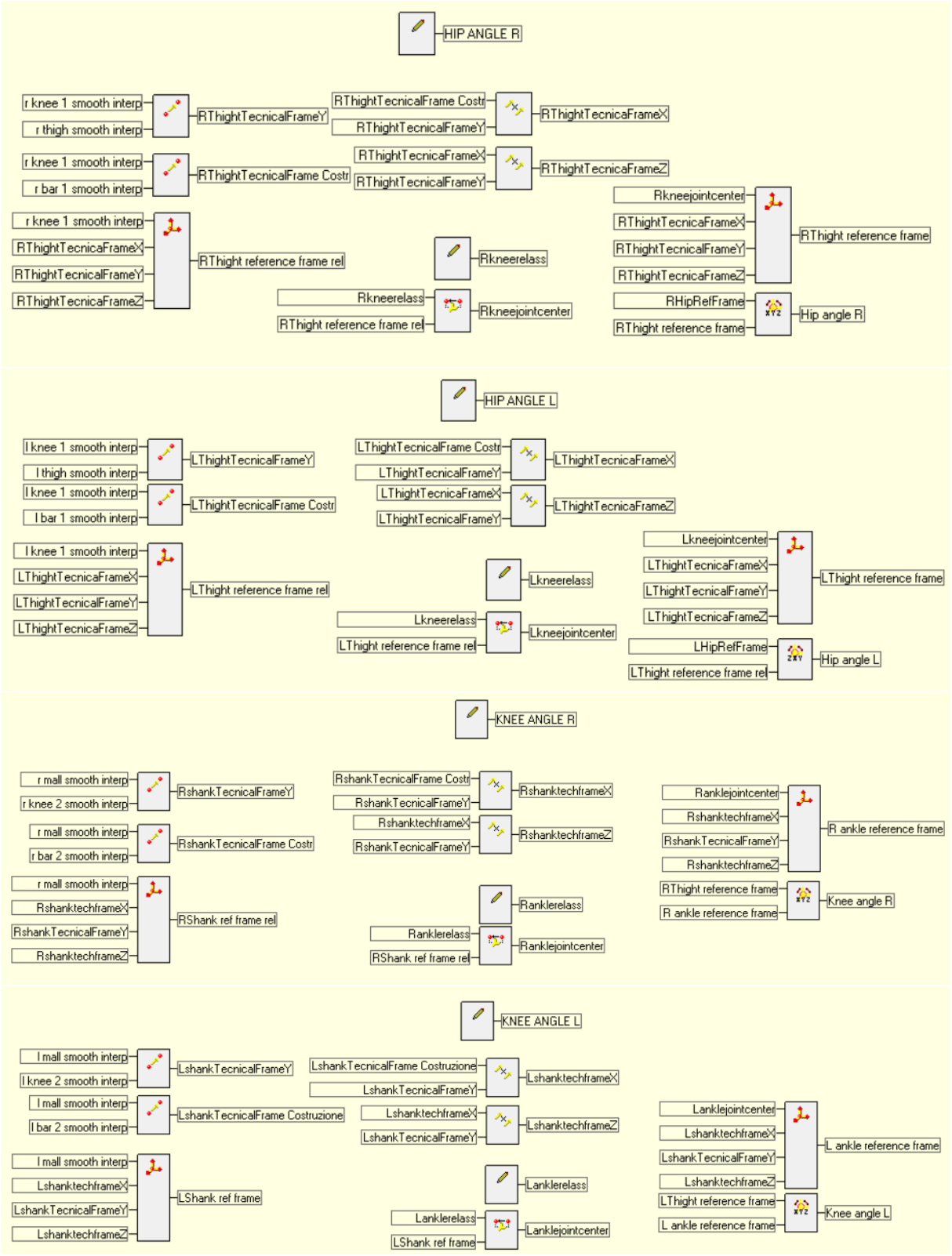

Figure B.1: SMARTAnalyzer Protocol created ad-hoc to obtain the joint angles of interest seen as gold standard

C | Appendix C: Ethical committee approval

Tervise Arengu Instituut

Tervise Arengu Instituudi inimuuringute eetikakomitee

Otsus nr 1128

Tervise Arengu Instituudi inimuuringute eetikakomitee (TAIEK) koosseisus K.Innos, C.Murd, A.Kull, A-R. Tereping, M.Tammaru, T.Pruunsild, M.Liibek arutas oma koosolekul 20. oktoobril 2022 ja otsustas lugeda kooskõlastatuks uuringu „**Digitaalse kaksiku numbrilise mudeli valideerimine OpenSense'is[a], kasutades IMU[b] mõõtmisi maismaal ja vees sooritatud füüsiliste harjutuste ajal füsioloogilise liikumisulatuse määramiseks**", mille vastutav uurija on **Jeffrey Tuhtan** (TTÜ Keskkonnaseire tehnoloogiate keskus), põhitäitjad on **Cecilia Monoli** (TTÜ doktorant) ning magistrandid **Filippo Motta** ja **Cristina Chieffo" .**

Uuring nr 2405, TAIEK koosoleku protokoll nr 45.

Otsus nr 1128 on väljastatud 27.10.2022

Kaire Innos
TAIEK aseesimees /allkirjastatud digitaalselt/

Marje Liibek
TAIEK sekretär /allkirjastatud digitaalselt/

Tervise Arengu Instituudi inimuuringute
eetikakomitee
Tervise Arengu Instituut, Hiiu 42, 11619 Tallinn
tel 659 3924
eetikakomitee@tai.ee
www.tai.ee

D | Appendix D: Informed Consent and Questionnaire

Informed Consent
Validation of an OpenSense computer simulation model based on IMU measurements for volleyball training exercises performed on land and in water

INFORMED CONSENT

Validation of a digital twin numerical model in OpenSense using IMU measurements during physical exercises performed on land and in water to establish physiological range of motion.

Dear Mr/Mrs,
You are being asked to take part in a research study. Before you decide to participate in this study, it is important that you understand why the research is being done and what it will involve. Please read the following information carefully. Please ask the researcher if there is anything that is not clear or if you need more information during the experimental phase or using the contact below. In order to participate in this study, you need to understand simple English directions, by signing you declare to be able to do that.
We want to thank you for your availability for reading this informed consent.

PRINCIPAL INVESTIGATOR
Jeffrey Tuhtan
Associate Professor of Enviromental Sensing and Intelligence Group, Tallinn University of Technology
Akadeemia tee 1, 12618 Tallinn, Estonia
+372 620 3556
jeffrey.tuhtan@taltech.ee

OTHER PEOPLE INVOLVED
Cecilia Monoli – PhD Student - cecilia.monoli@taltech.ee
Cristina Chieffo – Master Degree Student – cristina.chieffo@mail.polimi.it
Filippo Motta – Master Degree Student – filippo4.motta@mail.polimi.it

PURPOSE OF STUDY
The purpose of this study is to establish the physiological range of motion of people with an overall good physical condition, performing simple exercises on land and in water. The study involves physical exercises, by signing this consent you declare to not suffer from any cardiovascular or pulmonary diseases and to be able to perform a light aerobic training (simple motor tasks involving lower limbs). The study is performed in water, by signing you declare to be able to move inside a pool with a depth of water equal to 125cm.

STUDY PROCEDURES
All the experiments will be performed in the Elasmus SPA Mustamae, Akadeemia tee 30, 12611 Tallinn.

In the beginning, the researchers will ask you your age, your height, your weight, and your gender using an anonymous questionnaire.

Participant's Initials: _____

Informed Consent

Validation of an OpenSense computer simulation model based on IMU measurements for volleyball training exercises performed on land and in water

All the movements that needs to be performed will be also described and showed to you by the researchers and they will clarify all the questions you will might have.

You are invited to remove all your clothing and put on a bathing suit.

The researcher will place 7 non invasive sensors on both your legs and waist using an elastic band or adhesive tape.

You enter the pool, where you will stay for the entire duration of the experiment, if you want to withdraw, you can leave the pool at any time.

You will be asked to perform movements, previously well described and showed by researchers, to be done at your own speed and in the way you think is best:

- The first movement is the **squat**, in which you have to low your hips from a standing position reaching 90 degrees of joint angle and then stands back up. Number of repetitions: 5 and 10 seconds rest.
- The second movement is the **hip flexion/extension**. The movement starts in vertical standing position with arm around the waist of the body then flex the knee and keep an angle of 90 degrees. After one second flex the hip, raising the knee towards the chest, then pause for one second and return to starting position. Number of repetitions: 5 for each limb and 5 seconds rest between all the tasks.
- In the third movement, you are required to perform a **flexion/extension** of the **knee**, one leg at a time, starting from standing position. The exercise is composed by the fully flexion of the knee, until the foot reaches the gluteus and then return to standing position, keeping the hip locked. Number of repetitions: 5 for each limb and 5 seconds rest between all the tasks.
- The last movement is the standing **hip adduction/abduction**, where the leg analysed moves away from the midline of the body, keeping the knee extended and then returning to standing position. Number of repetitions: 5 for each limb and 5 seconds rest between all the tasks.

Then you will get out of the pool and repeat all the exercises on land.

The researchers will remove the sensors from your body.

Between all the tasks there will be a resting time of 5 minutes. Total time of experiment is about 30 minutes.

For all the duration of the experiment your motor data will be acquired by the sensors and you will be also videorecorded. Your face will not be in the camera frame, but in case it will be present it will be later blurred to avoid recognition. Some frames of the video could be published in the thesis for illustrative purposes. The footage will be deleted with the data at the end of the two years from the thesis defense.

Participant's Initials: _____

Informed Consent

Validation of an OpenSense computer simulation model based on IMU measurements for volleyball training exercises performed on land and in water

EXPERIMENTAL DURATION

The laboratory evaluation will last approximately one hour for each participant, including preparation and familiarization time with the tests.
The experimental protocol includes the following phases
1. Explanation of the experimental test procedure and signing of informed consent
2. Volunteer preparation
3. Familiarization with test procedures
4. Test execution (both in water and on land)
5. Removal of inertial sensors from the volunteer's body.

RISKS

You may decline to answer any or all questions and you may terminate your involvement at any time if you choose.

All the instrumentation that will be using during the study is not toxic or requires any invasive procedure.

Since the experiments comprehends the performing of an exercise there is the risk of injury, this risk is mitigated by the choice of very simple tasks and an adequate resting period between repetitions, so that fatigue doesn't occur.

A lifeguard will be present for all the duration of the acquisitions in case rescue is needed.

BENEFITS

There will be no direct benefit to you for your participation in this study. However, this study could be useful in future to predict the muscles responses and follow the improvements during a specific rehabilitation process both in case of strokes or joint prosthesis substitutions.

COST AND ALLOWANCE FOR PARTEICIPATION

Participation in the study is free of charge. Intellectual property products (publications, conference proceedings, presentations) created by the researchers involved will not be the property of the participant.

CONFIDENTIALITY

Your data and responses to the questionnaire will be assigned to a numerical number to ensure pseudonomysation, the list of names and codes will be accessible by the

Participant's Initials: _____

Informed Consent

Validation of an OpenSense computer simulation model based on IMU measurements for volleyball training exercises performed on land and in water
researchers only. If your face will appear in the video it will be blurred to avoid identification.

CONTACT INFORMATION

If you have questions at any time about this study, or you experience adverse effects as the result of participating in this study, you may contact the researcher whose contact information is provided on the first page. If you have questions regarding your rights as a research participant, or if problems arise that you do not feel you can discuss with the Primary Investigator (Jeffrey Tuhtan jeffrey.tuhtan@taltech.ee), please contact the Estonian National Institute for Health Development (TAIEK) at + 372 659 3900, tai@tai.ee.

PROCESSING AND DISSEMINATION OF COLLECTED INFORMATION

- Data concerning participants will be treated in a strictly anonymised form, in accordance with European privacy laws.
- The participant may revoke permission to use and disclose his/her data at any time; from that moment on, participation in the study will end and no further data will be collected.
- The researchers involved in the study will use the participant's data for the research described in this informed consent form.
- The results of the research may be presented at conferences and published in scientific journals of international relevance; in any case the data will be anonymised.

VOLUNTARY PARTICIPATION

Your participation in this study is voluntary. It is up to you to decide whether or not to take part in this study. If you decide to take part in this study, you will be asked to sign this consent form. After you sign the consent form, you are still free to withdraw at any time and without giving a reason. Withdrawing from this study will not affect the relationship you have, if any, with the researcher. If you withdraw from the study before data collection is completed, your data will be returned to you or destroyed.

CONSENT

I have read and I understand the provided information and have had the opportunity to ask questions. I understand that my participation is voluntary and that I am free to withdraw at any time, without giving a reason and without cost. I understand that I will be given a copy of this consent form. I voluntarily agree to take part in this study.

Participant's signature _____ Date _____

Participant's Initials: _____

Informed Consent
Validation of an OpenSense computer simulation model based on IMU measurements for volleyball training exercises performed on land and in water

Investigator's signature _____ Date _____

Participant's Initials: _____

QUESTIONNAIRE

Validation of an OpenSense computer simulation model based on IMU measurements for physical exercises performed on land and in water

I. Basic Information

Age:_____

Weight:_____

Height:_____

Gender:_____

II. General information

a. Are you a physically active person? YES ☐ NO ☐

If YES, how many time a week do you practice physical activity?

Once time a week ☐

Twice times a week ☐

Three or more times a week ☐

b. Did you undergo to any lower limb surgery in the last 2 years? YES ☐ NO ☐

If YES, specify which kind of surgery you had: _____

Staff Table:

Name	**Degree**	**Email**
Jeffrey A. Tuhtan	Associate Professor	jeffrey.tuhtan@taltech.ee
Cecilia Monoli	PhD Student	cecilia.monoli@taltech.ee
Cristina Chieffo	Master Degree Student	cristina.chieffo@mail.polimi.it
Filippo Motta	Master Degree Student	filippo4.motta@mail.polimi.it

E | Appendix E: Table of excursions of the Phase 2

SUBJECTS	SQUAT[°]		FRONTAL LEG SWING[°]	
	DRY	WET	DRY	WET
1	97,2 (6,5)	83,9 (8,4)	49,0 (11,6)	48,1 (5,8)
2	**56,5 (4,0)**	**59,2 (5,5)**	**30,8 (3,4)**	38,8 (12,3)
3	**102,9 (6,1)**	86,9 (2,5)	64,7 (2,9)	48,8 (4,5)
4	88,5 (5,9)	87,0 (15,5)	46,5 (5,3)	44,5 (3,2)
5	74,5 (5,2)	81,8 (2,6)	39,2 (4,9)	40,5 (3,4)
6	84,2 (1,9)	81,8 (2,2)	57,9 (13,4)	53,7 (6,5)
7	79,3 (4,3)	81,6 (6,0)	42,0 (4,7)	44,1 (6,3)
8	98,0 (5,8)	67,5 (9,6)	44,5 (2,9)	36,2 (6,9)
9	80,4 (2,3)	68,4 (5,2)	38,7 (10,9)	35,8 (3,3)
10	89,0 (5,6)	100,2 (3,8)	42,6 (2,8)	**33,4 (17,2)**
11	83,7 (2,2)	89,8 (4)	37,7 (6,5)	52,4 (7,9)
12	65,7 (6,1)	69,1 (3,6)	56,1 (6,4)	55,6 (3,7)
13	74,6 (7,3)	93,3 (8,6)	60,7 (8,0)	**60,1 (13,1)**
14	81,1 (8,0)	75,8 (3,0)	58,0 (6,1)	54,3 (12,4)
15	89,9 (5,5)	**100,6 (7,2)**	**65,3 (11,9)**	50,7 (14,2)

Table E.1: Table of the mean and SD of the excursions performed for the S and FLS exercises with the min and max values highlighted.

SUBJECTS	KNEE TO CHEST[°]		HEEL TO HAMSTRING[°]	
	DRY	WET	DRY	WET
1	106,6 (3,6)	82,7 (9,2)	111,9 (4,8)	95,5 (10,9)
2	**78,4 (5,4)**	80,9 (7,9)	103,3 (5,6)	**116,1 (8,0)**
3	117,7 (8,1)	97,7 (2,6)	116,1 (6,0)	100,6 (5,4)
4	118,6 (5,5)	88,8 (4,8)	121,9 (2,5)	98,4 (13,2)
5	81,0 (10,8)	75,9 (3,4)	**98,2 (8,5)**	92,1 (9,1)
6	81,5 (9,3)	76,6 (4,5)	115,1 (5,4)	102,0 (3,3)
7	89,2 (3,0)	**71,9 (2,8)**	100,0 (8,3)	93,6 (7,6)
8	96,0 (4,6)	74,8 (6,9)	115,0 (8,1)	106,6 (14,4)
9	82,5 (7,6)	76,3 (2,6)	104,6 (6,1)	**87,9 (10,8)**
10	89,9 (4,2)	94,4 (3,2)	98,6 (7,2)	92,6 (4,4)
11	83,1 (9,1)	86,4 (6,0)	110,3 (6,5)	105,1 (4,1)
12	102,3 (6,4)	91,7 (6,1)	111,1 (4,1)	104,4 (3,9)
13	78,5 (8,0)	87,0 (10,9)	106,6 (10,6)	90,5 (3,1)
14	**123,4 (7,7)**	**105,7 (6,8)**	**131,4 (8,9)**	97,3 (11,3)
15	91,0 (8,8)	79,4 (6,1)	113,1 (15,5)	91,7 (12,4)

Table E.2: Table of the mean and SD of the excursions performed for the KTC and Heel to Hamstring exercises with the min and max values highlighted.

F | Appendix F: Bland-Altman Plots

This appendix contains all the Balnd-Altman plots obtained from the comparison between TinyTag and optoelectronic system. Here reported all the graphs divided according to exercise (Squat, then the FLS, the KTC and HTH) and subject analysed.

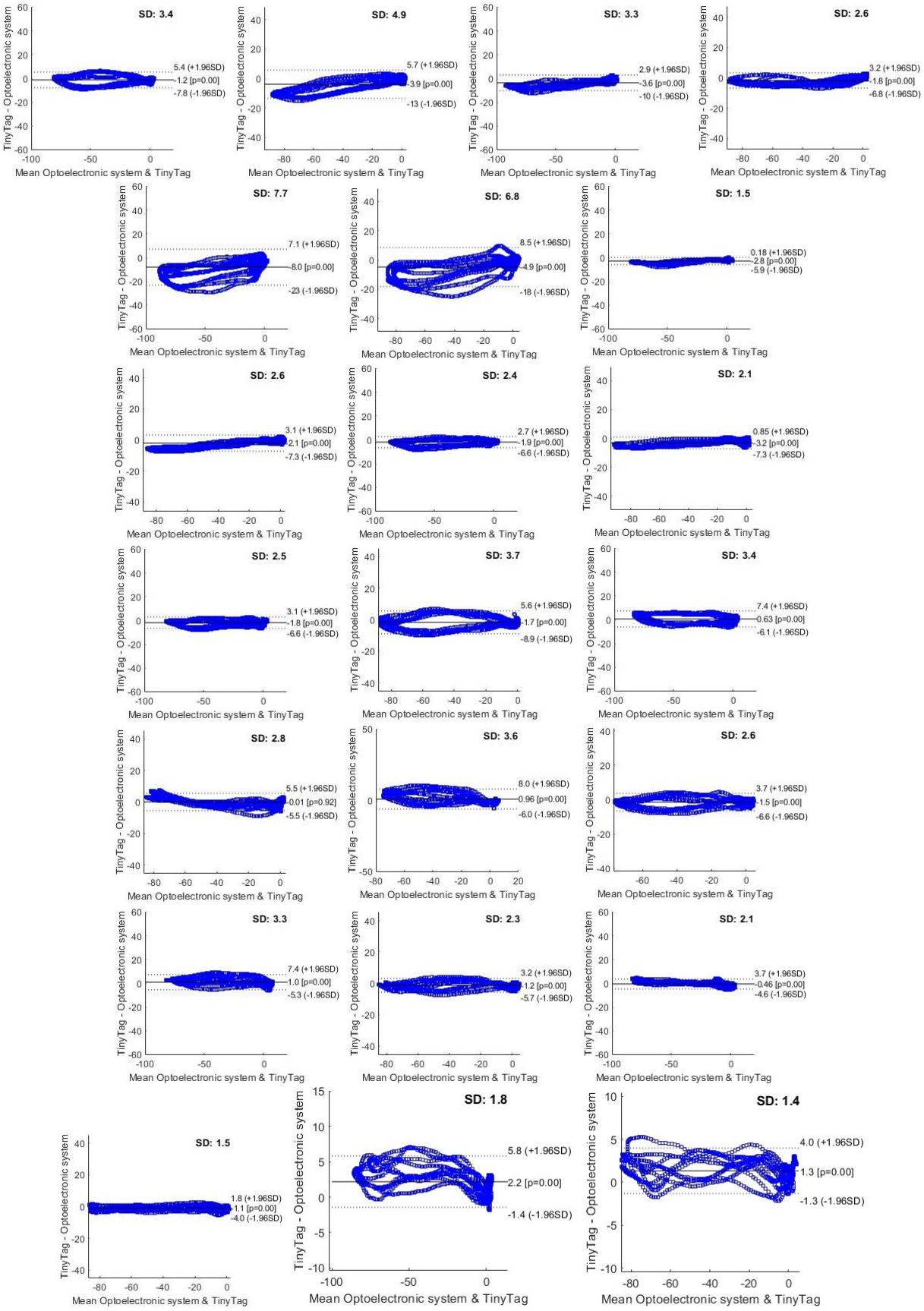

Figure F.1: Bland Altman plots of Squat exercise. Subject 1

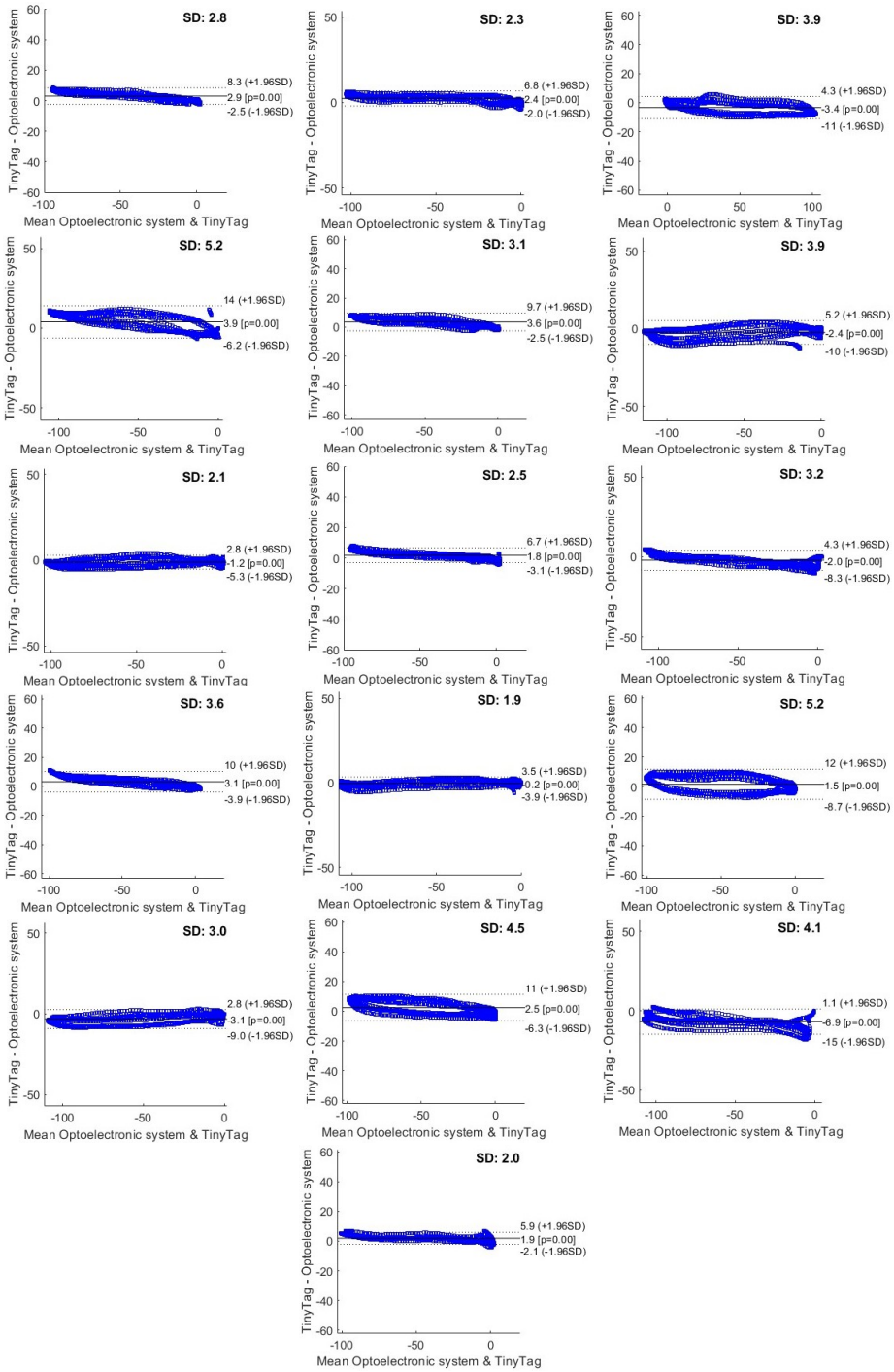

Figure F.2: Bland Altman plots of Squat exercise.Subject 2

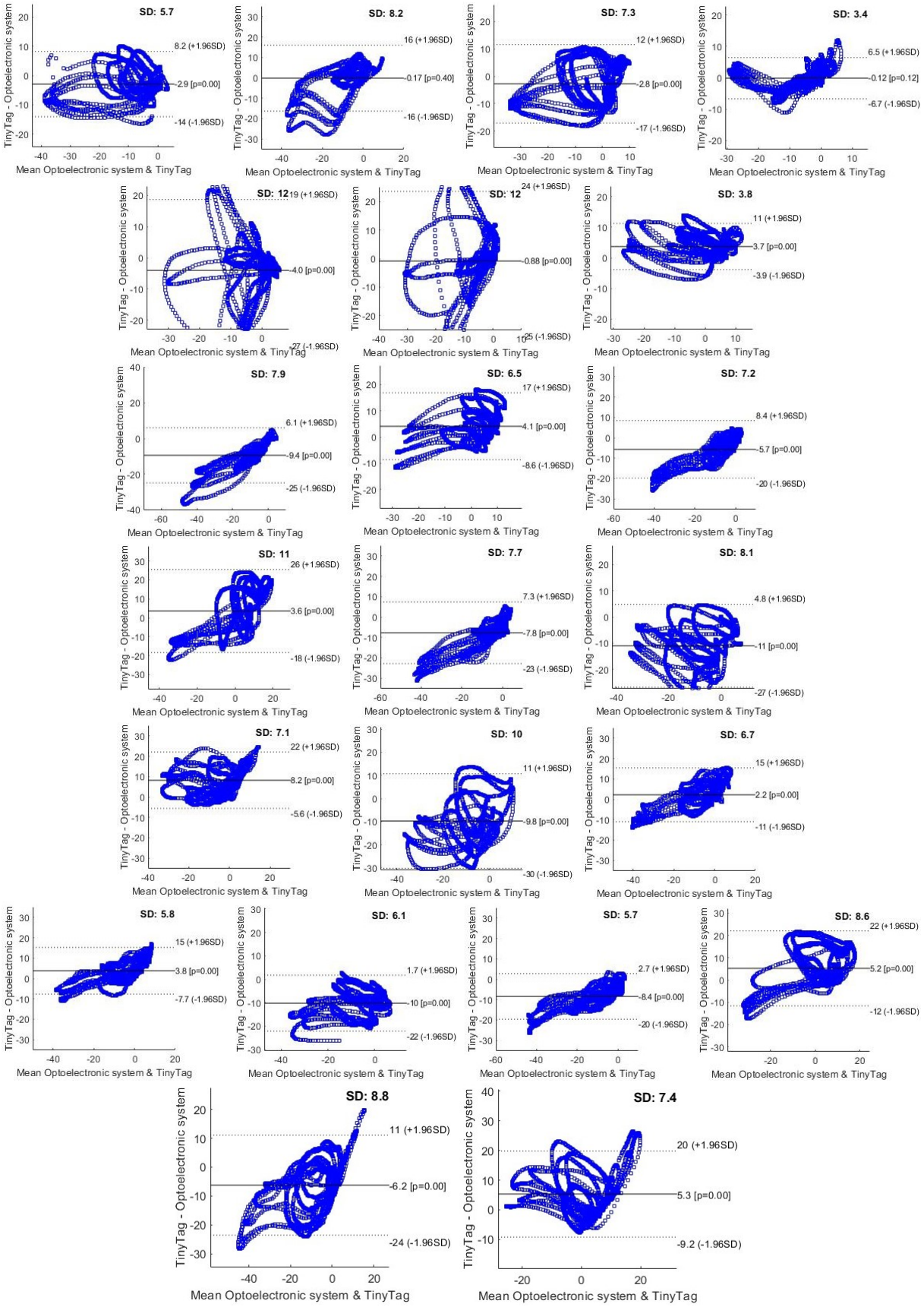

Figure F.3: Bland Altman plots of FLS exercise. Subject 1

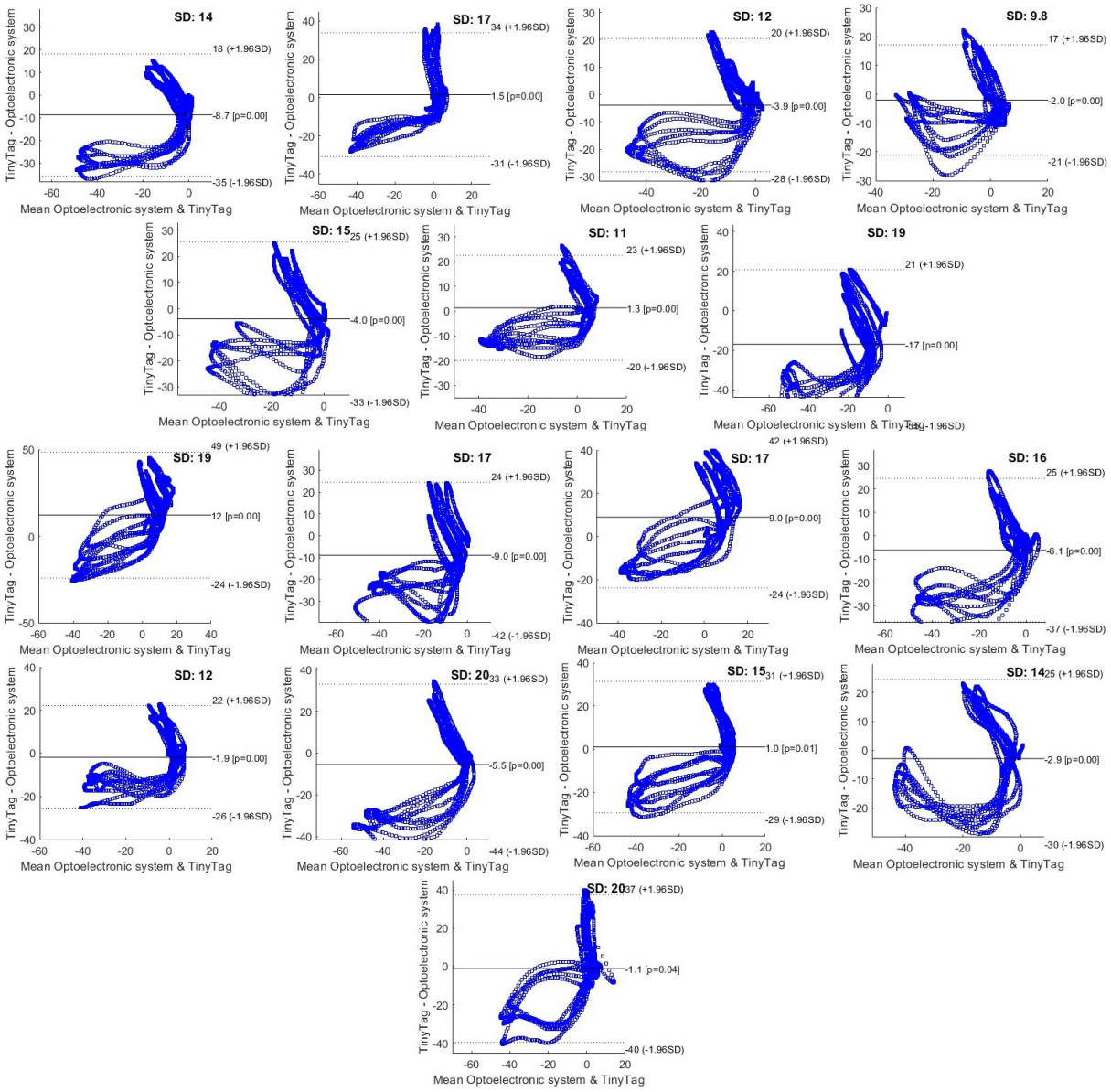

Figure F.4: Bland Altman plots of FLS exercise. Subject 2

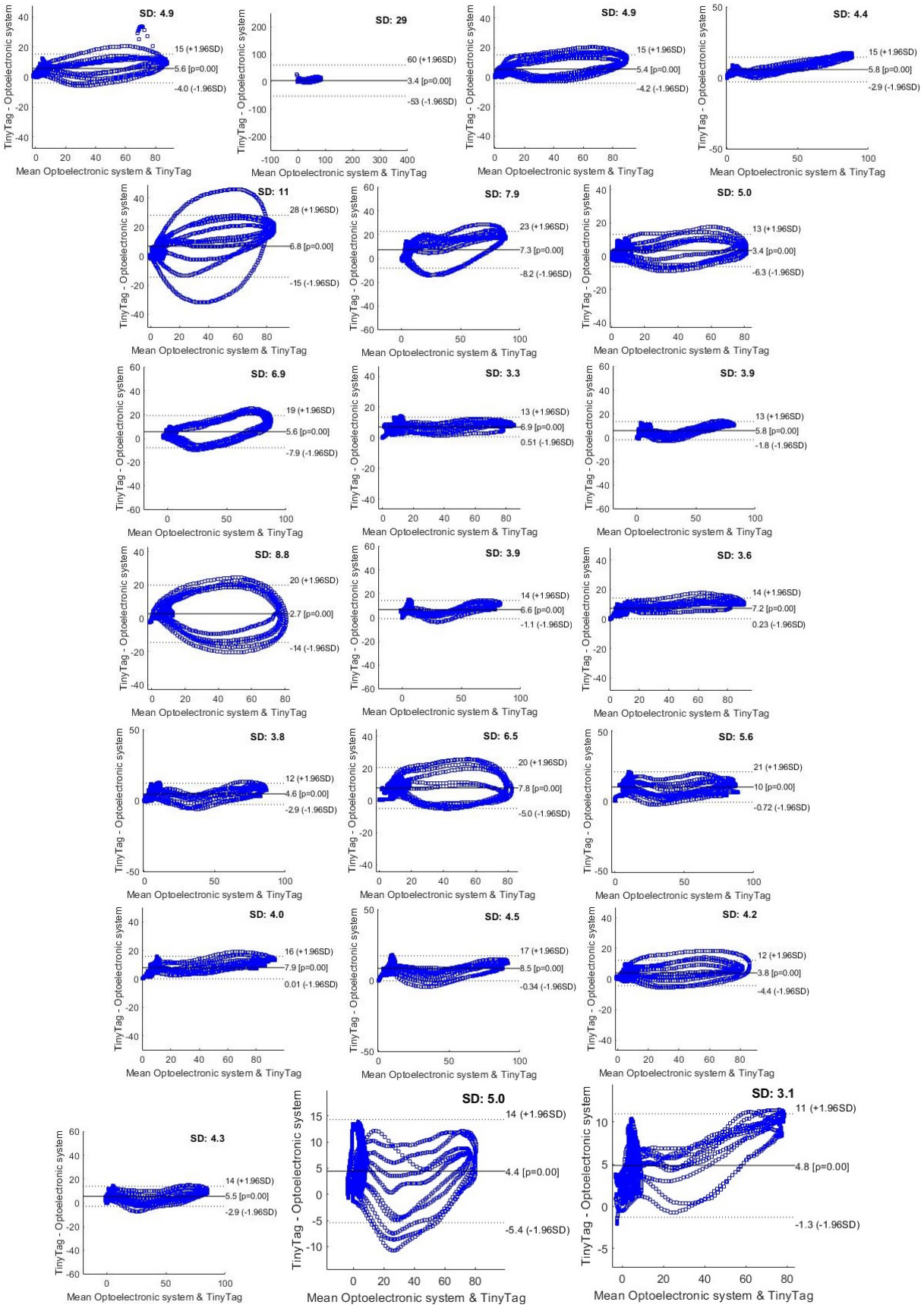

Figure F.5: Bland Altman plots of KTC exercise. Subject 1

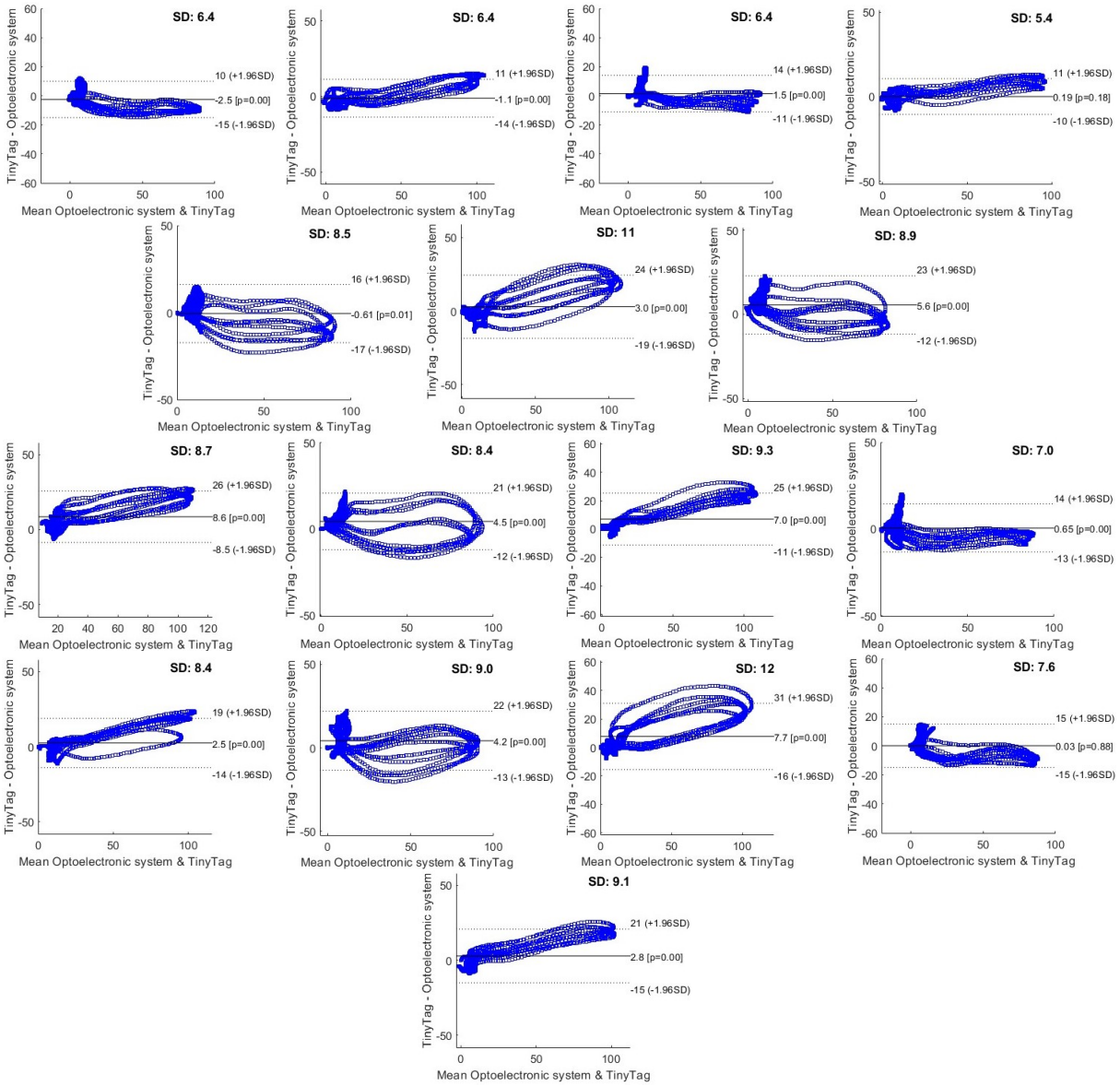

Figure F.6: Bland Altman plots of KTC exercise. Subject 2

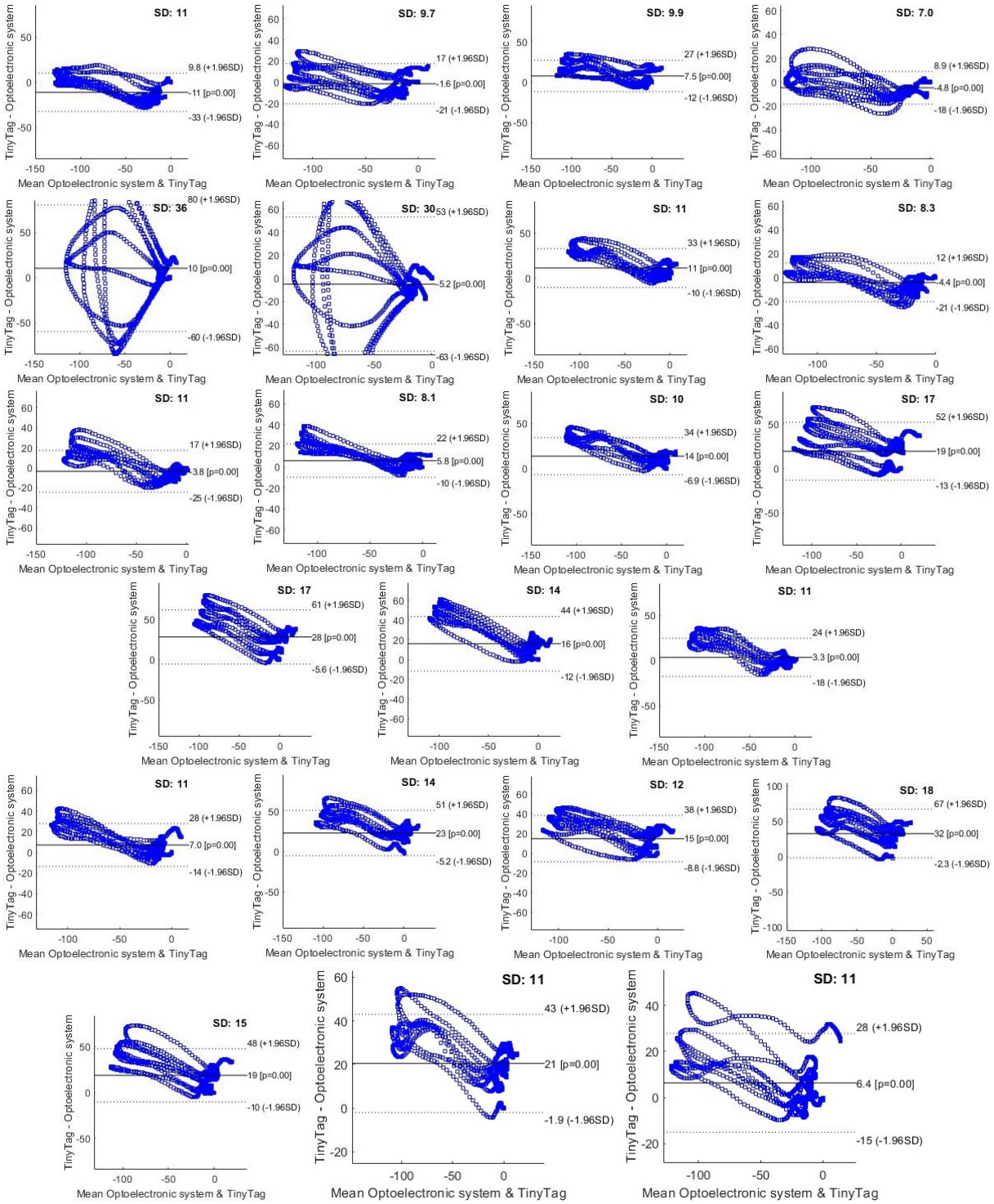

Figure F.7: Bland Altman plots of HTH exercise. Subject 1

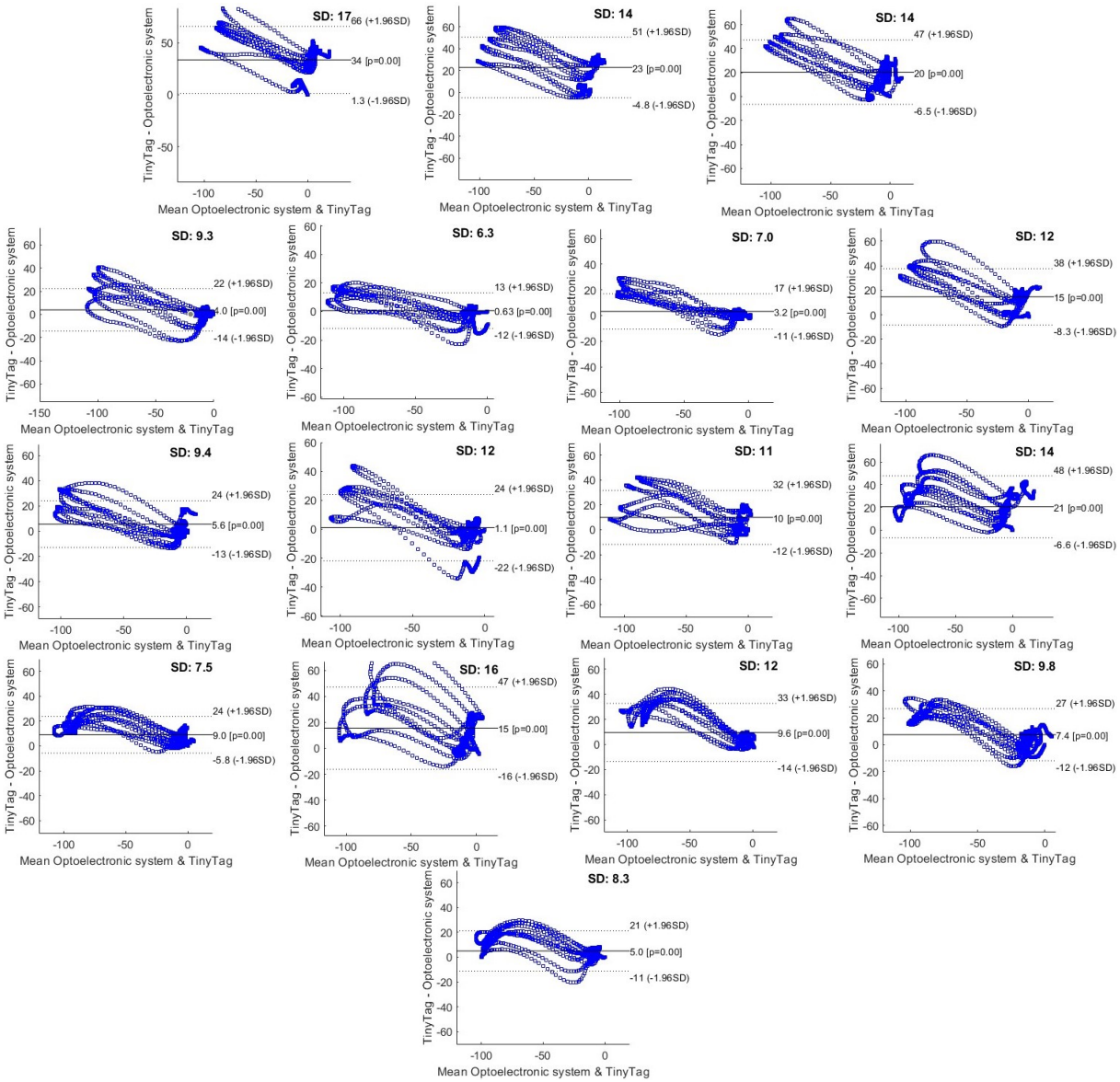

Figure F.8: Bland Altman plots of HTH exercise. Subject 2